POLITECHNIKA KRAKOWSKA

CRACOW UNIVERSITY OF TECHNOLOGY

THE INFLUENCE OF INERTIA FORCES ON SOIL SETTLEMENT UNDER HARMONIC LOADING

Natalia Pietrzak

Cracow, June 2017

ACKNOWLEDGEMENTS

I would like to express thanks to my supervisor, Prof. Bogumił Wrana, for formulating the basis of my research and constant guidance. I also wish to express my deep appreciation and gratitude for sharing his tremendous knowledge.

I will be eternally indebted to my father, mother and grandfather for everything which cannot be put into words, their love and support was a driving force throughout the whole challenging process.

I am also very grateful to my employer, Paweł Okroj, for his patience and understanding.

Finally, I wish to thank to my colleague, Sławomir Milewski, for his inestimable help with computer programming.

Table of Contents

Abstract

The thesis concerns dynamic analysis of a two-phase, fully saturated medium. The purpose is to determine the limits of validity of various simplification models. In order to do this a full set of governing, dynamic equations of saturated two phase media (Biot's model) and a series of simplifying models often used in practice, such as the *u-p* simplification model, the quasi-static consolidation model and the single-phase model, are considered. The displacement of the skeleton, displacement of fluid, pore water pressure, influence of the soil saturation level, and physical parameters on the dynamic (amplification) factor are shown and compared with each model with various formulations. Moreover, the dynamic factor, which is a multiplier for the static solution, is analyzed.

One dimensional (1D) and two dimensional (2D) problems were solely solved by the author. In the case of the 1D problems, an analytical solution was used. Regarding the 2D model, the Finite Element Method was utilized. In order to present and compare the results a customized computer program in Matlab was created. According to the results obtained all the simplifications have a significant impact. The level of discrepancy depends not only on the simplification used, but also on the parameters of the soil. What is worth mentioning here, is that the very commonly used single phase model, which does not include pore water pressure, implies a significant inaccuracy in both displacements and stresses.

1. Introduction.

1.1. Introduction.

Soil mechanics is a branch of engineering mechanics that describes the behavior of soil. It differs from fluid mechanics and solid mechanics in the sense that soil consists of a heterogeneous mixture of fluids (usually air and water) and particles (for example clay, silt, sand, and gravel) but soil may also contain organic solids, liquids, gases, and other matter. Soil mechanics provides the theoretical basis for analysis in geotechnical engineering using a great deal of knowledge from physics, chemistry, geology, theory of elasticity, theory of plasticity, and strength of materials. We can say that it is an interdisciplinary science, which is proved in (Wrana & Pietrzak, 2015).

Soil dynamics is a branch of geomechanics that describes processes which are unstable in time and which, as a consequence, require taking inertia forces into consideration. The study covers the numerical analysis of a two-phase media under harmonic loading.

The response of saturated porous media under a dynamic load is of high interest in many fields ranging from geomechanics to biomechanics. Problems like transient phenomena during impact loading, earthquakes, water wave loading, and consolidation are of significant interest in geomechanics. The nature of the response of the saturated porous media depends not only on the nature of the loading but also on the flow and deformation characteristics of the media. The response is said to be fully drained when the rate of loading is much smaller than the rate of pore fluid flow. The problem is said to be static if the steady-state pore fluid pressures depend only on the hydraulic conditions and are independent of the porous skeleton response leading to uncoupled flow and deformation problem. A one-phase media for all the calculations is adequate then. At the other extreme if the rate of loading is much faster than the rate of flow, the fluid follows the motion of the solid. This is an undrained condition, where the single-phase solution is also adequate.

Depending on the rate of loading and the characteristics of the flow and deformation there are three possible models :

- fully dynamic (the Biot's model (Biot, 1956))
- *u-p* formulation (partly dynamic (Zienkiewicz, et al., 1980))
- the consolidation equations (quasi-static (Terzaghi, 1960))

In the first model , the coupled equations of flow and deformations are formulated including an acceleration of both the solid skeleton and the fluid. In case of the *u-p* formulation, the coupled equations consider only the acceleration of the solid skeleton. The governing equations are represented only in terms of the solid displacement *u* and the pore fluid pressure *p*. When it comes to the quasi static case , all inertial terms are ignored.

1.2. Motivation and objectives.

Dynamic analysis plays a very important role in geotechnics. Currently, there are many simplified models used in practice, starting from the commonly used single phase model to other simplifications of two and three phase models. The aim of the thesis is to present the influence of the particular phases in the two-phase media model (the skeleton phase with its inertia and the water phase with its inertia). The thesis shows the differences not only in the theoretical equations, but also in the obtained results. One dimensional and two dimensional problems are analyzed. The following topics are raised in the thesis:

A) for the one dimensional problem:

1. Defining the fully dynamic (Biot's) model and deriving simplified formulations in dynamic analysis of the two phase media (*u-p* and quasi-static consolidation models).

2. Presenting discrepancies and limits of validities between the above formulations.

3. Analyzing the influence of the saturation level, physical parameters and extortion frequency of the dynamic factor.

B) for the two dimensional problem

1. Defining the *u-p* model, the *u-p* model omitting the change of water pressure with time and the commonly used single phase model.

2. Presenting discrepancies between the *u-p* model both including and then omitting the change of water pressure with time.

3. Presenting divergences between the two-phase model and the commonly used single phase model.

1.3. Thesis outline.

Chapter 2 of this research contains a brief history of the development of the theory of porous media. It mentions the most relevant scientists and gives an overview of three main eras in this field.

Chapter 3 presents details about propagation of elastic waves in a half-space soil due to dynamic loads in single phase (solid), two-phase (solid and fluid), and three-phase media (solid, fluid and gas). It mainly concentrates on dilatational and shear waves equations.

Chapter 4 is the introduction to the research part of the thesis. It gives the detailed review of equations, which are the starting point for the analysis. It covers stress-strain relations, equilibrium relations and it defines the boundary and initial conditions for the thesis purpose.

Chapter 5 explains the differences between three formulations for the one dimensional problem not only in theory but also by means of numerical example. The disparities between the models are thoroughly analyzed and compared. The limits of validities for each model are estimated. In the last section of this chapter the dynamic amplification factors are evaluated for different types of soil, frequencies and degrees of saturation.

Chapter 6 together with Appendix 1 gives the detailed view of the Finite Element Method approach to the two dimensional problem under plane strain condition. The strong and the weak formulation is presented. Again different formulations presenting alternative simplifications are compared and discussed. Appendix 1 presnts the FEM matrices for the plane strain condition.

Chapter 7 presents a brief summary and a possibility of extension of this study for further research.

2. Theory of porous media.

The space in naturally existing materials like soils, is usually not completely filled with the matter. There are some empty interspaces called pores. In general, three phases can be distinguished: solid skeleton with pores filled with fluid and gas phase. This complex microstructure determines the soil features. The skeleton which forms the body matrix and the contents in the pores have different material properties and different motions and the individual constituents are mutually influenced by each other. What is more, even some interaction phenomena occur. All these concepts confirm, that the soil, which is a three-phase media, is a very complex material, which has been investigated for decades by many scientists. As a large number of other solids contain pores it is not surprising that these media have been repeatedly investigated, the more so as these media play an important role in nearly all fields of engineering.

The history of porous media evaluation was widely discussed by R. de Boer (Boer, 1999; Boer, 1996). He explains all existing theories of as complex media as soil is. He divides the historical development into three periods. In the early era, in the 18th and 19th centuries, the fundamental principles of mechanics were discovered, the concept of volume fractions was started and the mixture theory was founded. In the period between 1910 and 1960, first attempts to clarify the mechanical interaction of liquids, gases, and rigid porous solids were performed and, for the first time, deformable saturated porous solids were treated. In the 1970s and 1980s theories of immiscible mixtures were developed which are still under study (Murray & Sivakumar, 2010) . Below I would try to describe shortly the aforementioned periods.

2.1. The Early Era.

In the 18th century first steps in soil mechanics were taken. Basic discoveries are mainly due to brilliant mathematician Leorhard Euler and excellent engineer Reinhard Woltman. Euler at the beginning of his soil mechanic adventure pointed out the elasticity in solid as a certain subtile matter in closed pores but he did not pay more attention to this matter. However he was the one, who formulated the axioms of continuum mechanics, which he called *cut principle* , balance of mass, balance of momentum and the balance of moment of momentum (Euler, 1736). Unfortunately the Euler's work was disturbed by the lack of principles of mechanics. He outlined in his book topics in mechanics that should be investigated in the future. Although he was not able to define clear rules and equations for raised subjects, he was definitely the pioneer of soil mechanics.

The concept of volume fraction was first used by an ingenious harbor construction director Reinhard Woltman (1757-1837). Not only did he formulate the volume fraction but he also noticed that the moisture content enlarges the cohesion. He particularly turned his attention to partially and totally water-saturated substances and was the first to use an expression *mixture* for soils as he noticed they consist of earth, fluid and air (Woltman, 1794).

The mixture theory is a second important branch of the porous media theory. First steps in this field were taken by Fick, who investigated the problem of diffusion. He analyzed the Fourier's heat transfer equation and noticed an analogy which lead him to the differential equation of the diffusion stream (Fick, 1855):

$$\frac{\partial y}{\partial t} = -k\left(\frac{\partial^2 y}{\partial^2 x} + \frac{1}{Q}\frac{dQ}{dx}\frac{\partial y}{\partial x}\right) \tag{2.1}$$

Where y is the concentration, t the time , k a constant which depends on the nature of the constituent, x the measure for the height of a container, and Q the cross section of the container.

Josef Stefan (1835-1893) on the contrary stated : "If the true processes in a mixture should be calculated, it is not sufficient anymore, to consider the mixture as a uniform body as common mechanics does; equations must be set up which contain the condition of equilibrium and the laws of motion for every individual constituent in the mixture". Stefan also introduced the interaction forces between the constituents and as a consequence he also formulated two one-dimensional equations for the two gases. Some scientists say that Stefan was the first who created the theory of the mixture, where different phases are treated as individual constituents considering the interaction forces.

Henry Darcy also played an important role in soil mechanics. He created basic constitutive relations for the problem of running water through a layer of sand. Although his investigations were purely experimental, the equations became essential. Then there were lots of other scientists who modified the Darcy's law trying to introduce some theoretical investigations.

2.2. The Classical Era.

The formulations of basic relations in the early stages had provided the sufficient background for further development of porous media. From 1913 to 1936 some important physical phenomena were described by Paul Fillunger and Karl von Terzaghi, professors in Vienna. They mainly worked on such phenomena as uplift, friction, capillarity and effective stress. Paul Fillunger was the first who stated that masonry dams are never impermeable, so water will certainly enter the

voids of the masonry. As a consequence the weight of the masonry decreases and there is an additional horizontal component as illustrated in Fig. 2.1 , reducing the stability of the dam (de Boer, et al., 1996) . In his papers (Fillunger, 1913) Fillunger analyzed the stresses in concrete and masonry gravity dams and gave the following equation :

$$\gamma_a = -k(n-n') \tag{2.2}$$

where n is the volume porosity, n' the surface porosity, and k the gradient of the pore-water pressure in the damn. The value of n' is between zero and one and it depends on representative elementary area caused by the cut.

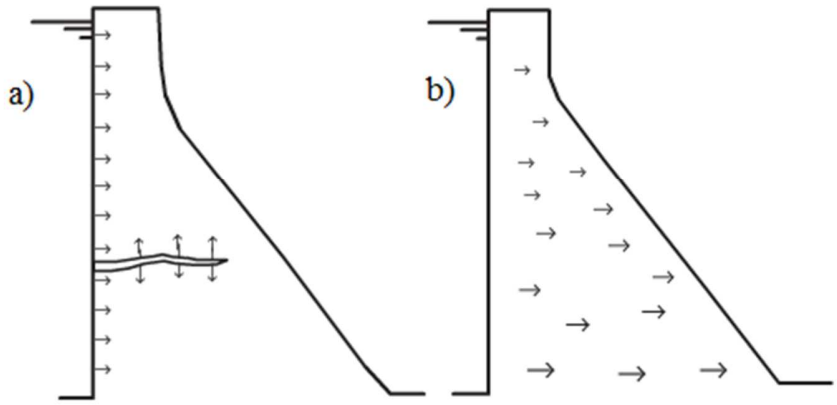

Fig. 2.1: Theories of uplift; a) The Early Era b) The classical Era

Karl von Terzaghi also touched the subject of uplift of dams on granular soils. He was a full advocate of designing for full uplift (von Terzaghi, 1925). He took up a study of the hydrodynamic uplift within the pores of cement mortar and concrete. Finally he introduced the equation for the uplift as :

$$\gamma_a = k(n-n_w) \tag{2.3}$$

where n_w is the effective surface porosity, a material property of the dam medium. In order to determine the value of n_w Terzaghi together with Rendulic performed series of triaxial compression tests and they finally made a conclusion that the value of nw is very close to one, which means that dams should be designed for full uplift. There was a long bitter dispute with Fillunger on this matter.

The theoretical treatment of capillary forces in saturated porous media was closely connected to the uplift problem. Karl von Terzaghi created the formula for the hydrostatic pressure of the pore liquid caused by capillarity (von Terzaghi, 1933). Fillunger strongly disapproved Terzaghi's statement but he also stated that the capillary suction for the liquid causes an additional pressure for the solid phase.

The third, even the most important mechanical effect in saturated porous solids, is the effect of effective stresses. The opinions on this matter were divided. Some scientists believed that the liquid pressure affects the porous solid materials whereas some of them strongly declined this possibility. The pioneer of the first concept was Fillunger. He assumed that the uniform internal pressure cannot cause a significant reduction in the strength. He came back to this problem few years later but his investigations were totally forgotten. It was Karl von Terzaghi that explained the effect of effective stresses to engineers' minds :

"The stresses in any point of a section through a mass of earth can be computed from the total principal stresses s1, s2,s3 which act in this point. If the voids of the earth are filled with water under a stress u, the total principal stresses consist of two parts. One part, u, acts in the water and in the solid in every direction with equal intensity. It is called the neutral stress (or porewater pressure). The balance, $\sigma_1' = \sigma_1 - \mathrm{u}$, $\sigma_2' = \sigma_2 - \mathrm{u}$, $\sigma_3' = \sigma_3 - \mathrm{u}$ represents an excess over the neutral stress u and it has its seat exclusively in the solid phase of the earth.

This fraction of the total principal stresses will be called the effective principal stresses . . ." (Terzaghi, 1936).

Neither Fillunger nor von Terzaghi considered this mechanism as being as important effect as a general principle. All of beforementioned discoveries (the uplift, the capillarity and the effective stresses) in fully saturated rigid and deformable porous solids make an incredible step forward in soil mechanics.

In The Classical Era also another important theory was discovered - the theory of consolidation. Firstly it was mathematically described by von Terzaghi, who formulated the one dimensional consolidation after performing a lot of experiments (Terzaghi, 1924) :

$$\frac{k}{a}\frac{\partial^2 w}{\partial z^2} = \frac{\partial w}{\partial t} \tag{2.4}$$

where *w* is the porewater overpressure, *k* and *a* are the permeability and the compression coefficients, *z* is a vertical coordinate and *t* the time. He made a series of assumptions like that clay is saturated and homogeneous, soil and water is incompressible and what is more Darcy's law was introduced when deriving the above equation. It is obviously very similar to the differential equation of heat propagation (Fourier's law). When Fillunger found the opportunity to compromise von Terzaghi, he immediately started to work on the same subject and after six months he formulated the one dimensional consolidation as :

$$\frac{\partial v_1}{\partial t} + v_1 \frac{\partial v_1}{\partial z} = \frac{g}{n\gamma_1}\left(-Z - \frac{\partial np}{\partial z}\right) \tag{2.5}$$

$$\frac{\partial v_2}{\partial t} + v_2 \frac{\partial v_2}{\partial z} = \frac{g}{(1-n)\gamma_2}\left(Z - \frac{\partial (1-n)p}{\partial z}\right) \tag{2.6}$$

$$\frac{\partial n}{\partial t} + \frac{\partial (n v_1)}{\partial z} = 0 \tag{2.7}$$

$$-\frac{\partial n}{\partial t} + \frac{\partial (1-n) v_2}{\partial z} = 0 \tag{2.8}$$

Fillunger stated that the pore-water [body 1] flows upwards and the solid [body 2] flows downwards with the settlement rate. If we disregard the effect of self-weight, then the external force for each body consists only of the resistance to this flow put up by the other body, and the coupling of the two motions is based on this. It is further recommended that this external force no longer be related to the mass unit but rather to the unit volume, and that it be imagined that the pore-water constantly, but with varying density fills the total space as well as the soil. It is then as if the flows were to exist in the same space: two flows which can influence each other only through resistance, but not according to the law of volume displacement (Fillunger, 1936). In each cross-section *z* of the double flow, there exists stress which is distributed on the two bodies or materials. If *n* is the pore space per unit of volume, then it follows from Delesse's law (where on each cut surface , in a uniform mixture, the surface ratios of each partial constituent must be equal to their volume ratios) that the partial stress $u^1 = np$ falls on the pore-water, and the partial stress $\sigma^s = (1-n)p$ falls on the solid particles in the clay. In fact, $p = u^1 + \sigma^s$. Invoking the Darcy's law, Fillunger arrived at $Z = -\frac{v_1 - v_2}{n_0 k'}\gamma_1$ where *k'* is the coefficient of permeability and n_0 is the initial porosity.

It is obvious that both scientists Terzaghi and Fillunger were brilliant and they contributed to an incredible development in the field of mechanics of porous media. Unfortunately their dispute ended tragically with Fillunger's suicide.

The porous media theory was further developed by the above scientists' followers. It was M.A. Biot that had the greatest impact on the development of the Terzaghi's direction. Unfortunately G.Heinrich, a follower of Fillunger, was nearly completely forgotten. In the period between 1935 and 1962 Biot published a number of scientific papers that lay the foundations of the theory of poroelasticity (now known as Biot theory), which describes the mechanical behaviour of fluidsaturated porous media. He also made a number of important contributions in areas of dynamics, irreversible thermodynamics and heat transfer, viscoelasticity and thermoelasticity, among others.

In 1941 Biot's generalization of the consolidation was published (Biot, 1941). The following basic properties of the soil were assumed :

- isotropy of the material,
- reversibility of stress-strain relations under final equilibrium conditions,
- linearity of the stress-strain relations,
- small strains,
- the water contained in the pores is incompressible,
- the water may contain air bubbles,
- the water flows through the porous skeleton according to Darcy's law.

He formulated equations governing consolidation for three dimensional case as follows:

$$G\nabla^2 u + \frac{G}{1-2\nu}\frac{\partial \varepsilon}{\partial x} - \alpha\frac{\partial \sigma}{\partial x} = 0 \tag{2.9}$$

$$G\nabla^2 v + \frac{G}{1-2\nu}\frac{\partial \varepsilon}{\partial y} - \alpha\frac{\partial \sigma}{\partial y} = 0 \tag{2.10}$$

$$G\nabla^2 w + \frac{G}{1-2\nu}\frac{\partial \varepsilon}{\partial z} - \alpha\frac{\partial \sigma}{\partial z} = 0 \tag{2.11}$$

$$\nabla^2 = \frac{\partial^2}{\partial x^2} + \frac{\partial^2}{\partial y^2} + \frac{\partial^2}{\partial z^2} \tag{2.12}$$

where

ε – the volume increase of the soil per unit initial volume

$G = \frac{E}{2(1+\nu)}$ – the shear modulus

$$\alpha = \frac{2(1+\nu)G}{3(1-2\nu)H}$$

The above constants E, ν, G are known by majority, these are Young's modulus, Poisson ratio and the shear modulus. There is one new constant *1/H* which is a measure of the compressibility of the soil for a change in water pressure also used later on in this chapter. The constant α measures the ratio of the water volume squeezed out to the volume change of the soil if the latter is compressed while allowing the water to escape ($\sigma = 0$).

There are three equations in (2.9), (2.10), (2.11) with four unknowns *u*, *v*, *w*, σ . In order to have a complete system we need one more equation. This is done by introducing Darcy's law governing the flow of water in a porous medium. We consider an elementary cube of soil and call V_x the volume of water flowing per second and unit area through the face of this cube perpendicular to the x axis. In the same way we define V_y, V_z . According to the Darcy's law these three components of the rate of flow are related to the water pressure by the relations :

$$\begin{aligned} v_x &= -k\frac{\partial \sigma}{\partial x} \\ v_y &= -k\frac{\partial \sigma}{\partial y} \\ v_z &= -k\frac{\partial \sigma}{\partial z} \end{aligned} \tag{2.13}$$

The physical constant k is called the coefficient of permeability of the soil. On the other hand, if we assume the water to be incompressible the rate of water content of an element of soil must be equal to the volume of water entering per second through the surface of the element, hence

$$\frac{\partial \theta}{\partial t} = -\frac{\partial v_x}{\partial x} - \frac{\partial v_y}{\partial y} - \frac{\partial v_z}{\partial z} \tag{2.14}$$

Combining all equations from (2.9) to (2.12) we obtain :

$$k\nabla^2\sigma = \alpha\frac{\partial \varepsilon}{\partial t} + \frac{1}{Q}\frac{\partial \sigma}{\partial t} \tag{2.15}$$

where σ is water pressure increment and Q is a physical constant, which is a measure of the amount of water which can be forced into the soil under pressure while the volume of the soil is kept constant. $\frac{1}{Q}$ is defined as :

$$\frac{1}{Q} = \frac{1}{R} - \frac{\alpha}{H} \tag{2.16}$$

where the coefficient $\frac{1}{H}$ is a measure of the compressibility of the soil for a change in water pressure , while $\frac{1}{R}$ measures the change in water content for a given change in water pressure. The two elastic constants and the constants *H* and *R* are the four distinct constants which under our assumption define completely the physical proportions of an isotropic soil in the equilibrium conditions. Other constants, like before mentioned α, have been derived from these four.

M.A. Biot used the above equation in his further works. His next article examines the consolidation settlement under a rectangular load distribution (Biot, 1940). In the calculation of foundations and the prediction of settlement we are not so much interested in the absolute value of the settlement but rather in the differences in settlement which can occur in loaded area due to differences in load intensity. Then differential settlements are direct cause of damage in buildings and structures carried by the soil. Biot tries to answer three questions in this article. First question is what happens at the edge of the loaded area – how much additional settlement is due to the water flowing from the loaded region to the unloaded region. Then he tries to explain how much restrain does the settlement of the loaded area encounter from the unloaded region. Finally he gives a quantitative answer to how much settlement does the unloaded area undergo in the vicinity of the load. In the article (Biot, 1940) he considers an infinitely deep layer of a completely saturated clay with rectangular load distribution as shown in figure below. The uniform load is suddenly applied at the instant *t=0* at the surface of the clay on the strip infinitely long in the *y* direction as in Fig. 2.2b. The water is assumed to escape freely at the surface so that the water pressure at the top is equal to atmospheric pressure. This a two-dimensional problem, where *v=0.*

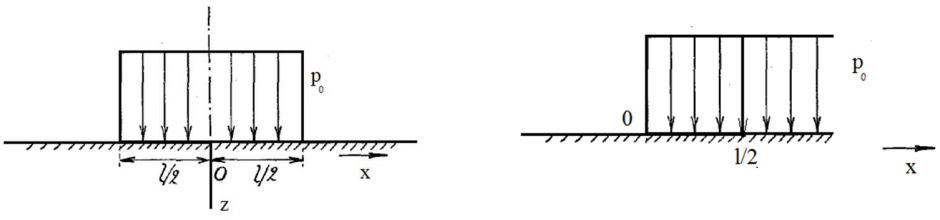

Fig. 2.2: Load distributions; on the left from x=-l/2 to x=l/2; on the right from x equal to zero to infinity

Starting from the below equations (writing symbolically $\frac{\partial}{\partial t} = p$) :

$$G\nabla^2 u + \frac{G}{1-2\nu}\frac{\partial \varepsilon}{\partial x} - \frac{\partial \sigma}{\partial x} = 0$$
$$G\nabla^2 w + \frac{G}{1-2\nu}\frac{\partial \varepsilon}{\partial z} - \frac{\partial \sigma}{\partial z} = 0 \qquad (2.17)$$
$$\nabla^2 \varepsilon = \frac{p\varepsilon}{c}$$

where

$c = \frac{k}{a}$ - coefficient of consolidation,

$a = \frac{1-2\nu}{2G(1-\nu)}$ - final compressibility,

the settlement is found most conveniently by the operational method after defining the boundary conditions :

a) all the variables vanish at infinite depth $z = \infty$

b) $\sigma = 0$ at $z = 0$

c) $\sigma = 2G\left(\frac{\partial w}{\partial z} + \frac{\nu\varepsilon}{1-2\nu}\right) = A\sin\lambda x$ at $z = 0$

d) $\frac{\partial u}{\partial t} + \frac{\partial w}{\partial x} = 0$ at $z = 0$

We can find the whole derivation of the solution in article (Biot, 1940), here below we have the settlement w_s of the soil surface at various time intervals for a load extending from *x=0* to *x=∞* an in Fig. 2.2b, where *l* is characteristic length which can be chosen arbitrarily. Then settlement curves are plotted as a function of x in Fig. 2.3 at time intervals corresponding to $\frac{ct^{\frac{1}{2}}}{l} = \frac{1}{8}, \frac{2}{8}, \frac{3}{8}, \frac{4}{8}, \frac{5}{8}$ and compared directly with the settlements w_{si} which would have occurred after the same time intervals if the load extended from infinity to infinity. The slope of the soil deflection at the edge of the loaded area (*x=0*) is infinite, it constitutes , therefore, a singular point probably associated with infinite stress. However this infinite slope does not show up in the plotted curve because it is highly localized effect. The settlements w_s and w_{si} are equal at first for *x>0* due to the water flowing out at the surface directly under the load , then w_s becomes slightly larger and finally for large values of time w_s becames smaller and smaller compared to w_{si}.

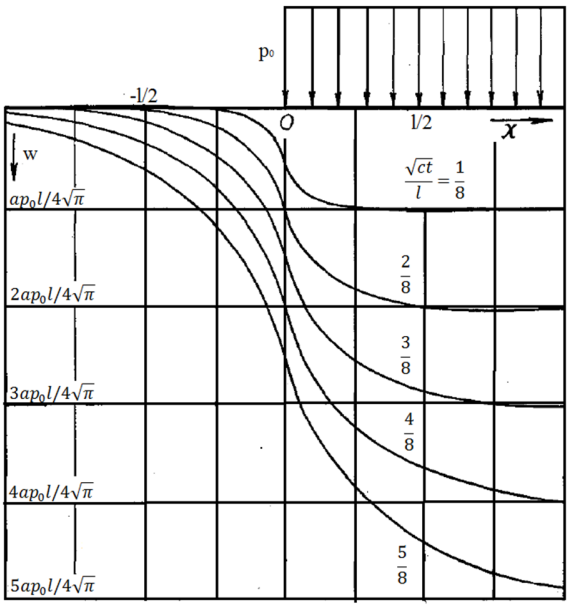

Fig. 2.3: Settlement of the soil surface at various time intervals

The same steps are taken for the second type of loading as in Fig. 2.2a. Below we also have the settlement graph, which we analyze similarly to the previous one. It can be noted that immediately after loading the settlement is little affected by the unloaded regions on both sides, while in the last phase the settlement is considerably reduced by the restraining effect of the unloaded regions.

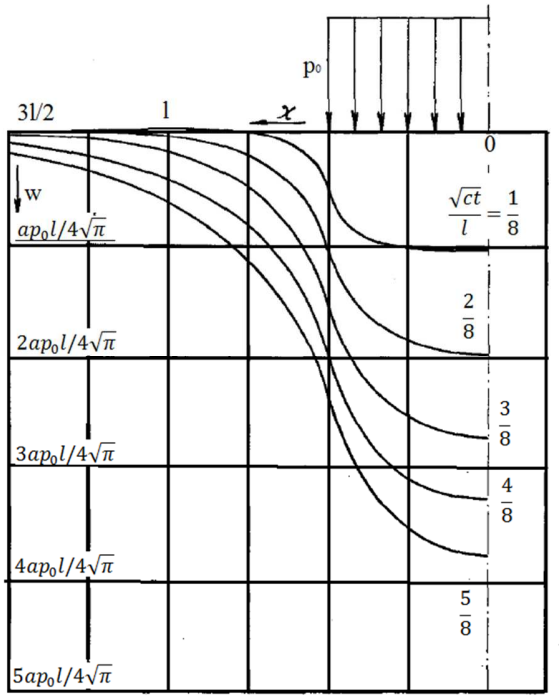

Fig. 2.4: Settlement of the soil surface at various time intervals for the load distribution represented in Fig. 2.2 a

Biot in his next publication together with his colleague (Biot & Clingan, 1941) investigates the problem when the top surface is completely impervious. It is clear that in this case the settlement is due to the fact, that the water contained in the soil flows from under the load to unloaded regions. Since it is assumed that the water cannot escape through the top surface . this will produce the swelling of the unloaded region in the vicinity of the load. Two dimensional consolidation for fully saturated clay with zero Poisson ratio is defined as :

$$G\nabla^2 u + G\frac{\partial \varepsilon}{\partial x} - \frac{\partial \sigma}{\partial x} = 0$$
$$G\nabla^2 w + G\frac{\partial \varepsilon}{\partial z} - \frac{\partial \sigma}{\partial z} = 0 \qquad (2.18)$$
$$\nabla^2 \varepsilon = \frac{p\varepsilon}{c}$$

The variables and symbols were defined when analyzing the equation (2.9). This time the boundary conditions are :

a) all the variables vanish at infinite depth $z = \infty$

b) $\frac{\partial \sigma}{\partial z} = 0$ at $z = 0$

c) $-\sigma + 2G\frac{\partial w}{\partial z} = -A\sin\lambda x$ at $z = 0$

d) $\frac{\partial u}{\partial t} + \frac{\partial w}{\partial x} = 0$ at $z = 0$

The second condition expresses that no water flows from the top surface. The last two conditions express that at the surface the normal stress is equal to the load and that the shearing stress is zero.

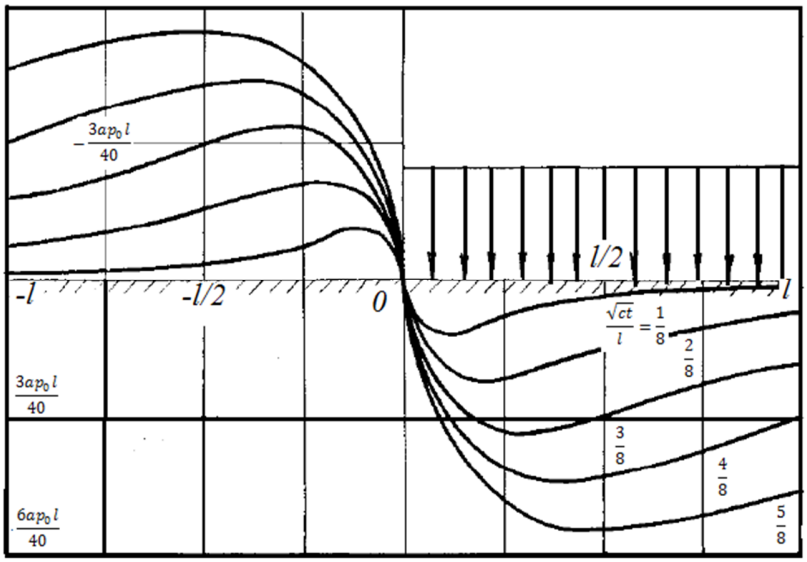

Fig. 2.5: Settlement of the soil surface at various time intervals for a uniform load extending from x=0 to x=∞

The settlement is composed of two parts : a purely elastic deflection which occurs at the instant of application of the load and a settlement due to consolidation which occurs gradually thereafter. In Fig. 2.5 we can see the settlements for the load shown in Fig. 2.2b. There is a considerable swelling of the unloaded area. For the load distribution presented in Fig. 2.2a the swelling is lower but for large values of time, the settlements are larger.

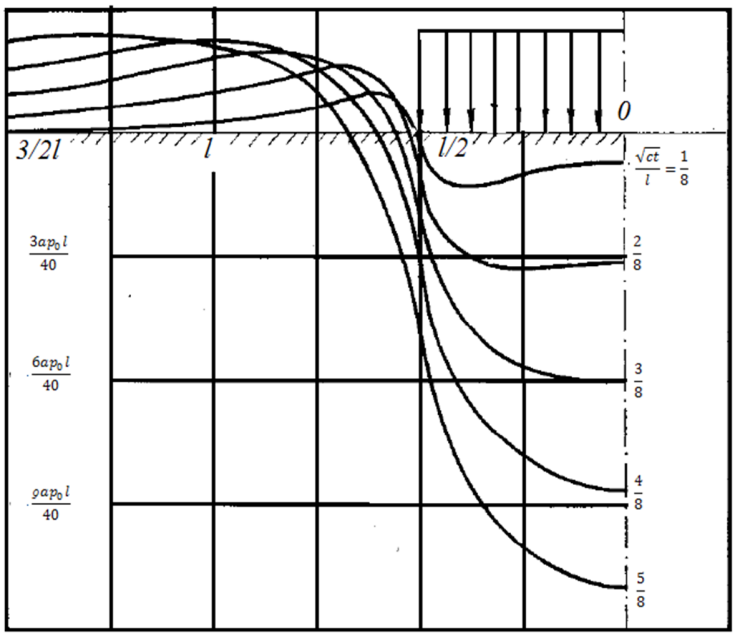

Fig. 2.6: Settlement of soil surface at various instants of time for a uniform load p_0 extending from x=-l/2 to x=l/2

M.A. Biot in 1955 extended the theory in the previous articles to the most general case of anisotropy (Biot, 1955). The method by which the theory is derived is also more general and direct. The same physical assumption is introduced , that the skeleton is purely elastic and contains a compressible viscous fluid. The theory in this article can therefore also be considered as a generalization of the theory of elasticity to porous materials. The author concentrates mostly on the case of transverse isotropy, which can be applied not only to soils but also to natural rock formations, since transverse isotropy is the type of symmetry usually acquired by rock under the influence of gravity.

In 1956 Biot's main field of interest was soil dynamics. He wrote an article which consisted of two parts, which are the basics for the thesis. In the first part (Biot, 1956) a theory is developed for the propagation of stress waves in a porous elastic solid containing a compressible viscous fluid and is restricted to the lower frequency range where the assumption of Poiseuille flow is valid. The extension to the higher frequencies are treated in the second part (Biot, 1956). The emphasis of these papers is on materials where fluid and solid are of comparable densities. The detailed information on the articles would be given in Chapter 3 and 4, where the current state of theory of soil dynamics will be presented.

2.3. The Modern Era.

Several papers on porous solids filled with fluids were published in the time period between 1960 and 1980 using the mixture theory without the volume fraction concept, so called modern continuum mechanics. Lots of scientists tried to formulate principles that help to formulate physical principles of balance and that close the dilemma about the validity of many of the approaches that had been used in the past. The new theory, known as multi-polar continuum mechanics, is based on some concepts developed by Truesdell an Toupin, who introduced generalized forces, body and surface forces and generalized stresses. Many other researchers tried to find the better understanding of the behavior of mixtures.

It seems that Morland (1972) was the first scientist to use the volume fraction concept in connection with modern mixture theories to describe the behavior of porous media as a "immiscible mixture". He constructed "a simple constitutive theory for a fluid-saturated porous solid" for the purely mechanical state. Before introducing the volume fraction concept, Morland considered the kinematics of the individual constituents, and formulated the state of stress and the balance of momentum for the individual constituents in the usual way. At the beginning Morland expressed the

partial density and the partial stress tensor of the constituent by the volume and surface fractions, and by the real densities and the real stress tensors, which were denoted by “effective”. It should be mentioned that while the decomposition of the partial density can be physically founded, there is, however, no physical foundation for the decomposition of the partial stress tensor. Then, Morland discussed the deformation state and decomposed the partial deformation gradient into a spherical part and a partial density preserving part F_a^*

$$F_\alpha = J_\alpha^{\frac{1}{3}} F_\alpha^{\ *} = \frac{\rho_0^{\alpha\,\frac{1}{3}}}{p^\alpha} F_\alpha^{\ *} \tag{2.19}$$

where ρ_0^α is the density in the reference configuration and J_α the determinant of F_α. The effective real deformation was then defined by

$$F_{\alpha R} = J_{\alpha R}^{\frac{1}{3}} F_\alpha^{\ *} \tag{2.20}$$

where

$$J_{\alpha R} = \frac{n^\alpha}{n_0^{\ \alpha}} J_\alpha \tag{2.21}$$

and where $n_0^{\ \alpha}$ denotes the volume fractions in the reference configuration. Morland also assumed a constitutive equation for $T^{\alpha R}$ which he defined as a functional depending on the effective deformation gradient

$$T^\alpha = m^\alpha F^\alpha \left[\frac{n^{\alpha\ 1/3}}{n_0^{\ \alpha}} F_\alpha \right] \tag{2.22}$$

and he proposed the following constitutive relation :

$$T^\alpha = -\rho^F \left[\frac{(n^F)^2}{n_0^{\ \alpha}} J_F \right] I \tag{2.23}$$

where the equivalence of the surface and volume fractions has been assumed.

We can find more information on constitutive relations, effective stresses in solid from that period in Morland’s excellent paper (Morland, 1972). Morland’s further treatment of the fluid-saturated porous solid was directed towards the geometrically-linear theory and toward a special

problem in the finite theory. Furthermore the elastic-plastic state of the porous solid was investigated, and a saturated, porous tuff model was treated.

Drumheller (1978) presented a theoretical treatment of porous solid using a mixture theory in which the volume fraction concept was introduced. The key point in his derivation was in the formulation of pore collapse relation to express the rate of change of the volume fraction. Bowen (1982) summarized all findings of the mixture theory and introduced the volume fractions concept for the saturated condition. The book from 2006 (Voyiadjis & Song, 2006) gives the profound information on the theory of porous media in the Modern Era.

The work of Biot also received great attention and was extensively used. The literature is replete with publications pertaining to the analytical solution of the general governing equations of motion for two-phase media based on the work of Biot. Deresiewicz (1960, 1962) solved Biot's governing equations of motion for an elastic half-space under harmonic time variations using displacement potentials. Derski used velocity terms to express the relative motion of different phases. Burridge and Vargas (1979) obtained the time domain fundamental solution (Green's function) for an infinite space. They also studied the disturbance in a poro-elastic infinite space due to application of an instantaneous point body force. Simon et al. (1984) presented an analytical one-dimensional solution for the transient response of an infinite domain by using Laplace transformations. Gazetas and Petrakis (1981) evaluated the compliance of a poroelastic half-space for swaying and rocking motions of an infinitely long, rigid and pervious strip that permitted complete drainage at the contact surface. Finally, Halpern and Christiano (1986) evaluated the compliances of three-dimensional square footings considering pervious as well as impervious cases.

For the numerical treatment of initial and boundary-value problems, quite different models have been used. These range from improved classical models proposed by Biot (Biot, 1955) (Biot, 1956) to such models which are based on the mixture theory restricted by the volume fraction concept. In this connection, one can read the extended paper by Zienkiewicz (Zienkiewicz, et al., 1990) which contains an improved Biot model as well as the treatise by Schrefler in which a model based on the mixture theory is treated.

Due to colossal devastation caused by earthquakes the scientists were forced to concentrate on dynamic problems as well. Prior to 1975, dynamic analysis were based on total stresses because of the deficiency in practical models that could predict pore water pressure. A widely used method was the Equivalent Linear Method ELM, which provided an approximate solution based on elastic soil stiffness and damping that are compatible with induced strains in the soil. In this method results

from laboratory tests relate the damping ratio and the shear modulus to cyclic shear strain levels. A linear solution is based on initial values of the shear modulus and the damping ratio. From the time variation of the shear strain , an equivalent strain magnitude is estimated and used to obtain new values of the shear modulus and the damping ratio. A new solution is calculated , and the procedure is repeated until convergence is achieved. The method became popular after Seed and co-workers and was implemented in computer applications as SHAKE (1972), QUAD (1983) and FLUSH (1975). However none of these models could predict either the increase of pore water pressure or its effect in the effective stresses. More information on this method can be found in (Yoshida, et al., 2002).

As the modern computational science developed and the rigorous numerical techniques such as finite element method became more and more popular, Biot's equations and mixtures theories found wide applications. A variational formulation of the dynamics of fluid-saturated porous solids was the basis of a numerical method that Ghaboussi and Dikman (1978) developed for the purpose of discretizing a partial media into finite elements. Shandu and Wilson (1969) first applied the finite element method to study fluid flow on saturated porous media. With the introduction of the FEM as a sound numerical technique, it became possible to extend the mixture theory to encompass elasto-plastic non-linear constitutive models and obtain reliable solutions of the field displacements and pressures. Prevost (1980) presented the general analytical procedure for non-linear effects in which he focused on the integration of the discretized field equations based on the mixture theories of Green and Naghdi. Later, he worked on several numerical applications to study the consolidation of inelastic porous media and on the non-linear transient phenomena and wave propagation effects in saturated porous media. Because of the increasing necessity of non-linear applications, Zienkiewicz and Shiomi (Zienkiewicz & Shiomi, 1984) classified different methods of analysis in a comprehensive paper on numerical solutions of the Biot formulation. These numerical solutions were further studied and used in several numerical applications related to the undrained, consolidating, and dynamic behaviour of saturated soils. A continuum theory for saturated porous media that is applicable for soils exhibiting large strains was formulated later by Kiousis and Voyiadjis using a Lagrangian reference frame.

I tried in this chapter to give an overview of the theories applied to soil mechanics during the longh time period. In the thesis I would develop the Biot's and Zienkiewicz's approach , the classical approach.

3. Theory of elastic waves in half space.

3.1. Single phase media.

3.1.1. Basic wave equations.

Propagation of elastic waves problem in a half-space soil due to dynamic loads is considered. The load can be placed on the soil surface (e.g. a passing car, train), can be caused by mechanical device resting on the foundation (e.g. harmonic excitation by electric turbine, impact loads by hammer,…) or can be derived from load inside half-space (e.g. traffic in a tunnel). Load causing a wave phenomenon can be periodic or aperiodic (Verruijt, 2010).

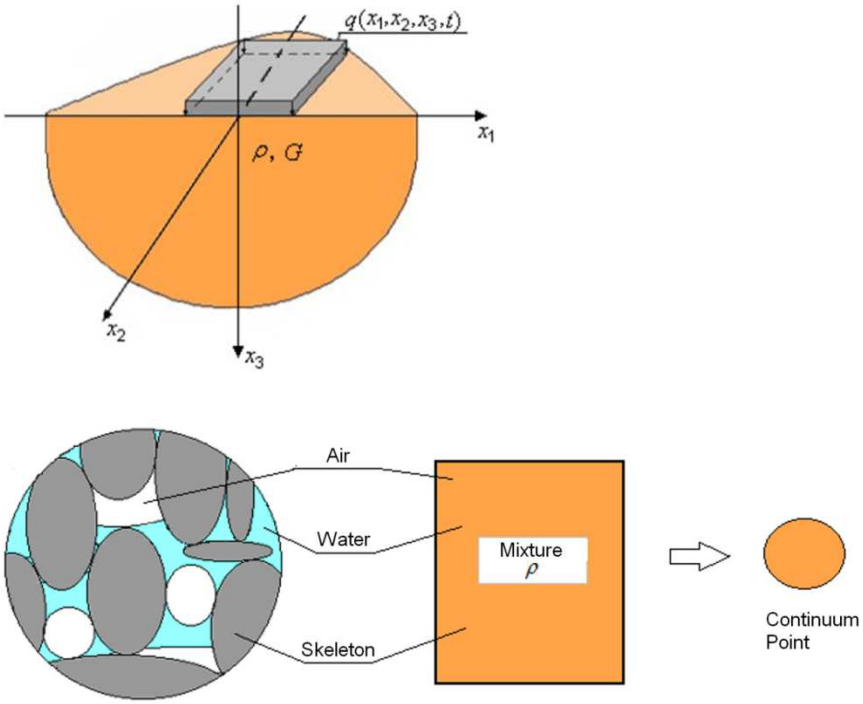

Fig. 3.1: Elastic half-space and continuum point of single-phase model (Wrana, 2016)

The basic equations of the dynamics problem in single-phase soil model are a set of the Navier equations which include inertia forces. In the Cartesian coordinate system, the equations are:

$$(\lambda + G)\frac{\partial}{\partial x_1}\left(\frac{\partial u_1}{\partial x_1} + \frac{\partial u_2}{\partial x_2} + \frac{\partial u_3}{\partial x_3}\right) + G\left(\frac{\partial^2 u_1}{\partial x_1^2} + \frac{\partial^2 u_1}{\partial x_2^2} + \frac{\partial^2 u_1}{\partial x_3^2}\right) + b_1 = \rho\frac{\partial^2 u_1}{\partial t^2} \qquad (3.1)$$

$$(\lambda+G)\frac{\partial}{\partial x_2}\left(\frac{\partial u_1}{\partial x_1}+\frac{\partial u_2}{\partial x_2}+\frac{\partial u_3}{\partial x_3}\right)+G\left(\frac{\partial^2 u_2}{\partial x_1^2}+\frac{\partial^2 u_2}{\partial x_2^2}+\frac{\partial^2 u_2}{\partial x_3^2}\right)+b_2=\rho\frac{\partial^2 u_2}{\partial t^2} \tag{3.2}$$

$$(\lambda+G)\frac{\partial}{\partial x_3}\left(\frac{\partial u_1}{\partial x_1}+\frac{\partial u_2}{\partial x_2}+\frac{\partial u_3}{\partial x_3}\right)+G\left(\frac{\partial^2 u_3}{\partial x_1^2}+\frac{\partial^2 u_3}{\partial x_2^2}+\frac{\partial^2 u_3}{\partial x_3^2}\right)+b_3=\rho\frac{\partial^2 u_3}{\partial t^2} \tag{3.3}$$

or $$(\lambda+G)\frac{\partial}{\partial x_1}\nabla\mathbf{u}+G\nabla^2 u_1+b_1=\rho\frac{\partial^2 u_1}{\partial t^2} \tag{3.4}$$

$$(\lambda+G)\frac{\partial}{\partial x_2}\nabla\mathbf{u}+G\nabla^2 u_2+b_2=\rho\frac{\partial^2 u_2}{\partial t^2} \tag{3.5}$$

$$(\lambda+G)\frac{\partial}{\partial x_3}\nabla\mathbf{u}+G\nabla^2 u_3+b_3=\rho\frac{\partial^2 u_3}{\partial t^2} \tag{3.6}$$

where:

ρ – volume density of soil

b_1, b_2, b_3 – components of mass force in the direction x_1, x_2, x_3.

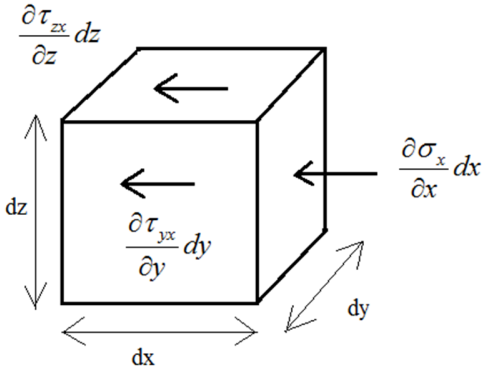

Fig. 3.2: Stresses acting on an element during wave propagation. The perturbation travels in *x* direction

3.1.2. Dilatational waves.

In consideration of wave propagation it is assumed that $b_1 = b_2 = b_3 = 0$, so that equations (3.1),(3.2) and (3.3) reduces to the homogeneous differential equations:

$$(\lambda + G)\frac{\partial}{\partial x_1}\varepsilon_v + G\nabla^2 u_1 = \rho\frac{\partial^2 u_1}{\partial t^2} \tag{3.7}$$

$$(\lambda + G)\frac{\partial}{\partial x_2}\varepsilon_v + G\nabla^2 u_2 = \rho\frac{\partial^2 u_2}{\partial t^2} \tag{3.8}$$

$$(\lambda + G)\frac{\partial}{\partial x_3}\varepsilon_v + G\nabla^2 u_3 = \rho\frac{\partial^2 u_3}{\partial t^2} \tag{3.9}$$

Differentiating the above equations: (3.7) with respect to x_1, (3.8) with respect to x_2, (3.9) with respect to x_3 obtained:

$$\lambda\frac{\partial^2}{\partial x_1^2}\left(\frac{\partial u_1}{\partial x_1} + \frac{\partial u_2}{\partial x_2} + \frac{\partial u_3}{\partial x_3}\right) + G\frac{\partial^2}{\partial x_1^2}\left(\frac{\partial u_1}{\partial x_1} + \frac{\partial u_2}{\partial x_2} + \frac{\partial u_3}{\partial x_3}\right) +$$

$$+G\frac{\partial}{\partial x_1}\left(\frac{\partial^2 u_1}{\partial x_1^2} + \frac{\partial^2 u_1}{\partial x_2^2} + \frac{\partial^2 u_1}{\partial x_3^2}\right) = \rho\frac{\partial}{\partial x_1}\frac{\partial^2 u_1}{\partial t^2} \tag{3.10}$$

$$\lambda\frac{\partial^2}{\partial x_2^2}\left(\frac{\partial u_1}{\partial x_1} + \frac{\partial u_2}{\partial x_2} + \frac{\partial u_3}{\partial x_3}\right) + G\frac{\partial^2}{\partial x_2^2}\left(\frac{\partial u_1}{\partial x_1} + \frac{\partial u_2}{\partial x_2} + \frac{\partial u_3}{\partial x_3}\right) +$$

$$+G\frac{\partial}{\partial x_2}\left(\frac{\partial^2 u_2}{\partial x_1^2} + \frac{\partial^2 u_2}{\partial x_2^2} + \frac{\partial^2 u_2}{\partial x_3^2}\right) = \rho\frac{\partial}{\partial x_2}\frac{\partial^2 u_2}{\partial t^2} \tag{3.11}$$

$$\lambda\frac{\partial^2}{\partial x_3^2}\left(\frac{\partial u_1}{\partial x_1} + \frac{\partial u_2}{\partial x_2} + \frac{\partial u_3}{\partial x_3}\right) + G\frac{\partial^2}{\partial x_3^2}\left(\frac{\partial u_1}{\partial x_1} + \frac{\partial u_2}{\partial x_2} + \frac{\partial u_3}{\partial x_3}\right) +$$

$$+G\frac{\partial}{\partial x_3}\left(\frac{\partial^2 u_3}{\partial x_1^2} + \frac{\partial^2 u_3}{\partial x_2^2} + \frac{\partial^2 u_3}{\partial x_3^2}\right) = \rho\frac{\partial}{\partial x_3}\frac{\partial^2 u_3}{\partial t^2} \tag{3.12}$$

Summing above equations (3.10),(3.11) and (3.12) we obtained:

$$(\lambda + 2G)\frac{\partial^2}{\partial x_1^2}\left(\frac{\partial u_1}{\partial x_1} + \frac{\partial u_2}{\partial x_2} + \frac{\partial u_3}{\partial x_3}\right) + (\lambda + 2G)\frac{\partial^2}{\partial x_2^2}\left(\frac{\partial u_1}{\partial x_1} + \frac{\partial u_2}{\partial x_2} + \frac{\partial u_3}{\partial x_3}\right) +$$

$$+(\lambda+2G)\frac{\partial^2}{\partial x_3^2}\left(\frac{\partial u_1}{\partial x_1}+\frac{\partial u_2}{\partial x_2}+\frac{\partial u_3}{\partial x_3}\right)=\rho\frac{\partial^2}{\partial t^2}\left(\frac{\partial u_1}{\partial x_1}+\frac{\partial u_2}{\partial x_2}+\frac{\partial u_3}{\partial x_3}\right) \tag{3.13}$$

or
$$\frac{(\lambda+2G)}{\rho}\left(\frac{\partial^2}{\partial x_1^2}\varepsilon_v+\frac{\partial^2}{\partial x_2^2}\varepsilon_v+\frac{\partial^2}{\partial x_3^2}\varepsilon_v\right)-\frac{\partial^2}{\partial t^2}\varepsilon_v=0 \tag{3.14}$$

or
$$\frac{(\lambda+2G)}{\rho}\nabla^2\varepsilon_v-\frac{\partial^2}{\partial t^2}\varepsilon_v=0 \tag{3.15}$$

Equation (3.15) is a homogeneous differential equation that describes the eigen-vibrations of half-space soil as a homogeneous isotropic elastic area. The first part defines the elasticity of soil, and the second one determines the inertia of a soil area by the variable. The equation describes the propagation of the dilatational wave, the volumetric wave or the pressure wave (flat or spherical, depending on the space dimension), see Fig. 3.3. Constant in eq.(3.15) is:

$$V_L^2=\frac{(\lambda+2G)}{\rho}=\frac{M}{\rho}=\frac{E(1-\nu)}{(1+\nu)(1-2\nu)\rho} \tag{3.16}$$

which defines the speed of dilatational wave.

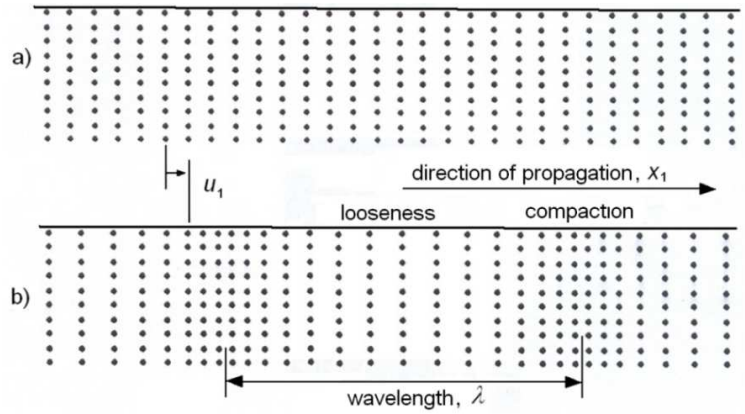

Fig. 3.3: The dilatational wave a) before the wave propagation; b) during the wave propagation (Santamarina, et al., 2001)

3.1.3. Shear waves.

Shear waves equations are obtained from eq. (3.7),(3.8) and (3.9) by reducing the dilatation part. Next differentiating it successively in respect to the variables: $x_1,\ x_2,\ x_3$.

The shear wave equation in the plane $x_2 - x_3$ obtained by differentiating eq.(3.8) with respect to x_3, eq.(3.9) with respect to x_2, and then adding the parties to give:

$$\frac{G}{\rho}\nabla^2\left(-\frac{\partial u_2}{\partial x_3}+\frac{\partial u_3}{\partial x_2}\right)-\frac{\partial^2}{\partial t^2}\left(-\frac{\partial u_2}{\partial x_3}+\frac{\partial u_3}{\partial x_2}\right)=0 \tag{3.17}$$

or

$$\frac{G}{\rho}\nabla^2\omega_1-\frac{\partial^2\omega_1}{\partial t^2}=0 \tag{3.18}$$

where $\omega_1=-\frac{\partial u_2}{\partial x_3}+\frac{\partial u_3}{\partial x_2}$ - rotation in the plane x_2-x_3. (3.19)

The shear wave equation in the plane x_1-x_3 obtained by differentiating equation (3.7) with respect to x_3, (3.9) with respect to x_1, and then adding the parties to give:

$$\frac{G}{\rho}\nabla^2\omega_2-\frac{\partial^2\omega_2}{\partial t^2}=0 \tag{3.20}$$

where $\omega_2=-\frac{\partial u_1}{\partial x_3}+\frac{\partial u_3}{\partial x_1}$ - rotation in the plane x_1-x_3. (3.21)

The shear wave equation in the plane x_1-x_2 obtained by differentiating equation (3.7) with respect to x_2, (3.8) with respect to x_1, and then adding the parties to give:

$$\frac{G}{\rho}\nabla^2\omega_3-\frac{\partial^2\omega_3}{\partial t^2}=0 \tag{3.22}$$

where $\omega_3=-\frac{\partial u_1}{\partial x_2}+\frac{\partial u_2}{\partial x_1}$ - rotation in the plane x_1-x_2. (3.23)

The shear wave equations (3.18), (3.20), (3.22) are homogeneous differential equations that describe the eigen-vibrations of half-space soil as a homogeneous isotropic elastic area. The first part defines the elasticity of soil, and the second one determines the rotation inertia of a soil area in the plane (x_2-x_3), (x_1-x_3) and(x_1-x_2). These are the equations of the dynamics of the variables $\omega_1, \omega_2, \omega_3$ and therefore describe the propagation of shear, rotating and distortion waves. In the equations (3.18), (3.20) and (3.22) is constant V_s - the shear wave velocity:

$$V_S=\sqrt{\frac{G}{\rho}}=\sqrt{\frac{E}{2(1+\nu)\rho}} \tag{3.24}$$

and the relation:

$$V_S = V_L \sqrt{\frac{1-2\nu}{2(1-\nu)}} \tag{3.25}$$

We can assume from the above equations the following :

- from eq.(3.25) it appears that, the dilatational waves velocity V_L is greater than the shear wave velocity V_S because $V_L = \sqrt{\frac{(\lambda+2G)}{\rho}} > V_S$.
- the dilatational wave is called the primary wave – P.
- the shear wave is called the distortion wave, the secondary wave – S (Fig. 3.4).

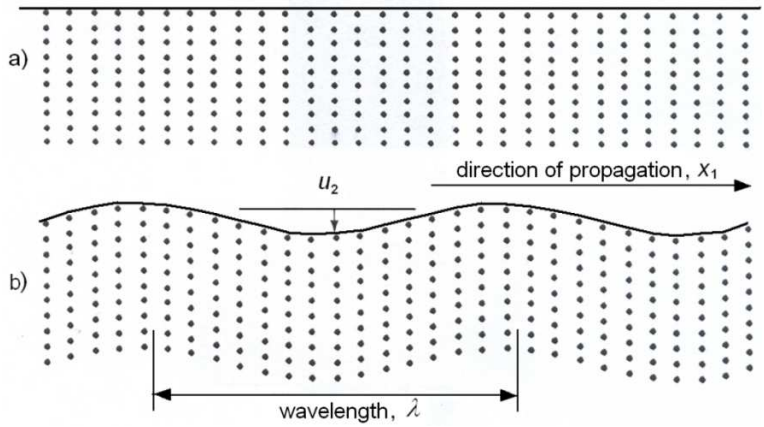

Fig. 3.4: The shear wave: a) before the wave propagation; b) during the wave propagation (Santamarina , et al., 2001)

3.1.4. Surface waves.

In addition to the dilatational and shear waves that propagate inside the half-space, there are also waves that propagate on the surface called surface waves. The thesis mainly concentrates on dilatational and shear waves. The surface waves are only discussed hereunder cursorily.

First type of a surface wave is a Rayleigh wave, which is a shear plane wave which propagates at a free surface of half-space and is strongly damped at depth. Rayleigh was the first to described this kind of wave in 1885, therefore the name of this wave comes from the name of the researcher, see Fig. 3.5. These waves occur during the earthquakes, explosions, etc., and play an

important role in seismic studies.

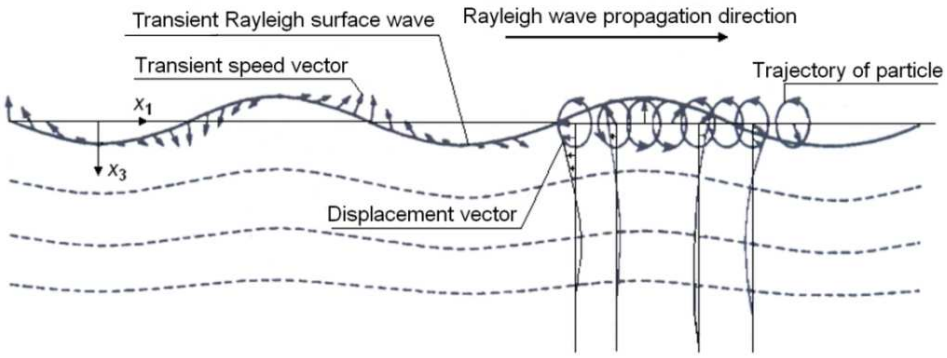

Fig. 3.5: Rayleigh wave (Fung, 1965)

Fig. 3.6 shows an example record of the horizontal component of the earthquake acceleration. The figure shows some typical time periods:

- The first time interval corresponds to the dilatational wave (P),
- The second time interval corresponds to the shear wave (S),
- The final, with large amplitudes, corresponds to the Rayleigh surface wave.

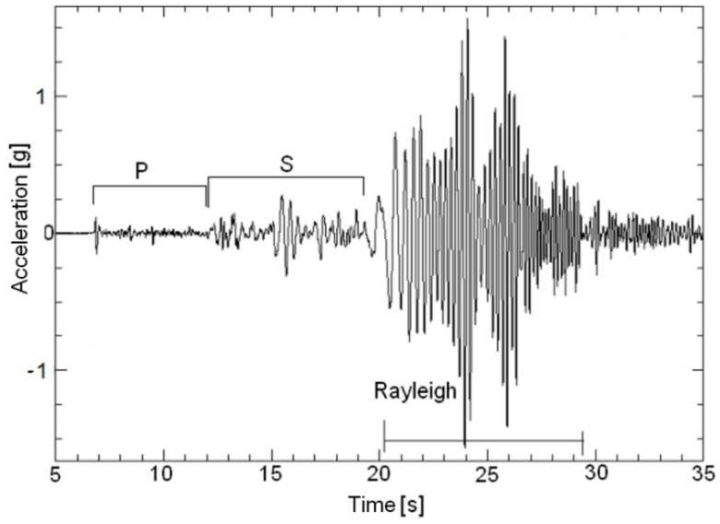

Fig. 3.6: Sample of acceleration during an earthquake (Wrana, 2016)

In the layered elastic half-space dilatational waves and shear waves refract and reflect on the layer surfaces. In the plane of the layer surface Love's surface wave also arises. Love's plane wave propagation is the plane perpendicular to the plane of Rayleigh surface wave propagation. The following is considered the simplest case of Love's wave, propagating in a weak layer with a stronger layer below (Fig. 3.7), the case was first considered by Love in 1911.

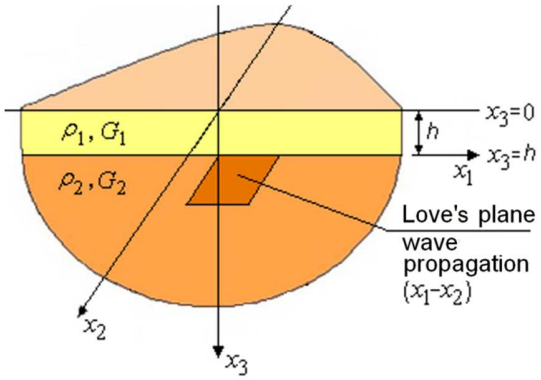

Fig. 3.7: Love's plane ($x_1 - x_2$) wave propagation on the layer surface $x_3 = h$

3.2. Two phase media- skeleton, fluid.

3.2.1. Introduction.

A soil mass consist of the solid particles and the voids in between them. These voids are filled with air or/and water. So there is a three phase system, but when the voids are only filled with air, or only filled with water then soil becomes a two phase system. When the voids are only filled with water, it is said to be saturated. A saturated porous medium is composed of a matrix and a porous space, the latter being filled by the fluid. The connected porous space is the space through which the fluid actually flows and whose two points can be joined by a path lying entirely within it so that the fluid phase remains continuous there. The matrix is composed of both a solid part and a possible occluded porosity, whether saturated or not, but through which no filtration occurs. The connected porosity is the ratio of the volume of the connected porous space to the total volume. In what follows the term "porosity", used without further specification, refers to the entire connected porosity.

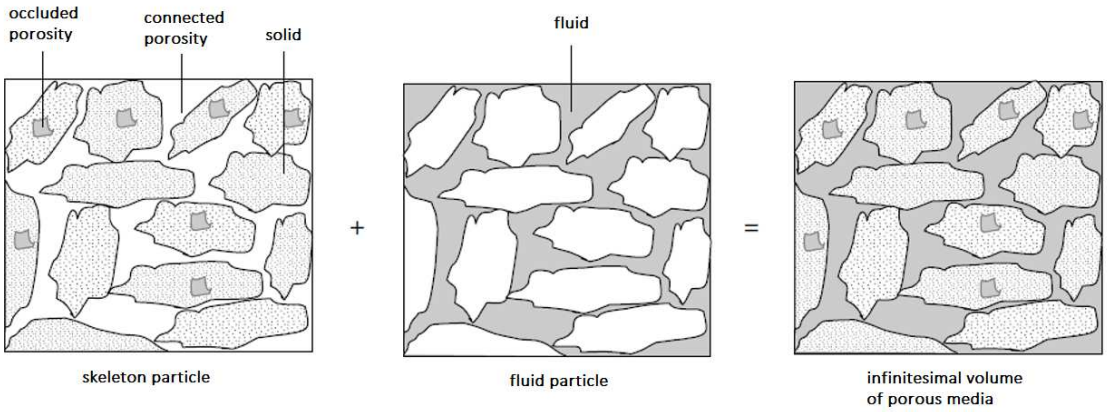

Fig. 3.8: The porous media as a superimposition of two continuous media: a skeleton particle and a fluid particle coincide with the same geometrical infinitesimal volume (Coussy, 2004)

A porous media can be treated as the superimposition of two continua, the skeleton continuum and the fluid continuum. Accordingly, as illustrated in Fig. 3.8, any infinitesimal volume can be treated as the superimposition of two material particles. The first is the skeleton particle formed from the matrix and the connected porous space emptied of fluid. The second is the fluid particle formed from the fluid saturating the connected porous space and from the remaining space without the matrix.

A continuous description of a medium, which is heterogeneous at the microscopic scale, requires the choice of a macroscopic scale at which the inner composition of matter is ignored in the analysis of the macroscopic physical phenomena. For instance, the porosity is associated with the elementary volume including sufficient material to be representative of the filtration process. More generally the hypothesis of continuity assumes the existence of a representative elementary volume which is relevant at the macroscopic scale for all the physical phenomena involved in the intended application. The physics is supposed to vary continuously from one to another of those juxtaposed infinitesimal volumes whose junction constitutes the porous medium. In addition, continuous deformation of the skeleton assumes that two skeleton particles, juxtaposed at a given time, were always so and will remain so.

In the following chapters all the calculations are done for fully saturated two-phase media which consists of solid skeleton and fully saturated pores as shown in Fig. 3.9. When subjected to external forces and no variations in pressure of the saturating fluid, the skeleton deforms. The description of this deformation differs in no way from that of a standard solid.

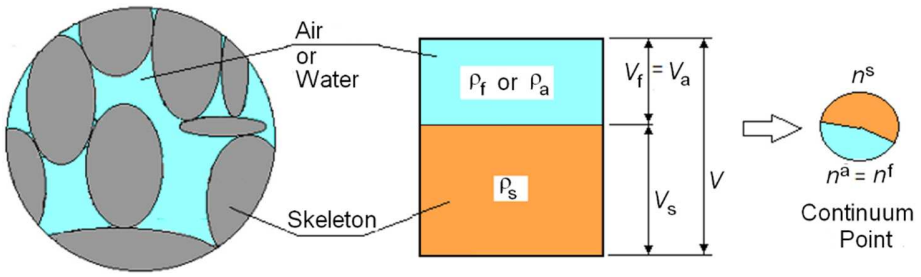

Fig. 3.9: Soil as a two-phase media, $n_s + n_f = 1$ (Wrana, 2016)

The behavior of the mixture of soil and water is affected by the deformation of the solid particles (skeleton), the relative motion (sliding) between particles and water, the deformation of pore water, and the movement of pore water through pores. A general formulation for such an interacting system is presented in this chapter, in which static case, consolidation and a variety of dynamic behavior can be obtained as special cases (Kubik, et al., 2000).

The wave propagation in saturated porous media as a soil skeleton fully saturated with fluid is described by Biot (Biot, 1956). Biot assumed that the motion of porous media on the micro level can be described by continuum mechanics of material. He used Lagrange postulate and Hamilton's principle to derive the equations of wave propagation.

The main assumptions of Biot theory, cursorily mentioned in Section 2.2, are as follows (presented in (Wrana, 2016)):

1. In the porous medium there is a relationship between the current and reference state. Displacement, velocity and deformations of particles are small. Constitutive equations, dissipation forces and inertia forces are linear. Thus, the strain energy, dissipation potential and kinetic energy is a square form of variables.
2. Principles of continuum mechanics can be applied to measure the macroscopic value. The size of averaged macroscopic elementary volume is based on microscopic structure.
3. The wavelength is large compared to the macroscopic dimensions of the elementary volume. This volume sufficiently and accurately determines properties, such as porosity, permeability and modulus of elasticity.
4. The isothermal state is under consideration.
5. The hydrostatic stress is assumed to fill the pores with viscous fluid.
6. The liquid phase is a continuum. The skeleton is a solid phase with discrete discontinuous areas.

The formulation of porous media dynamics is based on the kinetic energy equation, dissipation function and it leads to the equations of motion using Lagrange's postulate.

In the following equations in the introduced indications: "m" - refers to the skeleton, "s" - refers to the skeleton particles and "f" - refers to the liquid phase in the pores.

3.2.2. Kinetic energy.

In the Euler description the averaged macroscopic skeleton and the fluid velocity introduced:

$v_i^m = \frac{\partial u_i^m}{\partial t}$ or $\mathbf{v}^m = \frac{\partial}{\partial t}\mathbf{u}^m$ - macroscopic averaged velocity of skeleton,

$v_i^f = \frac{\partial u_i^f}{\partial t}$ or $\mathbf{v}^f = \frac{\partial}{\partial t}\mathbf{u}^f$ - macroscopic averaged velocity of fluid.

The kinetic energy of the particles at the microscopic level is:

$$T = \frac{1}{2}\int_{\Omega_s} \rho_s w_i^m \; w_i^m d\Omega + \frac{1}{2}\int_{\Omega_f} \rho_f w_i^f \; w_i^f d\Omega \tag{3.26}$$

where: w_i^m, w_i^f - skeleton and fluid velocity at microscopic level,

ρ_s - density of skeleton grains,

ρ_f - density of fluid in the pores,

$\Omega_s = (1-n)\Omega_b$, $\Omega_f = n\Omega_b$,

Ω_b - representative elementary macroscopic volume.

Isotropic material and averaged macroscopic velocity in volume Ω_b was assumed. The kinetic energy of the particles at the macroscopic level, similarly to form eq.(3.26) is (Biot, 1956):

$$T = \frac{1}{2}\Omega_b \left[\rho_{11} v_i^m \; v_i^m + 2\rho_{12} v_i^m \; v_i^f + \rho_{22} v_i^f \; v_i^f \right] \tag{3.27}$$

where:

ρ_{11} - density of skeleton at macro level,

ρ_{22} - density of fluid at macro level,

ρ_{12} - reciprocal density of skeleton and fluid at macro level.

The following considerations (below) are shown to determine the material constants ρ_{11} and ρ_{12} as a function of the skeleton and fluid parameters.

Assuming a constant fluid and skeleton density in a volume Ω_b , eq.(3.26), i.e. the kinetic energy of the particles at the microscopic level, can be written as:

$$T = \frac{1}{2}\rho_s \Omega_m \langle w_i^m w_i^m \rangle_s + \frac{1}{2}\rho_f \Omega_f \langle w_i^f w_i^f \rangle_f \tag{3.28}$$

where $\langle \circ \rangle$ means averaging in the representative volume.

Assuming balance of kinetic energy on the macroscopic and microscopic level, the density of mixture medium is received:

$$\rho = \rho_{11} v_i^m v_i^m + 2\rho_{12} v_i^m v_i^f + \rho_{22} v_i^f v_i^f = (1-n)\rho_s \langle w_i^m w_i^m \rangle_m + n\rho_f \langle w_i^f w_i^f \rangle_f \tag{3.29}$$

The momentum of the skeleton and the fluid is

$$\pi_i^s = \frac{\partial T}{\partial v_i^m} = \Omega_b \left(\rho_{11} v_i^m + \rho_{12} v_i^f \right) \tag{3.30}$$

$$\pi_i^f = \frac{\partial T}{\partial v_i^f} = \Omega_b \left(\rho_{22} v_i^f + \rho_{12} v_i^m \right) \tag{3.31}$$

If the relative velocity of the skeleton to the fluid is equal to zero, i.e. $v_i^s = v_i^f$ and the macroscopic velocity is equal to the microscopic velocity, then eq.(3.28) can be simplified:

$$\rho = (1-n)\rho_s + n\rho_f = \rho_{11} + 2\rho_{12} + \rho_{22} \tag{3.32}$$

The momentum of the skeleton and fluid at the microscopic level determined from the eq.(3.28) is:

$$\pi_i^m = \frac{\partial T}{\partial w_i^m} = \Omega_b (1-n)\, \rho_s w_i^m \tag{3.33}$$

$$\pi_i^f = \frac{\partial T}{\partial w_i^f} = \Omega_b n \rho_f \, w_i^f \tag{3.34}$$

Comparing equations (3.30),(3.31) with (3.33),(3.34) we obtain:

$$\rho_{11} + \rho_{12} = (1-n)\,\rho_s \tag{3.35}$$

$$\rho_{22} + \rho_{12} = n\,\rho_f \tag{3.36}$$

Substituting ρ_{11} and ρ_{22} to (3.28) we obtain the reciprocal density ρ_{12} (Nelson, 1988):

$$\rho_{12} = -\frac{(1-n)\rho_s \left[\langle w_i^m w_i^m \rangle_m - v_i^m v_i^m \right] + n\rho_f \left[\langle w_i^f w_i^f \rangle_f - v_i^f v_i^f \right]}{\left(v_i^f - v_i^m \right) \left(v_i^f - v_i^s \right)} \tag{3.37}$$

The reciprocal density is determined as the difference between the square of the average velocity of the particles at the micro level and the square of the velocity of the particles at the macro level with weights of skeleton and fluid mass.

Moreover, the reciprocal density can be determined on the basis of tortuosity as a measure of the difference velocity of fluid and skeleton at the micro and macro level.

$$\tau_s = \frac{\langle (w_i^m - v_i^f)\ (w_i^m - v_i^f) \rangle_m}{\left(v_i^f - v_i^m \right) \left(v_i^f - v_i^m \right)} \tag{3.38}$$

$$\tau = \frac{\langle (w_i^f - v_i^m)\ (w_i^f - v_i^m) \rangle_f}{\left(v_i^f - v_i^m \right) \left(v_i^f - v_i^m \right)} \tag{3.39}$$

$$\rho_{12} = -(1-n)\rho_s(\tau_s - 1) - n\rho_f(\tau - 1) \tag{3.40}$$

In the case of compatibility of the velocity at the microscopic and the macroscopic levels, with $\tau_s \approx 1$ we obtain

$$\rho_{12} = -n\rho_f(\tau - 1) \tag{3.41}$$

This case was considered by (Biot, 1956).

Assuming that $\frac{w_i^f}{v_i^f} = \frac{l}{L}$, where l is the distance between two points on the micro level, and L is the distance in a straight line (at the macro level), then the tortuosity defined in eq.(3.39) is:

$$\tau = \left(\frac{l}{L}\right)^2 \tag{3.42}$$

If ρ_{11} is be considered as a skeleton density moving in fluid, then we receive

$$\rho_{11} = (1-n)(\rho_s + r\rho_f) \tag{3.43}$$

where $r\ \rho_f$ is the density of fluid associated with the skeleton particles moving in the fluid. Using eq.(3.35), (3.41) and (3.43) the tortuosity can be defined as:

$$\tau = 1 + \left(\frac{1-n}{n}\right) r \tag{3.44}$$

Constant r =0.5 concerns the case of spherical grains moving in a fluid (Berryman, 1980).

3.2.3. Dilatational plane wave without damping.

Wave propagation is characterized as an example of dilatational plane wave, dilatation wave. In the isotropic medium dilatational wave can be separated from the shear one by acting of the divergence (div) or rotation (rot) operator on the differential equation of motion. In the case of an isotropic material, without loss of generality, a plane wave is considered. The equation below presents a generalized eigenproblem with two arrays **B** and **H**.

$$\mathbf{Be} = v_p^2\ \mathbf{He} \tag{3.45}$$

where

$$v_p = \frac{\omega}{k} \qquad \text{- phase velocity} \tag{3.46}$$

$$\mathbf{B} = \begin{bmatrix} K_B + \frac{4}{3}G_m & C \\ C & R \end{bmatrix},\ \mathbf{H} = \begin{bmatrix} \rho_{11} & \rho_{12} \\ \rho_{21} & \rho_{22} \end{bmatrix},\ \mathbf{e} = \begin{Bmatrix} e_1 \\ e_2 \end{Bmatrix} \tag{3.47}$$

G_m - shear modulus of the skeleton

$C = \dfrac{(1-n-K/K_s)nK_s}{1-n-K/K_s+nK_s/K_f}$ - constant in Biot notation

$R = \dfrac{n^2 K_s}{1-n-K/K_s+nK_s/K_f}$ - constant in Biot notation

$K_B = K+Q(\alpha-n)^2$, $\alpha = 1-\dfrac{K}{K_s}$ - coefficient of Biot effective stress , $\dfrac{1}{Q} = \dfrac{\alpha-n}{K_s}+\dfrac{n}{K_f}$, K - bulk modulus of skeleton in soil.

Equation (3.45) presents a generalized eigenproblem with two arrays **B** and **H**. From the solution of the eigenproblem (3.45) we obtained two eigenvalues v_{p1} and v_{p2} corresponding eigenvectors: $\mathbf{e}_1 = \begin{Bmatrix} e_{1,1} \\ e_{1,2} \end{Bmatrix}$ and $\mathbf{e}_2 = \begin{Bmatrix} e_{2,1} \\ e_{2,2} \end{Bmatrix}$ with corresponding to the two dilatational waves' velocity.

From the orthogonality condition of eigenvectors , *i,j*=1,2 taking into account the eq.(3.47) the equality is obtained

$$\left(K+\frac{4}{3}G_m\right)e_{1,1}e_{2,1} + C\left(e_{1,1}e_{2,2}+e_{1,2}e_{2,1}\right)+Re_{1,2}e_{2,2} = 0 \tag{3.48}$$

From the eq.(3.48) with the positive material constants *K, G_m, C, R* it appears that: if both components of the first eigenvector $\{e_{1,1}, e_{1,2}\}^{\mathrm{T}}$ are of the same sign, the components of the second vector $\{e_{2,1}, e_{2,2}\}^{\mathrm{T}}$ must have opposite signs. It means that in the dilatational wave propagation of saturated soil, the fluid and skeleton are in a phase, or fluid and skeleton are in an anti-phase.

Multiplying the left-side eq.(3.45) by $\mathbf{e}_1^T$ we receive $\mathbf{e}_1^T\mathbf{B}\mathbf{e}_1 = v_{p1}^2\mathbf{e}_1^T\mathbf{H}\mathbf{e}_1$, hence

$$v_{p1}^2 = \frac{(K+4G_m/3)e_{1,1}^2+2C\,e_{1,1}e_{1,2}+R\,e_{1,2}^2}{\rho_{11}e_{1,1}^2+2\rho_{12}e_{1,1}e_{1,2}+\rho_{22}e_{1,2}^2} \tag{3.49}$$

Similar operating may be performed with respect to a pair of v_{p2} , $\mathbf{e}_2$.

In equation (3.49) we take into account the property $\rho_{12} < 0$ according to (3.41). Analysis of the sign of the two eigenvector components $\mathbf{e}_1$ and $\mathbf{e}_2$ leads to the conclusion that:

- if one eigenvector has two components of the same sign, e.g. vector $\mathbf{e}_1$,

- then the second eigenvector has components of the opposite sign, e.g. vector $\mathbf{e}_2$ and in this case there is:

$$v_{p1}^2 > v_{p2}^2 \tag{3.50}$$

It follows that; the second wave velocity v_{p2} (skeleton and fluid in an anti-phase) is slower than the first velocity v_{p1} (skeleton and fluid in a phase). Biot proposed the following names of the waves: 1) the fast wave or wave of the first kind - waves traveling at a higher speed, and 2) the slow wave or waves of the second kind - waves traveling at a slower speed.

3.2.4. Shear waves without damping.

Equations of motion in the low frequency range for the fully saturated medium can be written as (Biot, 1956):

$$\frac{\partial \sigma_{ij}^m}{\partial x_j} = \rho_{11} \frac{\partial^2 u_i^m}{\partial t^2} + \rho_{12} \frac{\partial^2 u_i^f}{\partial t^2} + b \left(v_i^m - v_i^f \right) \tag{3.51}$$

$$-n \frac{\partial p_f}{\partial x_i} = \rho_{12} \frac{\partial^2 u_i^m}{\partial t^2} + \rho_{22} \frac{\partial^2 u_i^f}{\partial t^2} - b \left(v_i^m - v_i^f \right) \tag{3.52}$$

where here only *b* is a damping coefficient proportional to the velocity, viscous damping. (Coussy, 2004) on the basis of Darcy's law, proposed to adopt $b = n^2 \frac{\eta}{k}$, where: η is the coefficient of viscosity of the fluid, *k* is a coefficient of permeability.

Introducing $Y(t) = m \frac{d\delta(t)}{dt} + \frac{\eta}{k} \delta(t)$ (3.53)

and $m = \frac{\rho_{22}}{n^2} = \frac{\rho_f \tau}{n}$ (3.54)

we obtain:

$$-\frac{\partial p_f}{\partial x_i} = \rho_f \frac{\partial^2 u_i^m}{\partial t^2} + Y(t) \cdot \frac{\partial w_i}{\partial t} \tag{3.55}$$

In the above equations it is assumed that constant porosity does not depend on time.

Moreover, if we assume that the mass forces are equal to zero ($b = 0$) (Biot, 1956):

$$\frac{\partial \sigma_{ij}}{\partial x_j} = (\rho_{11} + \rho_{12}) \frac{\partial^2 u_i^m}{\partial t^2} + (\rho_{12} + \rho_{22}) \frac{\partial^2 u_i^f}{\partial t^2}$$

Assuming the relative displacement of skeleton to fluid:

$$w_i = n\,(u_i^f - u_i^m) \tag{3.56}$$

and taking into account the equations (3.35) and (3.36), equations of motion in the low frequency range can be written as:

$$\frac{\partial \sigma_{ij}}{\partial x_j} = \rho \frac{\partial^2 u_i^m}{\partial t^2} + \rho_f \frac{\partial^2 w_i}{\partial t^2} \tag{3.57}$$

The equations regarding the shear wave will be evaluated in two steps.

First step - the rotation operator applied to eq.(3.52) including (3.51):

$$\mathrm{rot}\left(\frac{\partial \sigma_{ij}^m}{\partial x_j} \right) = \mathrm{rot}\left[\rho \frac{\partial^2 u_i^m}{\partial t^2} - n\rho_f \left(\frac{\partial^2 u_i^m}{\partial t^2} - \frac{\partial^2 u_i^f}{\partial t^2} \right) \right] \tag{3.58}$$

or

$$\mathrm{rot}\left(\mathrm{div}\boldsymbol{\Sigma}\right) = \rho \frac{\partial^2}{\partial t^2}\left(\mathrm{rot}\mathbf{u}^m\right) - n\rho_f \left[\left(\frac{\partial^2}{\partial t^2}\left(\mathrm{rot}\mathbf{u}^m\right) - \frac{\partial^2}{\partial t^2}\left(\mathrm{rot}\mathbf{u}^f\right) \right) \right] \tag{3.59}$$

or entering a notation: $\boldsymbol{\Omega}^s = \mathrm{rot}\mathbf{u}^s$, $\boldsymbol{\Omega}^f = \mathrm{rot}\mathbf{u}^f$

$$\mathrm{rot}\left(\mathrm{div}\boldsymbol{\Sigma}\right) = \rho \frac{\partial^2 \boldsymbol{\Omega}^m}{\partial t^2} - n\rho_f \frac{\partial^2 \left(\boldsymbol{\Omega}^m - \boldsymbol{\Omega}^f \right)}{\partial t^2} \tag{3.60}$$

where $\boldsymbol{\Sigma} = \begin{bmatrix} \sigma_{11} & \sigma_{12} & \sigma_{13} \\ \sigma_{21} & \sigma_{22} & \sigma_{23} \\ \sigma_{31} & \sigma_{32} & \sigma_{33} \end{bmatrix}$ – Cauchy stress tensor.

From experiment of compression test of the mixture in drainage conditions (Biot & Willis, 1957) we have the following relation:

$$\boldsymbol{\sigma}^m = 2G\left(\boldsymbol{\varepsilon}^m - \frac{1}{3}\varepsilon_v^m \mathbf{m}\right) + K\,\varepsilon_v^m \mathbf{m} + C\,\varepsilon_v^f \mathbf{m} \tag{3.61}$$

the above coefficients K,C were already discussed in Section 3.2.3. The rest is defined as:
$\boldsymbol{\varepsilon} = \{\varepsilon_{11}, \varepsilon_{22}, \varepsilon_{33}, \varepsilon_{12}, \varepsilon_{13}, \varepsilon_{23}\}^{\mathrm{T}}$ – strain vector of skeleton in Voight's notation,

ε_v^m – volumetric strain of skeleton,

ε_v^f – volumetric strain of fluid,

$$s_{ij} = \varepsilon_{ij} - \frac{1}{3}\varepsilon_v \delta_{ij} \tag{3.62}$$

or $\mathbf{s} = \boldsymbol{\varepsilon} - \frac{1}{3}\varepsilon_v \mathbf{m}$ – strain deviator of skeleton and fluid mixture medium

where $\mathbf{m} = \{1, 1, 1, 0, 0, 0\}^{\mathrm{T}}$.

From the eq.(3.61) taking into account the eq.(3.62) we receive (Wrana, 2016):

$$\mathrm{div}\sigma_{ij}^m = 2G_m \mathrm{div}\varepsilon_{ij}^m + \left(K - \frac{2}{3}G_m\right)\mathrm{grad}\varepsilon_v^m + C\,\mathrm{grad}\varepsilon_v^f \,. \tag{3.63}$$

Applying rotation operator we receive

$$\mathrm{rot}\left(\frac{\partial\,\sigma_{ij}^m}{\partial\,x_j}\right) = 2G_m \mathrm{rot}\left(\frac{\partial\,\varepsilon_{ij}^m}{\partial\,x_j}\right) + \left(K - \frac{2}{3}G_m\right)\mathrm{rot\ grad}\varepsilon_v^m + C\ \mathrm{rot\ grad}\varepsilon_v^f \,. \tag{3.64}$$

Because $\mathrm{rot\,grad}\,\varepsilon_v^m = 0$ and $\mathrm{rot\,grad}\,\varepsilon_v^f = 0$, (3.58), taking into account the (3.63), we shall have the form

$$2G_m \mathrm{rot}\left(\frac{\partial\,\varepsilon_{ij}^m}{\partial\,x_j}\right) = \rho\ \mathrm{rot}\left(\frac{\partial^2 u_i^m}{\partial\,t^2}\right) - n\rho_f \mathrm{rot}\left(\frac{\partial^2 u_i^m}{\partial\,t^2} - \frac{\partial^2 u_i^f}{\partial\,t^2}\right) \tag{3.65}$$

True equality is:

$$2\mathrm{rot}\left(\frac{\partial \varepsilon_{ij}^{m}}{\partial x_j}\right)=2\mathrm{rot}\left[\frac{\partial}{\partial x_j}\left(\frac{\partial u_i^m}{\partial x_j}+\frac{\partial u_j^m}{\partial x_i}\right)\right]=\mathrm{rotgrad}\varepsilon_v^m+\frac{\partial^2 \mathrm{rot}u_i^m}{\partial x_j^2}=\frac{\partial^2 \mathrm{rot}u_i^m}{\partial x_j^2} \tag{3.66}$$

the eq.(3.65) can be written using the eq.(3.32):

$$G_m\frac{\partial^2 \boldsymbol{\Omega}^m}{\partial x_j^2}=(1-n)\rho_s\frac{\partial^2 \boldsymbol{\Omega}^m}{\partial t^2}+n\rho_f\frac{\partial^2 \boldsymbol{\Omega}^f}{\partial t^2}. \tag{3.67}$$

Second step - derivation of the eq.(3.55) used

$$0=\rho_f\frac{\partial^2 \boldsymbol{\Omega}^m}{\partial t^2}-nY(t)\cdot\frac{\partial \boldsymbol{\Omega}^m}{\partial t}+nY(t)\cdot\frac{\partial \boldsymbol{\Omega}^f}{\partial t}. \tag{3.68}$$

We consider, without loss of generality, a plane wave propagating in the direction of the axis x_1 polarized in the direction x_2. Adopted solution in the vectors has the form: $\boldsymbol{\Omega}^m=\{0,0,S^m\}^{\mathrm{T}}$, $\boldsymbol{\Omega}^f=\{0,0,S^f\}^{\mathrm{T}}$, with notation $S^m=\frac{\partial u_2^m}{\partial x_1}$, $S^f=\frac{\partial u_2^f}{\partial x_1}$

$$S^m=S_1\exp[i(\omega t-kx_1)] \tag{3.69}$$

$$S^f=S_2\exp[i(\omega t-kx_1)] \tag{3.70}$$

where k - complex wave number including the function of damping in the eq.(3.68).

Substituting the solution (3.69) and (3.70) to (3.67) and (3.68) we receive

$$\left[G_m-v_c^2(1-n)\rho_s\right]S_1-n\rho_f v_c^2 S_2=0 \tag{3.71}$$

$$-\left(\rho_f+\mathrm{i}\frac{1}{\omega}Y_0 n\right)S_1+\left(\mathrm{i}\frac{1}{\omega}Y_0 n\right)S_2=0 \tag{3.72}$$

where $v_c=\omega/k$ - complex shear wave speed. The solution is

$$v_c=\sqrt{\frac{G_m}{\rho-\mathrm{i}\omega\rho_f^2 Y_0^{-1}}}. \tag{3.73}$$

The phase velocity v_s is obtained dividing the angular frequency by the real part of the complex wave number:

$$v_{S\mp} = \frac{\omega}{\mathrm{Re}(k)} = \frac{1}{\mathrm{Re}\left(\frac{1}{v_{c_-^+}}\right)}. \tag{3.74}$$

The factor of wave decay is defined as the imaginary part of the complex wave number:

$$\alpha = I\,\mathrm{m}(k) = \omega \mathrm{Im}\left(\frac{1}{v_c}\right). \tag{3.75}$$

In the low frequency range, the amplitude defined by the formula (3.61c) can be written as $Y_0 = \mathrm{i}\omega\, m + \eta / \kappa$, which after substituting to (3.73) leads to the formula:

$$v_c = \sqrt{\frac{G_m}{\rho - \rho_f^2 \left[m - \mathrm{i}\eta/(\omega\kappa)\right]^{-1}}}. \tag{3.76}$$

In the case without damping ($\eta / \kappa = 0$), in (3.76) complex shear wave velocity is given by:

$$v_c = \sqrt{\frac{G_m}{\rho - \rho_f^2 / m}} = \sqrt{\frac{G_m}{\rho - n\rho_f / \tau}}. \tag{3.77}$$

Shear wave amplitudes obtained from the eq.(3.72) :

$$S_2 = \left(1 - \frac{\rho_f}{n\, m}\right) S_1 = \left(1 - \frac{1}{\tau}\right) S_1. \tag{3.78}$$

In the above equation expression in brackets is positive, because $\tau \geq 1$, thus the amplitude of the shear wave of skeleton and fluid are of the same sign. From the eq.(3.72) we receive $S_1 = S_2$, indicating no relative movement between the skeleton and the fluid in the propagation of shear waves. In the case of zero-frequency, , $\omega = 0 \rightarrow v_c = \sqrt{\frac{G_m}{\rho}}$.

Remark: Since $m \geq 0$, the shear wave without damping speed (3.77) is greater than the average speed $v_c = \sqrt{\frac{G_m}{\rho}}$.

3.2.5. Example.

The gravel as the water-saturated porous medium is considered. The material parameters of soil are: K_s=35 GPa; ρ_s=2,65 t/m3; K_m=1,7 GPa; G_m=1,855 GPa; n=0,3; κ=1 Darcy; τ=2; K_f=2,4 GPa; ρ_f=1,00 t/m3 and η=1 (Carcione, 1998). Substituting the data to the equation of the dilatational wave phase velocity and to the shear wave velocity , the results are in frequency-dependent range f [Hz]- Fig. 3.10.

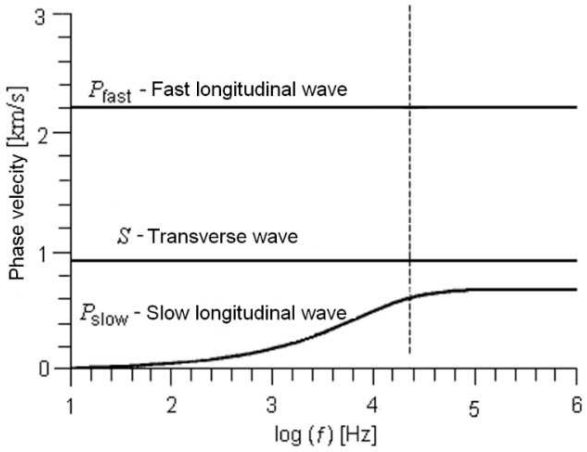

Fig. 3.10: Comparison of the phase velocity of dilatational and shear waves in the fully saturated gravel (Wrana, 2016)

3.3. Three phase media – skeleton, fluid and gas .

3.3.1. Introduction.

The most precise model of the soil is a three-phase model, taking into account- skeleton, water and air. The basic equations much differ, because there is an additional phase that needs to be taken into consideration. Consequently the constitutive equations, equations of motion and wave propagation changes, which have an impact on the final results. The picture below presents the outline of the three-phase media.

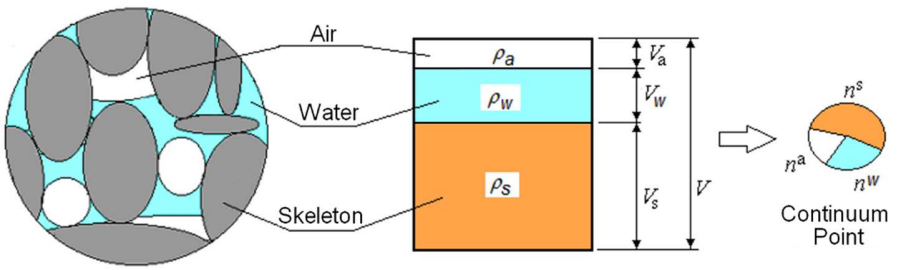

Fig. 3.11: Soil as a three-phase media

The first proposal to unsaturated soil description gave Bishop (Bishop, 1959), he extended the Terzaghi equation to three phase medium as:

$$\sigma'_m = \sigma_m - p_a + \bar{\chi}\,(p_a - p_w). \tag{3.79}$$

where:

σ'_m - effective average stress, σ_m - total average stress, $\bar{\chi}$ - function of saturation degree S, p_a- air pressure in pores, p_w– water pressure in pores.

Unsaturated soil is a soil consisting of three phases: skeleton, water and air. In the mixtures theory, such soil is a continuous medium, i.e. at the same point of medium there are three phases. In the consideration of wave propagation problem the following assumptions are used:

a) small deformation,
b) incompressible soil grains,
c) material of skeleton is isotropic and linearly elastic,
d) consider laminar flow of water and air in the pores in accordance with the law of Darcy.

The gravity forces, chemical changes and electric fields are omitted. It is also assumed that the soil mixture material is a homogeneous continuous medium in which there are no phenomena of reflection and refraction wave and phase changes.

3.3.2. Equation of motion.

The equation of wave propagation in porous soil medium consists with skeleton, water and air per unit volume of soil is considered. Having regarded the inertia forces of skeleton, water and air we obtained:

$$\mathrm{div}\boldsymbol{\sigma} = \rho_s(1-n)\ddot{\mathbf{u}}^s + \rho_w n^w \ddot{\mathbf{u}}^w + \rho_a n^a \ddot{\mathbf{u}}^a . \tag{3.80}$$

where

ρ_w – density of water

ρ_a – density of air

n^w – volumetric contents of water phase, $n^w = nS$

n^a – volumetric contents of air phase, $n^a = n(1-S)$

n^s – volumetric contents of skeleton phase $n^s + n^w + n^a = 1$

S – degree of saturation

Darcy's law of laminar flow through the soil is applied. In the case of anisotropic material and omitting gravitational force (Coussy, 2004) we can obtain:

$$n^w\left(\dot{\mathbf{u}}^w - \dot{\mathbf{u}}^s\right) = -\frac{k_w}{g\rho_w}\left(\mathrm{grad}p_w + \rho_w\ddot{\mathbf{u}}^w\right). \tag{3.81}$$

$$n^a\left(\dot{\mathbf{u}}^a - \dot{\mathbf{u}}^s\right) = -\frac{k_a}{g\rho_a}\left(\mathrm{grad}p_a + \rho_a\ddot{\mathbf{u}}^a\right). \tag{3.82}$$

where

p_w – water pressure in pores

p_a – air pressure in pores

k_w – permeability coefficient of water phase in the soil

k_a – permeability coefficient of air phase in the soil

g – acceleration due to gravity

It is necessary to introduce constitutive equations for the three-phase media in order to move forward with the equations of motion. They are defined as follows (Fredlung & Morgenstern, 1976):

$$\begin{bmatrix} d\varepsilon_v^s \\ dn^w \\ dn^a \end{bmatrix} = \begin{bmatrix} m_1^s & m_2^s \\ m_1^w & m_2^w \\ m_1^a & m_2^a \end{bmatrix} \begin{bmatrix} d\left(\sigma_m + p_a\right) \\ d\left(p_a - p_w\right) \end{bmatrix}. \tag{3.83}$$

m_1^s, m_2^s – coefficients of volumetric increment of skeleton representing the physical parameter

$$m_1^s = \frac{3(1-2v^s)}{2(1+v^s)G}$$

v^s – Poisson ratio of soil skeleton

Compatibility condition of volume three phases, i.e. $d\varepsilon_v^s = dn^w + dn^a$, leads to the equations:

$$m_1^{\ s} = m_1^{\ w} + m_1^{\ a} \tag{3.84}$$

$$m_2^s = m_2^w + m_2^a \,. \tag{3.85}$$

where

m_1^w , m_1^w – coefficient of volumetric increment of water

m_1^a , m_1^a – coefficients of volumetric increment of air

The total stress of three phase soil medium equation is based on the assumption on linear elasticity behavior of skeleton grains with including water and air pressure in the pores (Fredlund & Rahardjo, 1993), so:

$$\mathrm{d}\,\boldsymbol{\sigma} = \mathbf{D}\,\mathrm{d}\boldsymbol{\varepsilon} - \chi \mathrm{d}p_w \mathbf{m} - (1-\chi)\mathrm{d}p_a \mathbf{m} \tag{3.86}$$

where: χ- volume change coefficient defined as:

$$\chi = m_2^s / m_1^s \tag{3.87}$$

After the substitution (3.86) to (3.83) we have:

$$\mathrm{d}\boldsymbol{\varepsilon} = \mathbf{D}^{-1}\mathrm{d}\boldsymbol{\sigma} + \frac{\chi}{3K^s}\mathrm{d}p_w \mathbf{m} + \frac{1-\chi}{3K^s}\mathrm{d}p_a \mathbf{m} \tag{3.88}$$

$$\mathrm{d}n^w = \frac{\psi_w}{3K^s}\mathbf{m}^{\mathrm{T}}\mathrm{d}\boldsymbol{\sigma} + c_{ww}\mathrm{d}p_w + c_{wa}\mathrm{d}p_a \tag{3.89}$$

$$\mathrm{d}n^a = \frac{\psi_a}{3K^s}\mathbf{m}^{\mathrm{T}}\mathrm{d}\boldsymbol{\sigma} + c_{aw}\mathrm{d}p_w + c_{aa}\mathrm{d}p_a \tag{3.90}$$

where:

$$\mathbf{m} = \{1,1,1,0,0,0\}^T$$

$$\psi_w = \frac{m_1^w}{m_1^s} \tag{3.91}$$

$$\psi_a = \frac{m_1^a}{m_1^s} \tag{3.92}$$

$$c_{ww} = \frac{\chi\psi_w}{K^s} + \frac{m_1^s m_2^w - m_2^s m_1^w}{m_1^s} \tag{3.93}$$

$$c_{wa} = \frac{(1-\chi)\psi_w}{K^s} + \frac{m_1^s m_2^w - m_2^s m_1^w}{m_1^s} \tag{3.94}$$

$$c_{aw} = \frac{\chi \psi_a}{K^s} + \frac{m_1^s m_2^a - m_2^s m_1^a}{m_1^s} \tag{3.95}$$

$$c_{aa} = \frac{(1-\chi)\psi_a}{K^s} + \frac{m_1^s m_2^a - m_2^s m_1^a}{m_1^s}. \tag{3.96}$$

The effect of temperature and dissipation of energy are omitted. The complementary elastic energy (work of deformation on stress increments) can be submit, according to (Loret & Khalili, 2000) :

$$\mathrm{d}H_s = \boldsymbol{\varepsilon}^{\mathrm{T}} \mathrm{d}\boldsymbol{\sigma} + n^w \mathrm{d}p_w + n^a \mathrm{d}p_a \tag{3.97}$$

From the eq.(3.97) received:

$$\boldsymbol{\varepsilon} = \frac{\partial H_s}{\partial \boldsymbol{\sigma}} \qquad n^w = \frac{\partial H_s}{\partial p_w} \qquad n^a = \frac{\partial H_s}{\partial p_a} \tag{3.98}$$

and

$$\mathrm{d}\boldsymbol{\varepsilon} = \frac{\partial^2 H_s}{\partial \boldsymbol{\sigma} \partial \boldsymbol{\sigma}} \mathrm{d}\boldsymbol{\sigma} + \frac{\partial^2 H_s}{\partial \boldsymbol{\sigma} \partial p_w} \mathrm{d}p_w + \frac{\partial^2 H_s}{\partial \boldsymbol{\sigma} \partial p_a} \mathrm{d}p_a \tag{3.99}$$

$$\mathrm{d}n^w = \left(\frac{\partial^2 H_s}{\partial p_w \partial \boldsymbol{\sigma}} \right)^{\mathrm{T}} \mathrm{d}\boldsymbol{\sigma} + \frac{\partial^2 H_s}{\partial p_w \partial p_w} \mathrm{d}p_w + \frac{\partial^2 H_s}{\partial p_w \partial p_a} \mathrm{d}p_a \tag{3.100}$$

$$\mathrm{d}n^a = \left(\frac{\partial^2 H_s}{\partial p_a \partial \boldsymbol{\sigma}} \right)^{\mathrm{T}} \mathrm{d}\boldsymbol{\sigma} + \frac{\partial^2 H_s}{\partial p_a \partial p_w} \mathrm{d}p_w + \frac{\partial^2 H_s}{\partial p_a \partial p_a} \mathrm{d}p_a . \tag{3.101}$$

where

$\mathrm{d}n^s$ – increment of volumetric contents of skeleton phase

$\mathrm{d}n^w$ – increment of volumetric contents of water phase

$\mathrm{d}n^a$ – increment of volumetric contents of air phase

Comparison of equations (3.88),(3.89),(3.90) with equations (3.99),(3.100) and (3.101) we find that a coefficients in equations (3.88),(3.89),(3.90) depend on the Hessian H_s. Since the Hessian matrix is symmetric, it holds:

$$m_1^w = m_2^s . \tag{3.102}$$

Using the equality $\mathrm{d}m^w = \mathrm{d}\left(\rho_w V^w\right)$ we can received:

$$\mathrm{d}n^w = \frac{\mathrm{d}m^w}{\rho_w} - n^w \frac{\mathrm{d}p_w}{K^w}. \tag{3.103}$$

where

dm^w – increment of water mass per unit volume of soil

K^w – bulk modulus of water phase in soil

Similarly, obtained with the air phase

$$\mathrm{d}n^a = \frac{\mathrm{d}m^a}{\rho_a} - n^a \frac{\mathrm{d}p_a}{K^a}. \tag{3.104}$$

Assuming small displacement amplitude, from mass conservation equations (Wrana, 2016) we can obtain:

$$\frac{\mathrm{d}m^w}{\rho_w} = -n^w \mathrm{div}\left(\mathbf{u}^w - \mathbf{u}^s\right) = -n^w\left(\varepsilon_v^w - \varepsilon_v^s\right) \tag{3.105}$$

$$\frac{\mathrm{d}m^a}{\rho_a} = -n^a \mathrm{div}\left(\mathbf{u}^a - \mathbf{u}^s\right) = -n^a\left(\varepsilon_v^a - \varepsilon_v^s\right) \tag{3.106}$$

Substituting (3.103),(3.104) and (3.83) to (3.105),(3.106) and (3.86) constitutive equations were obtained:

$$\boldsymbol{\sigma} = G\left(\boldsymbol{\varepsilon} - \frac{1}{3}\varepsilon_v^s \mathbf{m}\right) + H\varepsilon_v^s \mathbf{m} + n^w\left[\chi L + (1-\chi)C\right]\varepsilon_v^w \mathbf{m} + n^a\left[\chi C + (1-\chi)N\right]\varepsilon_v^a \mathbf{m} \tag{3.107}$$

$$p_w = W\varepsilon_v^s - n^w L\varepsilon_v^w - n^a C\varepsilon_v^a \tag{3.108}$$

$$p_a = M\varepsilon_v^s - n^w C\varepsilon_v^w - n^a N\varepsilon_v^a \tag{3.109}$$

where:

$$H = \frac{2Gv^s}{1-2v^s} - \chi W - (1-\chi)M \tag{3.110}$$

$$W=-\frac{K^w A}{D}+n^w L+n^a C \tag{3.111}$$

$$M=-\frac{K^a B}{D}+n^w C+n^a N \tag{3.112}$$

$$L=\frac{K^w\left[n^a m_1^s+K^a\left(m_1^s m_2^w-m_2^s m_1^w\right)\right]}{D} \tag{3.113}$$

$$N=\frac{K^a\left[n^w m_1^s+K^w\left(m_1^s m_2^w-m_2^s m_1^w\right)\right]}{D} \tag{3.114}$$

$$C=\frac{K^w K^a\left(m_1^s m_2^w-m_2^s m_1^w\right)}{D} \tag{3.115}$$

$$A=n^a m_1^w+K^a\left(m_1^s m_2^w-m_2^s m_1^w\right) \tag{3.116}$$

$$B=n^w m_1^a+K^w\left(m_1^s m_2^w-m_2^s m_1^w\right) \tag{3.117}$$

$$D=\left(m_1^s m_2^w-m_2^s m_1^w\right)\left(n^a K^w+n^w K^a\right)+n^a n^w m_1^s \tag{3.118}$$

$$m_1^s=\frac{3(1-2\nu^s)}{2(1+\nu^s)G} \tag{3.119}$$

and with the equations: (3.84), (3.85), (3.101) received:

$$m_1^a=(1-\chi)m_1^s \tag{3.120}$$

$$m_2^w=\chi m_1^s-m_2^a \tag{3.121}$$

$$m_1^w=m_2^s=\chi m_1^s. \tag{3.122}$$

Substituting the constitutive equations in the equations of motion (3.80), (3.81) and (3.82) received:

$$\begin{aligned}&(H+2G+n^w W+n^a M)\,\mathrm{grad}\varepsilon_v^s-G(\mathrm{grad}\varepsilon_v^s-\nabla^2 u^s)+\\&\quad n^w\left[\chi L+(1-\chi)C-n^w L-n^a C\right]\mathrm{grad}\varepsilon_v^w+\\&\quad n^a\left[\chi C+(1-\chi)N-n^a N-n^w C\right]\mathrm{grad}\varepsilon_v^a+\\&+\frac{g\left(n^w\right)^2\rho_w}{k_w}\left(\dot{\mathbf{u}}^w-\dot{\mathbf{u}}^s\right)+\frac{g\left(n^a\right)^2\rho_a}{k_a}\left(\dot{\mathbf{u}}^a-\dot{\mathbf{u}}^s\right)-(1-n)\rho_s\ddot{\mathbf{u}}^s=0\end{aligned} \tag{3.123}$$

$$-n^w W \mathrm{grad}\varepsilon_v^s + \left(n^w\right)^2 L \mathrm{grad}\varepsilon_v^s + n^w n^a C \mathrm{grad}\varepsilon_v^a - \frac{g\left(n^w\right)^2 \rho_w}{k_w}\left(\dot{\mathbf{u}}^w - \dot{\mathbf{u}}^s\right) - n^w \rho_w \ddot{\mathbf{u}}^w = 0 \tag{3.124}$$

$$-n^a M \mathrm{grad}\varepsilon_v^s + \left(n^a\right)^2 N \mathrm{grad}\varepsilon_v^a + n^a n^w C \mathrm{grad}\varepsilon_v^w - \frac{g\left(n^a\right)^2 \rho_a}{k_a}\left(\dot{\mathbf{u}}^a - \dot{\mathbf{u}}^s\right) - n^a \rho_a \ddot{\mathbf{u}}^a = 0 \tag{3.125}$$

In the case of a two-phase fully water saturated soil model with incompressible grains (Biot model) the relevant parameters are: $S_r = 1$, $m_1^s = m_2^s = m_1^w = m_2^w$. Three above equations reduce to two equations:

$$\left[\frac{2G\left(1-\nu^s\right)}{1-2\nu^s} + \left(1-n\right)^2 \frac{K^w}{n}\right]\mathrm{grad}\varepsilon_v^s - G\left(\mathrm{grad}\varepsilon_v^s - \nabla^2 \mathbf{u}^s\right) + \left(1-n\right) K^w \mathrm{grad}\varepsilon_v^w + \frac{n^2 g \rho_w}{k_w}\left(\dot{\mathbf{u}}^w - \dot{\mathbf{u}}^s\right) - \left(1-n\right)\rho_s \ddot{\mathbf{u}}^s = 0 \tag{3.126}$$

$$\left(1-n\right)\frac{K^w}{n}\mathrm{grad}\varepsilon_v^s + K^w \mathrm{grad}\varepsilon_v^w - \frac{ng\rho_w}{k_w}\left(\dot{\mathbf{u}}^w - \dot{\mathbf{u}}^s\right) - \rho_w \ddot{\mathbf{u}}^w = 0 \tag{3.127}$$

3.3.3. Dilatational and shear wave propagation.

The theory of discontinuous wave propagation in an unsaturated soil was used (Coussy, 2004). In this theory displacement and velocity are described by continuous function and acceleration by discontinuous function (skip function). The velocity of wave propagates depend on the soil parameters. There are three cases of phase motion:

a) air and water move independently relative to skeleton,
b) air moves relative to skeleton, water and skeleton move with the same velocity,
c) air, water and skeleton move with the same velocity, this case corresponding to undrainage problem of porous material.

***Case a*)**

In this case wave propagation problem is described by equations (3.123), (3.124) and (3.125). To solve the wave propagation problem, the jump Hadamard operator is used, marked with double square brackets [[ ]], where a discontinuity: $[\![\ddot{\mathbf{u}}^s]\!]$, $[\![\ddot{\mathbf{u}}^w]\!]$ and $[\![\ddot{\mathbf{u}}^a]\!]$ means (Kosiński, 1986):

$$[\![\ddot{\mathbf{u}}^s]\!] = \ddot{u}_n^s\mathbf{n} + \ddot{u}_t^s\mathbf{t}; \quad [\![\ddot{\mathbf{u}}^w]\!] = \ddot{u}_n^w\mathbf{n} + \ddot{u}_t^w\mathbf{t}; \quad [\![\ddot{\mathbf{u}}^a]\!] = \ddot{u}_n^a\mathbf{n} + \ddot{u}_t^a\mathbf{t} \tag{3.128}$$

where **t** is a unit vector located in a plane tangent to the wave front, **n** is a unit vector normal to the surface of the wave front in the direction of propagation. Taking into account $\mathrm{grad}\varepsilon_v^s = [\![\mathbf{n}\cdot\ddot{\mathbf{u}}^s]\!]\mathbf{n}$, $\mathrm{grad}\varepsilon_v^w = [\![\mathbf{n}\cdot\ddot{\mathbf{u}}^w]\!]\mathbf{n}$, $\mathrm{grad}\varepsilon_v^a = [\![\mathbf{n}\cdot\ddot{\mathbf{u}}^a]\!]\mathbf{n}$, equations (3.123), (3.124) and (3.125) can be written as:

$$\begin{aligned}(H + 2G + n^wW + n^aM)[\![\mathbf{n}\cdot\ddot{\mathbf{u}}^s]\!]\mathbf{n} + \\ +n^w[\chi L + (1-\chi)C - n^wL - n^aC][\![\mathbf{n}\cdot\ddot{\mathbf{u}}^w]\!]\mathbf{n} + \\ +n^a[\chi C + (1-\chi)N - n^wC - n^aN][\![\mathbf{n}\cdot\ddot{\mathbf{u}}^a]\!]\mathbf{n} + \\ +[G - c^2(1-n)\rho_s][\![\ddot{\mathbf{u}}^s]\!] = 0\end{aligned} \tag{3.129}$$

$$-n^wW[\![\mathbf{n}\cdot\ddot{\mathbf{u}}^s]\!]\mathbf{n} + (n^w)^2L[\![\mathbf{n}\cdot\ddot{\mathbf{u}}^w]\!]\mathbf{n} + n^wn^aC[\![\mathbf{n}\cdot\ddot{\mathbf{u}}^a]\!]\mathbf{n} - n^w\rho_w[\![\ddot{\mathbf{u}}^w]\!] = 0 \tag{3.130}$$

$$-n^aM[\![\mathbf{n}\cdot\ddot{\mathbf{u}}^s]\!]\mathbf{n} + n^an^wC[\![\mathbf{n}\cdot\ddot{\mathbf{u}}^w]\!]\mathbf{n} + (n^a)^2N[\![\mathbf{n}\cdot\ddot{\mathbf{u}}^a]\!]\mathbf{n} - c^2n^a\rho_a[\![\ddot{\mathbf{u}}^a]\!] \tag{3.131}$$

where *c* is velocity of wave propagation.

Substituting (3.128) to (3.129), (3.130), (3.131) and multiplying by the vector **t**, received:

$$\left[G - c^2(1-n)\rho_s\right]\ddot{u}_t^s = 0 \tag{3.132}$$

$$c^2n^w\rho_w\ddot{u}_t^w = 0 \tag{3.133}$$

$$c^2n^a\rho_a\ddot{u}_t^a = 0 \tag{3.134}$$

from which it follows that

$$\ddot{u}_t^s \neq 0 \quad \rightarrow \quad c^2 = V_s^2 = \frac{G}{(1-n)\rho_s} \tag{3.135}$$

$$\ddot{u}_t^w = \ddot{u}_t^a = 0. \tag{3.136}$$

Equation (3.135) describes a shear wave (*S-wave*) propagating in a plane tangent to the wave front at a speed of V_s. Substituting (3.128) to (3.129), (3.130), (3.131) and multiplying by the vector **n**, obtained:

$$(\mathbf{K} - c^2\mathbf{M})\begin{Bmatrix}\ddot{u}_n^s\\ \ddot{u}_n^w\\ \ddot{u}_n^a\end{Bmatrix} = 0 \tag{3.137}$$

where:

$$\mathbf{K}=\begin{bmatrix} H+2G+ & n^w\begin{pmatrix}\chi L+(1-\chi)C-\\ -n^wL-n^aC\end{pmatrix}, & n^a\begin{pmatrix}\chi C+(1-\chi)N-\\ -n^wC-n^aN\end{pmatrix} \\ +n^wW+n^aM, & & \\ -n^wW, & (n^w)^2L, & n^wn^aC \\ -n^aM, & n^an^wC, & (n^a)^2N \end{bmatrix} \tag{3.138}$$

$$\mathbf{M}=\begin{bmatrix}(1-n)\rho_s, & 0, & 0\\ 0, & n^w\rho_w, & 0\\ 0, & 0, & n^a\rho_a\end{bmatrix}. \tag{3.139}$$

K is a symmetric matrix (Wrana, 2016). Equation (3.137) presents three different dilatational waves (*P- waves*), which propagate in the normal direction to the wave front. From condition of zero determinant of matrix $(\mathbf{K}-c^2\mathbf{M})$ we can obtain wave speeds:

$$\det\left(\mathbf{K}-c^2\mathbf{M}\right)=0 \tag{3.140}$$

where $c^2=V_P^2$.

Equation (3.140) leads to equation on variable V_P^2:

$$\left(V_P^2\right)^3-\left(a_{p1}^2+a_{p2}^2+a_{p3}^2\right)\left(V_P^2\right)^2+\left(a_{p1}^2a_{p2}^2+a_{p1}^2a_{p3}^2+a_{p2}^2a_{p3}^2+A_1+A_2-A_3\right)V_P^2+$$
$$-\left(a_{p1}^2a_{p2}^2a_{p3}^2+A_1a_{p3}^2+A_2a_{p2}^2-A_3a_{p1}^2-A_0\right)=0 \tag{3.141}$$

where:

$$a_{p1}^2=\frac{H+2G+n^wW+n^aM}{(1-n)\rho_s} \tag{3.142}$$

$$a_{p2}^2=\frac{n^wL}{\rho_w} \tag{3.143}$$

$$a_{p3}^2=\frac{n^aN}{\rho_a} \tag{3.144}$$

$$A_0=\frac{\left[\chi L+(1-\chi)\,C-n^wL-n^aC\right]\,n^wn^aMC}{(1-n)\,\rho_s\rho_w\rho_a}+\frac{\left[\chi C+(1-\chi)\,N-n^wC-n^aN\right]\,n^wn^aWC}{(1-n)\,\rho_s\rho_w\rho_a} \tag{3.145}$$

$$A_1 = \frac{n^w W\left[\chi L + (1-\chi) C - n^w L - n^a C\right]}{(1-n)\rho_s \rho_w} \tag{3.146}$$

$$A_2 = \frac{n^w M\left[\chi C + (1-\chi) N - n^w C - n^a N\right]}{(1-n)\rho_s \rho_a} \tag{3.147}$$

$$A_3 = \frac{n^w n^a C^2}{\rho_w \rho_a}. \tag{3.148}$$

In eq.(3.141) we have variable V_P^2, hence the solution of this equation is the value of positive and negative V_p, which correspond to the propagation according to the velocity vector, and contrary to the vector. Similar results obtain from eq. (3.135) where there is a variable V_s^2.

***Case b*)**

In this case there is no relative water to skeleton displacement: $\mathbf{u}^w - \mathbf{u}^s = \mathbf{0}$, thus the equations (3.123), (3.124) and (3.125) reduced to form:

$$\begin{aligned}[H + 2G + n^w \chi L + n^w (1-\chi) C + n^a (M - n^w C)]\mathrm{grad}\varepsilon_v^s - \\ -G(\mathrm{grad}\varepsilon_v^s - \nabla^2 \mathbf{u}^s) + n^a[\chi C + (1-\chi) N - n^a N]\mathrm{grad}\varepsilon_v^a + \\ + \frac{(n^a)^2 \rho_a g}{k_a}(\dot{\mathbf{u}}^a - \dot{\mathbf{u}}^s) - \left[(1-n)\rho_s + n^w \rho_w\right]\ddot{\mathbf{u}}^s = 0\end{aligned} \tag{3.149}$$

$$\begin{aligned}-n^a (M - n^w C)\mathrm{grad}\varepsilon_v^s + (n^a)^2 N \mathrm{grad}\varepsilon_v^a - \frac{(n^a)^2 \rho_a g}{k_a}(\dot{\mathbf{u}}^a - \dot{\mathbf{u}}^s) - \\ - n^a \rho_a \ddot{\mathbf{u}}^a = 0.\end{aligned} \tag{3.150}$$

As in the case a) to solve the wave propagation problem the Hadamard jump operator [[]] is used, which leads to the determination of one shear wave and two dilatational waves. Velocity of these waves are determined:

$$V_S^2 = \frac{G}{(1-n)\rho_s + n^w \rho_w} \tag{3.151}$$

and $$V_P^2 = \frac{1}{2}\left[\left(b_{p1}^2 + b_{p2}^2\right) \pm \sqrt{\left(b_{p1}^2 - b_{p2}^2\right)^2 + 4B_0}\right] \tag{3.152}$$

where:

$$B_0 = -\frac{n^a\left[\chi C + (1-\chi)\,N - n^a N\right]\left(M - n^w C\right)}{\left[(1-n)\rho_s + n^w \rho_w\right]\rho_a} \tag{3.153}$$

$$b_{p1}^2 = \frac{H + 2G + n^w \chi L + n^w (1-\chi)\,C + n^a\left(M - n^w C\right)}{(1-n)\rho_s + n^w \rho_w} \tag{3.154}$$

$$b_{p2}^2 = \frac{n^a N}{\rho_a}. \tag{3.155}$$

Similarly, when there is a lack of air to skeleton displacement: $\mathbf{u}^a - \mathbf{u}^s = \mathbf{0}$, received one shear wave speed V_S and two different dilatational wave speeds V_P:

$$V_S^2 = \frac{G}{(1-n)\rho_s + n^a \rho_a} \tag{3.156}$$

and $$V_P^2 = \frac{1}{2}\left[\left(c_{p1}^2 + c_{p2}^2\right) \pm \sqrt{\left(c_{p1}^2 - c_{p2}^2\right)^2 + 4C_0}\right] \tag{3.157}$$

where:

$$C_0 = -\frac{n^w\left[\chi L + (1-\chi)C - n^w L\right]\left(W - n^a C\right)}{\left[(1-n)\rho_s + n^a \rho_a\right]\rho_w} \tag{3.158}$$

$$c_{p1}^2 = \frac{H + 2G + n^a \chi C + n^a (1-\chi)\,N + n^w\left(W - n^a C\right)}{(1-n)\rho_s + n^a \rho_a} \tag{3.159}$$

$$c_{p2}^2 = \frac{n^w L}{\rho_w}. \tag{3.160}$$

Case c)

In this case there is no water to skeleton and no air to skeleton displacement, undrained case, $\mathbf{u}^a - \mathbf{u}^w - \mathbf{u}^s = \mathbf{u}$. Equation of motion simplifies to the form:

$$\mathrm{div}\boldsymbol{\sigma} = \rho\ddot{\mathbf{u}} \tag{3.161}$$

where $\rho = (1-n)\rho_s + S_r n \rho_w + (1-S_r) n \rho_a$. (3.162)

Taking into account the constitutive equations from 3.3.2 in the above equation the following were obtained:

$$\left[\frac{2G(1-v^s)}{1-2v^s}+\chi\frac{K^wA}{D}+(1-\chi)\frac{K^aB}{D}\right]\mathrm{grad}\varepsilon_v-G(\mathrm{grad}\varepsilon_v-\nabla^2\mathbf{u})-\rho\ddot{\mathbf{u}}=0 \tag{3.163}$$

In this case, there is the one shear wave propagation at the speed of:

$$V_S^2=\frac{G}{\rho} \tag{3.164}$$

and the one dilatational wave propagation at the speed of:

$$V_P^2=\frac{\left[2G(1-v^s)/(1-2v^s)\right]+\left(d_{p1}/d_{p2}\right)}{\rho} \tag{3.165}$$

where:

$$d_{p1}=K^wK^a\left(-\chi^2+m_2^w/m_1^s\right)+n\left[\chi^2K^w(1-S_r)+(1-\chi)^2K^aS_r\right]/m_1^s \tag{3.166}$$

$$d_{p2}=n\left[S_rK^a+(1-S_r)K^w\right]\left(-\chi^2+m_2^w/m_1^s\right)+n^2S_r(1-S_r)/m_1^s\,. \tag{3.167}$$

When the pores are completely filled with air (dry soil, $S_r=0$) or if the pores are completely filled with water (irrigated soil, $S_r=1$ $\mathrm{S_r}=0$) the shear wave velocity is defined by the formula (3.163) taking account of the volume density ρ:

with $\mathrm{S_r}=0$, $\rho=(1-n)\rho_s+n\rho_a$ (3.168)

with $\mathrm{S_r}=1$, $\rho=(1-n)\rho_s+n\rho_w$. (3.169)

Hence the dilatational wave velocity will define, in accordance with the equation (3.164):

with $\mathrm{S_r}=0$, $V_P^2=\dfrac{\left[2G(1-v^s)/(1-2v^s)\right]+\left(K^a/n\right)}{(1-n)\rho_s+n\rho_a}$ (3.170)

with $\mathrm{S_r}=1$, $V_P^2=\dfrac{\left[2G(1-v^s)/(1-2v^s)\right]+\left(K^w/n\right)}{(1-n)\rho_s+n\rho_w}$. (3.171)

Comments

1. The above considerations apply to the low-frequency.
2. The above consideration does not include energy dissipation caused by the laminar water motion in the pores. It should be emphasized (Brutsaert, 1964), that in the low frequency range relative water to skeleton motion in the pores is negligibly small. In the high frequency range water moves freely in the pores and energy dissipation may be omitted.
3. In paper (Miura, et al., 2001) shows the wave speed depend on frequency for variety irrigated

soil, from clays to soft rock. The authors showed that the coefficient of permeability is the main parameter of soil, which determines the bandwidth of low frequency. Reduction of permeability coefficient causes the extension frequency bandwidth. From in situ soil geophysical measurement to a few hundred kHz carried out by (Santamarina , et al., 2001) and (Miura, et al., 2001) shows that the largest components of soil response are in the low frequency range.

4. Two phase medium – equations of motion.

4.1. Introduction.

The following section is concentrated on further description of the two-phase media, which was also described in Section 3.2. and expended hereunder for the thesis' purpose.

The behavior of saturated porous soil-structure systems subjected to dynamic or static loads should be defined by taking into consideration the coupling between flow and deformation. The Fig. 4.1 shows the schematic of such a soil-structure system.

The behavior of the mixture of soil and water is affected by the deformation of the solid particles (skeleton), the relative motion (sliding) between particles and water, the deformation of pore water, and the movement of pore water through pores. A general formulation for such an interacting system is presented in this section, in which static case, consolidation and a variety of dynamic behavior can be obtained as special cases.

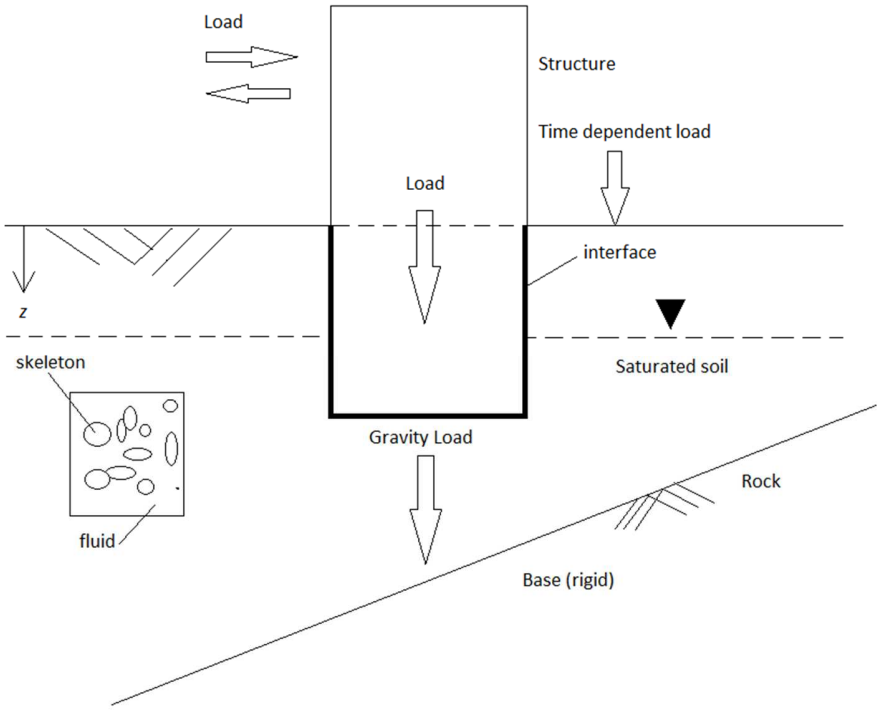

Fig. 4.1: Schematic of structure-foundation system (Desai & Zaman, 2014)

Biot theory describes the wave propagation in saturated porous media as a soil skeleton fully saturated with fluid. Biot (Biot, 1956) assumed that the motion of porous media on the micro level can be described by continuum mechanics of material. He used Lagrange postulate and Hamilton's principle to derive the equations of wave propagation.

The main assumptions of Biot theory are as mentioned in 3.4.1. The formulation of porous media dynamics is based on the kinetic energy equation, dissipation function and it leads to the equations of motion using Lagrange's postulate.

Again – as in all the following equations in the introduced indications: "m" - refers to the skeleton, "s" - refers to the skeleton particles and "f" - refers to the liquid phase in the pores.

4.2. Stress-strain relations.

Before the formulations presented by Biot will be used, various terms relevant to saturated porous materials will be depicted. Fig. 3.9 shows the schematic of a porous material consisting of solid (particles) and fluid (water) and the diagram. The porosity *n* is defined as:

$$n = \frac{V_v}{V_v + V_s} \tag{4.1}$$

where V_v is the volume of pores equal to the volume of fluid ($=V_f$) and V_s is the volume of solids. The density, ρ, of the mixture is expressed as

$$\rho = (1-n)\rho_s + n\rho_f \tag{4.2}$$

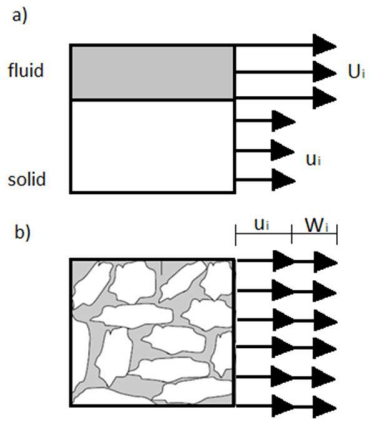

Fig. 4.2: Displacements in element with two phases. a) Displacement of different phases; b) relative displacement of fluid (Desai & Zaman, 2014)

The symbolic deformations of solids and fluids are shown in Fig. 4.2 . The terms in this figure are as follows: u_i (i=1,2,3) are the displacement components for the solid in 1 (x), 2 (y), and 3 (z) directions, and U_i (i=1,2,3) denotes displacement components of the fluid. Relative displacements can occur between the solid and the fluid for loadings such as dynamic. Then, w_i (i=1,2,3) denotes such relative displacements between solid and fluid, averaged over the face of the solid skeleton, given by

$$w_i = \frac{Q_i}{A_i} = n(U_i - u_i) \tag{4.3}$$

where A_i is the area normal to the ith direction. The volume of fluid moving through an area of the skeleton normal to the ith direction, Q_i, is expressed as

$$Q_i = A_i n(U_i - u_i) \tag{4.4}$$

For small strains, the strain tensor, ε_{ij}, is given by

$$\varepsilon_{ij} = \frac{1}{2}(u_{i,j} + u_{j,i}) \tag{4.5}$$

where $u_{i,j}$ denotes derivative of solid displacement u_i (i=1,2,3) and so on. The change in the volume of fluid in a unit volume of the skeleton, ξ, is given by

$$\xi = w_{i,i} \tag{4.6}$$

where (i,i) denote the summation, that is, $w_{i,i} = w_{1,1} + w_{2,2} + w_{3,3}$.

Biot (Biot, 1941; Biot, 1956) has developed the formulation for coupled, solid-fluid behavior by assuming linear elastic material behavior. For those solid (soil)- fluid (water) media which behave nonlinearly, and may experience elastic, plastic, and creep deformations. Zienkiewicz and Shiomi (Zienkiewicz & Shiomi, 1984; Zienkiewicz, 1982) have presented equations by assuming incremental plasticity, which account for the nonlinear behavior. Accordingly the total incremental stress $d\sigma_{ij}$ is divided into two components as

$$d\sigma_{ij} = d\sigma'_{ij} + dp\delta_{ij} \tag{4.7}$$

where $d\sigma'_{ij}$ is the incremental effective stress tensor, dp denotes the incremental pore water pressure and δ_{ij} is the Kronecker delta. Similarly, the total strain increment, $d\varepsilon_{ij}$, can be expressed as:

$$d\varepsilon_{ij} = (d\varepsilon_{ij})_{\sigma'} + (d\varepsilon_{ij})_p \tag{4.8}$$

where $(d\varepsilon_{ij})_{\sigma'}$ denotes the incremental strains caused by the deformation of soil or rock grains and skeleton due to the effective stress, and $(d\varepsilon_{ij})_p$ denotes the strain caused by the deformations of solid grains due to pore water pressure.

The constitutive equations for an elastic-plastic material in terms of the effective quantities can be expressed as

$$d\sigma'_{ij} = C^{ep}_{ijkl} + d\varepsilon'_{kl} \tag{4.9}$$

$$d\sigma' = C^{ep} + d\varepsilon \tag{4.10}$$

The first equation (4.9), is expressed in tensor notation, while the second one, eq.(4.10), is expressed in matrix notation. Here, $C^{ep}_{ijkl} = C^{e}_{ijkl} - C^{p}_{ijkl}$ where the first term relates to elastic behavior while the second term arises from inelastic or plastic behavior. The latter is derived based on the particular yield criterion or function chosen (e.g., conventional plasticity: von Mises, Drucker-Prager and Mohr Coulomb) or continuous yielding (e.g. critical state and cap), and related flow rule (Desai, 2000).

The bulk elastic behavior of solid grains (skeleton) can be expressed as

$$(d\varepsilon_{ij})_p = \frac{dp}{3K_s}\delta_{ij} \tag{4.11}$$

where K_s denotes the bulk modulus of the solid grains. The substitution of equations (4.8) through (4.11) in eq.(4.7) leads to

$$d\sigma_{ij} = C^{ep}_{ijkl} d\varepsilon_{kl} - \left(\frac{dp}{3K_s}\right) C_{ijkl} + dp\delta_{ij} \tag{4.12}$$

The common terms without dp in the last two terms can be expressed as

$$\delta_{ij} - \frac{C^{ep}_{ijkl}}{3K_s}\delta_{kl} = \alpha\delta_{ij} + \beta_{ij} \tag{4.13}$$

where α is a scalar term. Assuming that the deviatoric part, β, can be neglected (Zienkiewicz & Shiomi, 1984), eq. (4.12) reduces to

$$d\sigma_{ij} = C^{ep}_{ijkl} d\varepsilon_{kl} + \alpha dp\delta_{ij} \tag{4.14}$$

For elastic materials , C^{ep}_{ijkl} reduces to C^{e}_{ijkl} as

$$C^{e}_{ijkl} = 2\mu\delta_{ik}\delta_{jl} + \lambda dp\delta_{ij}\delta_{kl} \tag{4.15}$$

where μ and λ are Lame's constants. Now, by using equations (4.13) and (4.15) α can be deduced as

$$\alpha = 1 - \frac{\lambda + (2/3)\mu}{K_s} = 1 - \frac{K}{K_s} \tag{4.16}$$

where K is the bulk modulus of the soil-water mixture, which for elastoplastic material can be derived as

$$K = \frac{\delta_{ij} C^{ep}_{ijkl} \delta_{kl}}{9} \tag{4.17}$$

The following four items (given below in order of importance) can influence the volume change behavior of the mixture (Zienkiewicz, 1982):

- the increased volume due to a change in strain i.e.: $\mathrm{d}\varepsilon_{ii} = \delta_{ij} d\varepsilon_{ij} = \mathbf{m}^T \boldsymbol{\varepsilon}$,
- the additional volume stored by compression of void due to water pressure increase: $n d\mathrm{p}/K_f$
- the additional volume stored by the compression of grains by the water pressure increase: $(1-n)dp/K_s$, where K_s is the bulk modulus of skeleton
- the change in volume of the solid phase due to a change in the intergranular effective contact stress $\sigma' = \sigma + \delta_{ij} p : \frac{\frac{1}{3}\delta_{ij}\mathrm{d}\sigma_{ij}'}{K_s} = (K/K_s)(\mathrm{d}\varepsilon_{\mathrm{V}} + \mathrm{d}p/K_s)$, where K is average bulk modulus of the soil-water mixture and ε_{V} the total volumetric strain.

In view of the above four contributions, the volume change of the mixture, the continuum condition, can be expressed as

$$d\xi = d\varepsilon_{ii} + \frac{dp}{K_s}(1-n) + \frac{dpn}{K_f} - \frac{d\sigma'_{ii}}{3K_s} \tag{4.18}$$

The substitution of equation (4.7) and (4.14) into the above equation leads to (Zienkiewicz & Shiomi, 1984):

$$dp = Q\left(\alpha d\varepsilon_{kk} + d\xi\right) \tag{4.19}$$

where α was defined previously and Q is expressed as

$$Q = \frac{K_f K_s}{K_s \overline{n} + K_f(\alpha - n)} \tag{4.20}$$

Equation (4.14) and (4.18) can be applied for both elastic and elastic-plastic material behavior assuming that the bulk modulus for solid grains and fluid are invariant.

If the bulk modulus for the solid grains is much higher than that for the soil skeleton, that is, if $K_s >> K$ the values of α tend to unity. Than eq.(4.14) can be expressed as

$$d\sigma'_{ij} = d\sigma_{ij} - dp\delta_{ij} = C_{ijkl} d\varepsilon_{kl} \tag{4.21}$$

The above equation denotes the effective stress concept (Terzaghi, 1943; Terzaghi, 1960), implying that the deformation of the solid skeleton is affected by the effective stress.

4.3. Equilibrium equations.

As noted before, the solid and fluid components of the mixture are coupled. Equations of motion of fully saturated porous soil model include set of three equations: linear momentum balance for the mixture, mass balance for the water phase and mass balance for the mixture. Unknowns variable are three values: skeleton displacement, water displacement and water pore pressure. According to (Zienkiewicz & Shiomi, 1984; Zienkiewicz, 1982; Biot, 1962; Shao , 1997; Desai & Galagoda, 1989; Wathugala & Desai, 1990; Desai, 2000), those equations are given by:

1. Linear momentum balance for the soil-water mixture.

$$\sigma_{ij,j} + (1-n)\rho_s b_i + n\rho b_i - (1-n)\rho_s \ddot{u}_i^s - n\rho_f \ddot{u}_i^f = 0 \tag{4.22}$$

where b_i denotes the components of body force per unit mass, u^f and u^s are the displacements of the fluid and the skeleton, respectively, ρ_f and ρ_s are the densities of fluid and solid grains, respectively.

If we substitute equations (4.2), (4.3) and (4.21) into eq.(4.22), include convective element and assume that w_i is the vector of relative velocity of pore water ($w_i = \dot{u}_i{}^f - \dot{u}_i{}^s = \dot{u}_i{}^f - \dot{u}_i$), it simplifies to

$$\sigma_{ij,j} - \rho\ddot{u}_i - \rho_f(\dot{w}_i + w_j w_{i,j}) + \rho b_i = 0 \tag{4.23}$$

or

$$\mathbf{L}^{\mathrm{T}}\boldsymbol{\sigma} - \rho\ddot{\mathbf{u}} + \rho^f(\dot{\mathbf{w}} + \mathbf{w}\nabla^{\mathrm{T}}\mathbf{w}) + \rho\mathbf{b} = 0 \tag{4.24}$$

where

$$\mathbf{L}^{\mathrm{T}} = \begin{bmatrix} \frac{\partial}{\partial x_1} & 0 & 0 & \frac{\partial}{\partial x_2} & 0 & \frac{\partial}{\partial x_3} \\ 0 & \frac{\partial}{\partial x_2} & 0 & \frac{\partial}{\partial x_1} & \frac{\partial}{\partial x_3} & 0 \\ 0 & 0 & \frac{\partial}{\partial x_3} & 0 & \frac{\partial}{\partial x_2} & \frac{\partial}{\partial x_1} \end{bmatrix} \tag{4.25}$$

$$\mathbf{w}\nabla^{\mathrm{T}}\mathbf{w} = \begin{Bmatrix} w_1 w_{1,1} + w_2 w_{1,2} + w_3 w_{1,3} \\ w_1 w_{2,1} + w_2 w_{2,2} + w_3 w_{2,3} \\ w_1 w_{3,1} + w_2 w_{3,2} + w_3 w_{3,3} \end{Bmatrix}$$ - convective vector

$\mathbf{w} = \dot{\mathbf{u}}^{\mathbf{f}} - \dot{\mathbf{u}}^{\mathbf{s}} = \dot{\mathbf{u}}^{\mathbf{f}} - \dot{\mathbf{u}}$ - vector of relative velocity of pore water with respect to velocity of skeleton

$\dot{\mathbf{w}}$ - vector of relative acceleration of pore water with respect to acceleration of skeleton

Equation (4.23) is an extension of the linear momentum balance for the soil-water mixture including convective vector. Overall density of the soil-water mixture is given by eq.(4.2).

2. Linear momentum balance for the water.

$$-p_{,i} - R_i - \rho_f \ddot{u}_i^s - \rho_f (\dot{w}_i + w_j w_{i,j}) / n + \rho_f b_i = 0 \tag{4.26}$$

or

$$-\nabla p - \mathbf{R} - \rho^f \ddot{\mathbf{u}}^s - \rho^f \left(\dot{\mathbf{w}} + \mathbf{w}\nabla^{\mathrm{T}}\mathbf{w}\right)/n + \rho^f \mathbf{b} = 0 \tag{4.27}$$

where R_i represents the viscous drag forces, which assuming the Darcy seepage law, can be written as

$$k_{ij} R_j = w_i \tag{4.28}$$

In eq.(4.28) the permeability coefficients k_{ij} is used with dimensions of [length]^3[time]/[mass] which is different from the usual soil mechanics convention which has the dimension of velocity k', i.e., [length]/[time]. Their values are related by $k = k'/\rho_f g$ where ρ_f are the water density and g gravitational acceleration at which the permeability is measured. When these units, R_j has the dimension of force.

Equation (4.26) is an extension of the linear momentum balance for the pore water including convective component $\rho_f w_j w_{i,j}$. The other components are: $(-p_{,i})$ -is the gradient pore water pressure, $\rho_f \ddot{u}_i^s$ - is the inertia force of skeleton , $\rho_f \dot{w}_i$ - is the inertia force of pore water, $\rho_f b_i$ - is the water body force, R_i - is the viscous drag force.

3. Mass balance for the mixture.

Mass balance equation for the soil-water mixture balance the flow divergence $w_{i,i}$ by the augmented storage in the pores of a unit volume of soil occurring in time d*t*. This storage is composed of several before mentioned components given below in order of importance:

Adding all the storage increase contributions from eq. (4.18) together with a source term which represents temperature changes $\dot{s}_0$ and a second-order term due to the change in fluid density in the process $n\dot{\rho}_f / \rho_f$ we can finally write the flow conservation equation

$$w_{i,i} + \dot{\varepsilon}_v + \frac{n\dot{p}}{K_f} + \frac{(1-n)\dot{p}}{K_s} - \frac{K}{K_s}(\dot{\varepsilon}_v + \frac{\dot{p}}{K_s}) + \frac{n\dot{\rho}_f}{\rho_f} + \dot{s}_0 = 0 \tag{4.29}$$

or

$$w_{i,i} + \left(1 - \frac{K}{K_s}\right)\dot{\varepsilon}_v + \left(\frac{n}{K_f} + \frac{(1-n)}{K_s} - \frac{K}{K_s K_s}\right)\dot{p} + \frac{n\dot{\rho}_f}{\rho_f} + \dot{s}_0 = 0 \tag{4.30}$$

The following designation is used:

$$\frac{1}{Q} = \frac{n}{K_f} + \frac{1-n}{K_s} - \frac{K}{K_s K_s} = \frac{n}{K_f} + \frac{\alpha - n}{K_s} \tag{4.31}$$

Given above notation, the Equation

$$w_{i,i} + \dot{\varepsilon}_v + \frac{n\dot{p}}{K_f} + \frac{(1-n)\dot{p}}{K_s} - \frac{K}{K_s}(\dot{\varepsilon}_v + \frac{\dot{p}}{K_s}) + \frac{n\dot{\rho}_f}{\rho_f} + \dot{s}_0 = 0 \tag{4.29}$$

can be written:

$$w_{i,i} + \alpha\dot{\varepsilon}_v + \frac{\dot{p}}{Q} + \frac{n\dot{\rho}_f}{\rho_f} + \dot{s}_0 = 0 \tag{4.32}$$

or

$$\nabla^T \mathbf{w} + \alpha \mathbf{m}\dot{\varepsilon}_v + \frac{\dot{p}}{Q} + \frac{n\dot{\rho}_f}{\rho_f} + \dot{s}_0 = 0 \tag{4.33}$$

The set of three governing equations for the two-phase media gathered together are as follows:

$$\begin{cases} \sigma_{ij,j} + (1-\bar{n})\rho_s b_i + \bar{n}\rho b_i - (1-\bar{n})\rho_s \ddot{u}_i^s - \bar{n}\rho_f \ddot{u}_i^f = 0 \\ -p_{,i} - R_i - \rho_f \ddot{u}_i^s - \rho_f (\dot{w}_i + w_j w_{i,j})/n + \rho_f b_i = 0 \\ w_{i,i} + \dot{\varepsilon}_v + \frac{n\dot{p}}{K_f} + \frac{(1-n)\dot{p}}{K_s} - \frac{K}{K_s}(\dot{\varepsilon}_v + \frac{\dot{p}}{K_s}) + \frac{n\dot{\rho}_f}{\rho_f} + \dot{s}_0 = 0 \end{cases} \tag{4.34}$$

4.4. Boundary and initial conditions.

Behavior of two-phase medium (skeleton and water in the pores) in dynamic analysis is described by equations (4.23) – linear momentum balance for the soil-water mixture ; (4.26) – linear momentum balance for the water; (4.32) – mass balance for the mixture and (4.7) – constitutive equations. Unknowns in these equations are:

p - pore water pressure

$\mathbf{w} = \{w_1, w_2, w_3\}^T$ - average velocity vector of water flow inside inside the pore with respect to skeleton

$\mathbf{u} = \{u_1, u_2, u_3\}^T$ - displacement vector of soil skeleton

We can divide the boundary conditions to those regarding the soil skeleton and those regarding the pore water :

- the boundary conditions for the pore water are: known relative flow velocity with respect to skeleton $\bar{w}$ through the boundary Γ_w and pore water pressure $p=q$ on the boundary Γ_p, where $\Gamma = \Gamma_w \cup \Gamma_p$.
- the boundary conditions for the soil skeleton are: known displacement $\bar{\mathbf{u}}$ on the boundary Γ_u and known normal stress $\mathbf{n}\boldsymbol{\sigma} = \bar{\mathbf{t}}$ on the boundary Γ_t , where $\Gamma = \Gamma_u \cup \Gamma_t$.

The above information can be symbolically presented as in Fig. 4.3.

Skeleton phase	Pore water phase
$\Gamma = \Gamma_t \cup \Gamma_u$	$\Gamma = \Gamma_t \cup \Gamma_u$
$\mathbf{t} = \mathbf{n}\boldsymbol{\sigma} = \bar{\mathbf{t}}$ on Γ_t	$p = q$ on Γ_p
$\mathbf{u} = \bar{\mathbf{u}}$ on Γ_u	$\mathbf{w} = \bar{\mathbf{w}}$ on Γ_w

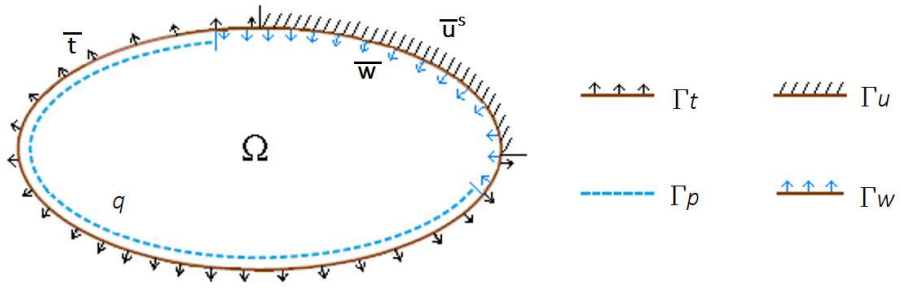

Fig. 4.3: Boundary conditions of two phase fully saturated soil model (Wrana, 2016)

The initial conditions, similarly as the boundary conditions, can be divided into those regarding the soil skeleton and those regarding the pore water:

- the initial conditions for the soil skeleton are: known displacement at time t_0, $\mathrm{u}(t = t_0) = \mathrm{u}_0$ and known velocity at time t_0, $\dot{\mathrm{u}}(t = t_0) = \dot{\mathrm{u}}_0$.
- the initial conditions for the pore water are: known the relative flow velocity with respect to skeleton at time t_0, $\mathbf{w}(t = t_0) = \mathbf{w}_0$ and known pore water pressure at time t_0, $p(t = t_0) = p_0$.

5. Solution methods. One dimensional problem of consolidation and dynamics.

Simplified set of equations (4.23), (4.26) and (4.32) after eliminating the relative flow velocity, body forces ($\rho b_i = \rho_f b_i = 0$) and implementing the following simplifications:

- omitting in equations (4.23) and (4.26) member $\dot{w}_i + w_j w_{i,j}$, which is very small when related to soil skeleton displacement **u** or pore water pressure *p*,
- omitting the water density changes in time $\dot{\rho}_f$,
- omitting the effects of temperature changes in time $\dot{s}_0$,

can be presented as follows:

$$\sigma_{ij,j} - \rho \ddot{u}_i - \rho_f \dot{w}_i = 0 \tag{5.1}$$

$$-p_{,i} - R_i - \rho_f \ddot{u}_i - \rho_f \dot{w}_i / n = 0 \tag{5.2}$$

$$w_{i,i} + \alpha \dot{\varepsilon}_v + \frac{\dot{p}}{Q} = 0 \tag{5.3}$$

Unknowns in these equations are:

p - pore water pressure,

$\mathbf{w} = \{w_1, w_2, w_3\}^T$ - average velocity vector of water flow inside the pore with respect to skeleton,

$\mathbf{u} = \{u_1, u_2, u_3\}^T$ - displacement vector of soil skeleton.

The boundary conditions from Fig. 4.3 imposed on these variables complete the problem.

5.1. Comparison of fully dynamic, partly dynamic and quasi static model.

5.1.1. Fully dynamic idealization – Biot model.

For the one-dimensional case we assume $u_1 = u$, $u_2 = u_3 = 0$ and $1/Q = n/K_f$. For an isotropic material, D is given by and for small strains the stress relation is $\boldsymbol{\sigma} = \boldsymbol{\sigma}'' - p = \mathrm{D}\boldsymbol{\varepsilon} - p = \mathrm{D}u_{,x} - p$, in the next relation we introduce $\mathbf{w} = \dot{\mathbf{u}}^f$ where $\mathbf{u}^f$ is the displacement of fluid.

From Equation (5.3) we have relation $p = \frac{K_f}{n}\left(u^s{}_{,x} + u^f{}_{,x}\right)$. Substituting this relation into the two remaining equations we obtain (Wrana & Pietrzak, 2013):

$$\left(D + \frac{K_f}{n}\right)\mathrm{u}^s{}_{,xx} + \frac{K_f}{n}\mathrm{u}^f{}_{,xx} = \rho \ddot{\mathrm{u}}^s + \rho_f \ddot{\mathrm{u}}^f \tag{5.4}$$

$$\frac{K_f}{n}\left(\mathrm{u}^s{}_{,xx} + \mathrm{u}^f{}_{,xx}\right) = \rho_f \ddot{\mathrm{u}}^s + \frac{\rho_f}{n}\ddot{\mathrm{u}}^f + \frac{\rho_f g \mathrm{w}}{k} \tag{5.5}$$

For a periodic applied surface load $\mathrm{q} = \mathrm{Q}e^{\mathrm{i}\omega t}$ a periodic solution arises after the dissipation of the initial transient in the form $\mathrm{u}^s = \mathrm{U}(\mathrm{x})e^{\mathrm{i}\omega t}$, $\mathrm{u}^f = \mathrm{v} = \mathrm{V}(\mathrm{x})e^{\mathrm{i}\omega t}$.

With following notations

$$K=\frac{\frac{K_f}{n}}{D+\frac{K_f}{n}},\qquad \beta=\frac{\rho_f}{\rho},\qquad \alpha=\frac{\pi\beta Lg}{kV_L}=\frac{\beta g\pi}{2\bar{f}k},\qquad z=\frac{x}{L},$$

where: L – depth of soil layer

$V_L=\sqrt{\frac{D+\frac{K_f}{n}}{\rho}}$ - compression wave velocity in porous soil,

$f=\frac{\omega}{2\pi}$ - frequency of excitation,

$\bar{f}=\frac{V_L}{4L}$ - reference frequency,

$\eta=\frac{f}{\bar{f}}=\frac{\omega L}{2\pi V_L}$ - frequency ration as proportion of excitation to reference frequency, one

can obtain Biot equations in the form of

$$U_{,zz}+KV_{,zz}=-\eta^2\pi^2U-\eta^2\pi^2\beta V \tag{5.6a}$$

$$KU_{,zz}+KV_{,zz}=-\eta^2\pi^2\beta U-\left[\frac{\eta^2\pi^2\beta}{n}-i\eta\alpha\right]V\,. \tag{5.6b}$$

5.1.2. Partly dynamic idealization – u-p formulation.

In this case , the coupled equations of flow and deformation consider only the acceleration of solid skeleton and not that of pore fluid. It is called u-p formulation as in this case the governing equations can be represented only in terms of solid displacement, u and pore fluid pressure, p.

The reduced system in general form when omitting inertia forces of the fluid becomes:

$$\sigma_{ij,j}-\rho\ddot{u}_i=0 \tag{5.7}$$

$$-p_{,i}-R_i-\rho_f\ddot{u}_i=0 \tag{5.8}$$

$$w_{i,i}+\alpha\dot{\varepsilon}_{11}+\frac{\dot{p}}{Q}=0\,. \tag{5.9}$$

The appropriate equation set for one-dimensional problem (5.6a) and (5.6b) , after substituting new variables introduced in the previous section, becomes (Wrana & Pietrzak, 2013):

$$U_{,zz}+KV_{,zz}=-\eta^2\pi^2U \tag{5.10a}$$

$$KU_{,zz}+KV_{,zz}=-\eta^2\pi^2\beta U+i\eta\alpha V\,. \tag{5.10b}$$

5.1.3. Quasi static idealization – consolidation model.

If we ignore all second time derivatives, in other words all inertial terms, the equations simplify to :

$$\sigma_{ij,j} = 0 \tag{5.11}$$

$$-p_{,i} - R_i = 0 \tag{5.12}$$

$$w_{i,i} + \alpha\dot{\varepsilon}_{11} + \frac{\dot{p}}{Q} = 0 \tag{5.13}$$

The resulting system corresponds to quasi-static case , which is used frequently in soil mechanics. If the phenomena is sufficiently slow the full set of equation is considerably reduced and after similar transformations as in previous cases, we obtain :

$$U_{,zz} + KV_{,zz} = 0, \tag{5.14a}$$

$$KU_{,zz} + KV_{,zz} = i\eta\alpha V \tag{5.14b}$$

We solve all the aforementioned (in 5.1.1, 5.1.2, 5.1.3) differential equations analytically reducing them to two uncoupled differential equations of fourth order.

5.1.4. Numerical example.

The one-dimensional soil layer subjected to a periodic surface force is considered as shown in Fig. 1. To complete the solution, boundary conditions must be applied at z=0 and z=1. These conditions are:

with z=0: pore pressure p=0, stress on external surface $\sigma = q = \bar{q}e^{i\omega t}$,

with z=1: displacement of skeleton u=0, displacement of fluid v=0.

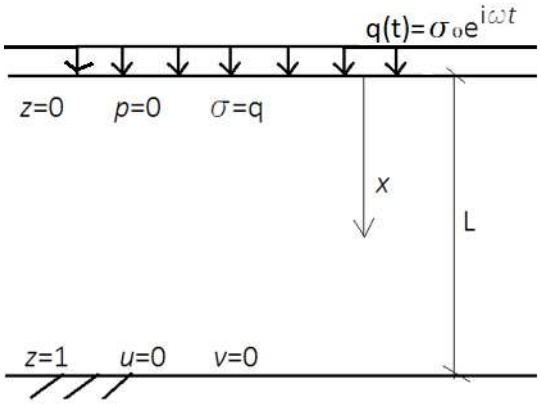

Fig. 5.1: Soil layer subjected to periodic loading

Numerical analysis is performed with typical parameters for a wide range of sands: porosity n=1/3, coefficient K=0.973, and β=1/3. The calculations of skeleton displacement – u and fluid displacement – v are carried out for three sets of models: FD- exact solution (Biot's model), PD- u-p model and QS- quasi-static model. All the calculations are done using the dimensionless η parameter which is the ratio of the excitation frequency to the comparative frequency which is 10Hz in our case: $\eta = \frac{f}{\bar{f}} = \frac{f}{10Hz}$. The value of 10Hz is a typical excitation for soil vibrators. There are generally considered five values of η : 0.1, 0.8, 1.0, 1.2, 5.0. These values comply with soil vibrators.

The three figures below (Fig. 5.2, Fig. 5.3 and Fig. 5.4) show the displacement of the skeleton and of the fluid and also the fluid pressure for Biot's model, versus normalized depth. There are varied values and shapes of the aforementioned unknowns for different η (or different excitation frequency in other words).

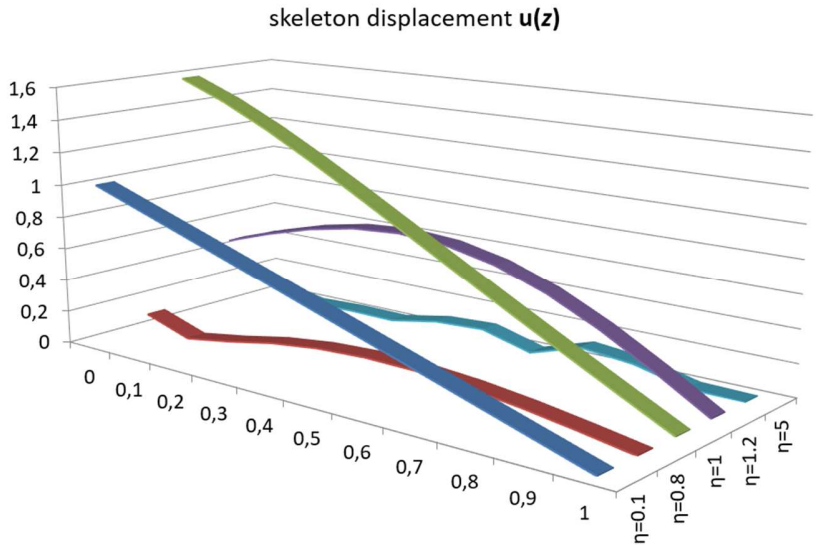

Fig. 5.2: Displacement of the soil skeleton versus normalized depth for FD analysis for five different η

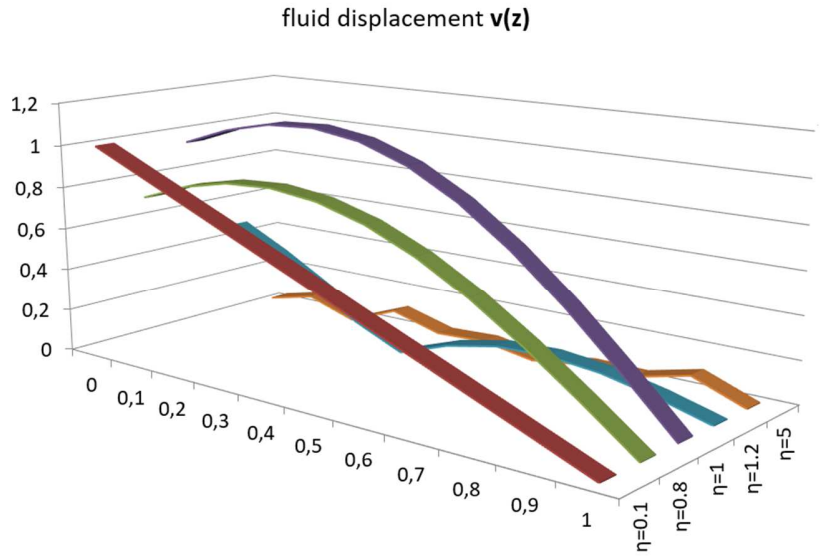

Fig. 5.3: Displacement of the fluid versus normalized depth for FD analysis for five different η

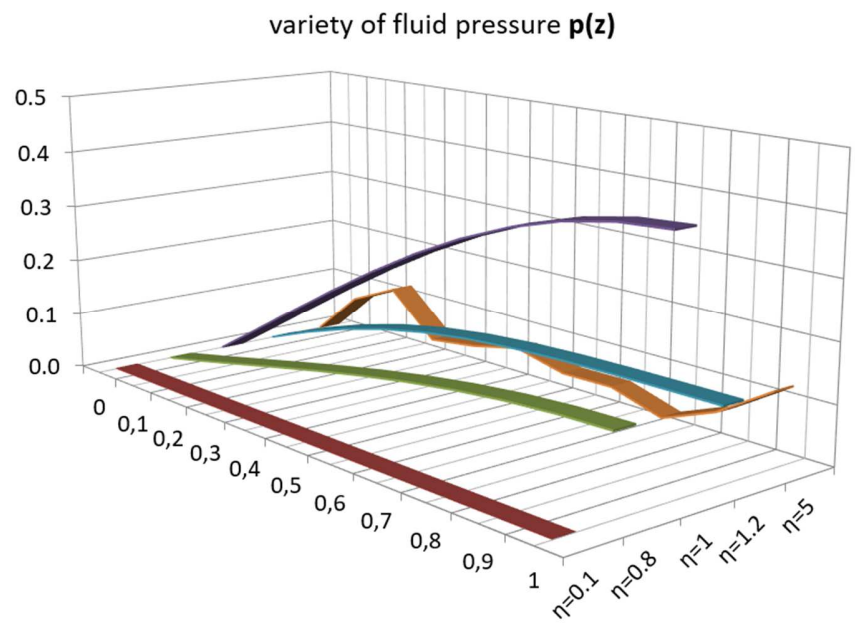

Fig. 5.4: General variation of the fluid pressure versus normalized depth for FD analysis for five different η

The set of figures below (Fig. 5.5, Fig. 5.6 and Fig. 5.7) on the contrary, present the comparison of the skeleton and the fluid displacement for analyzed formulations and for three exemplary η.

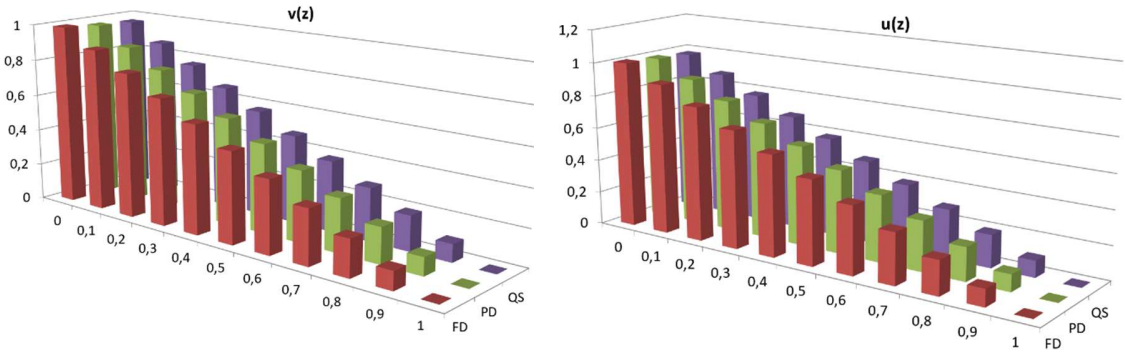

Fig. 5.5: Skeleton and fluid displacement versus normalized depth for Biot's, u-p and consolidation model for η=0,1

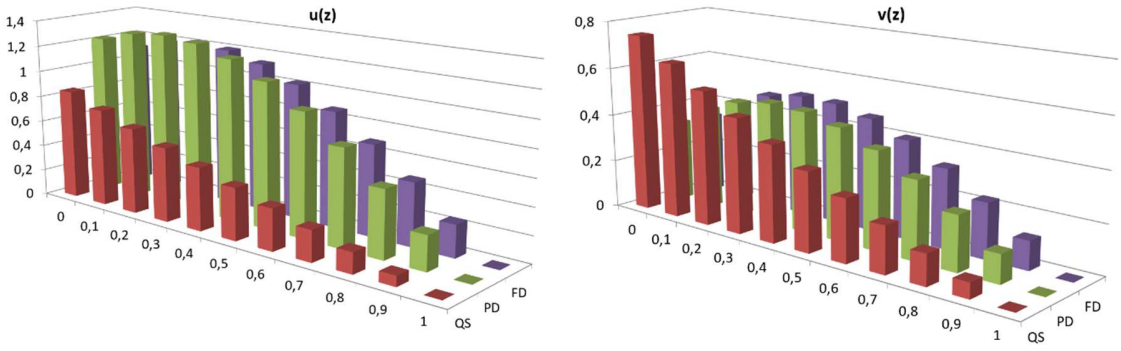

Fig. 5.6: Skeleton and fluid displacement versus normalized depth for Biot's, u-p and consolidation model for η=1

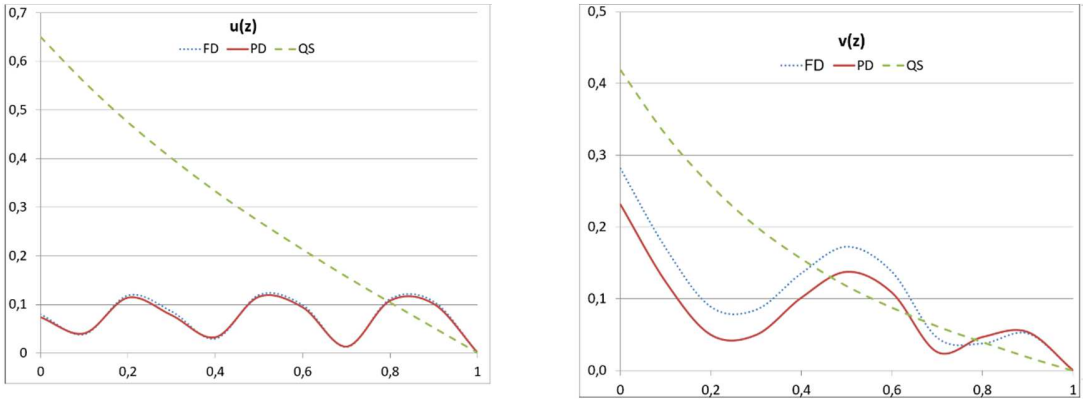

Fig. 5.7: Skeleton and fluid displacement versus normalized depth for Biot's, u-p and consolidation model for η=5

For η=5 (Fig. 5.7) there is a different type of graph used, because it shows the oscillations and the violent changes much better than the column graph.

When it comes to the fluid pressure, the disparity between analyzed models is also bigger for higher frequencies as shown in Fig. 5.8 presenting the pressure as a function of depth.

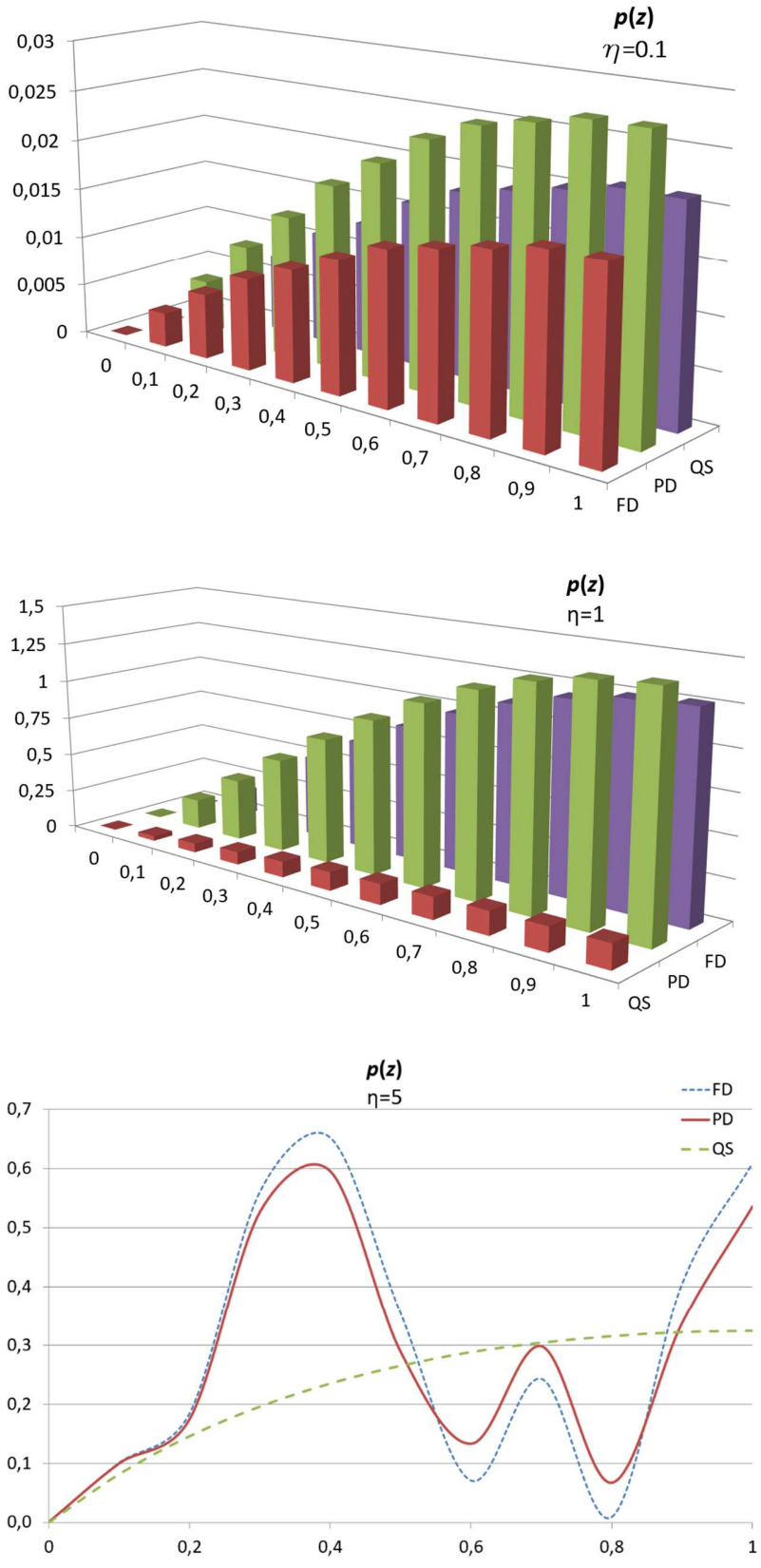

Fig. 5.8: Fluid pressure versus normalized depth for Biot's, u-p and consolidation model for η=0.1, η=1 and η=5 respectively

The analytical study described helps us to determine the limits of applicability of the various assumptions in the particular case of a linear one-dimensional and periodic problem. An extrapolation of the conclusions can be made to other more realistic problems of soil mechanics giving some quantitative basis for the recommended analysis procedure and avoiding a priori assumptions.

The main question which is raised in the thesis is when the PD or even QS model is sufficient and whether FD analysis is necessary to conduct. There are three main conclusions which can be done after calculations in previous sections :

- for low excitation frequency ($\eta \leq 0.1$) the three analyzed models have similar results, so there is no point in doing expanded calculations accompanying the PD or FD idealization ;
- the influence of the fluid inertia forces is very low even for $\eta = 1$, so it is not an error to neglect them for $\eta \leq 1$ (PD idealization is sufficient) ;
- if the skeleton displacement is of main interest, it is possible to conduct the PD idealization (which neglects the fluid inertia forces) even for relatively high excitation frequency ($\eta = 5$).

5.2. Influence of soil physical parameters on harmonic response.

5.2.1. Introduction.

The Equations (5.4) and (5.5) for the fully dynamic idealization can be written as follows (Wrana & Pietrzak, 2013):

$$\left(D + \frac{1-n}{n} D_f \right) \mathrm{u}^s{}_{,xx} + D_f \mathrm{u}^f{}_{,xx} = (1-n)\rho_s \ddot{\mathrm{u}}^s + n\rho_f \ddot{\mathrm{u}}^f \tag{5.15}$$

$$D_f \left(\frac{1-n}{n} \mathrm{u}^s{}_{,xx} + \mathrm{u}^f{}_{,xx} \right) = \rho_f \ddot{\mathrm{u}}^s + \frac{n\rho_f g}{k} \left(\dot{\mathrm{u}}^f - \dot{\mathrm{u}}^s \right) \tag{5.16}$$

where

$D_f = \frac{K_f}{n}$ - bulk modulus of the air-fluid mixture

n - porosity

and introducing the following

$$\chi = \frac{D}{D_f},\ \beta = \frac{1}{n + (1-n)G_s},\ c_w = \sqrt{\frac{D_f}{\rho_f}},\ w = n\left(u^f - u^s\right) = n\left(v - u\right),\ G_s = \frac{\rho_s}{\rho_f}$$

the above equations (5.14) and (5.15) become:

$$\frac{1}{\beta}\ddot{u} + \ddot{w} = c^2{}_w \left(\left(\frac{1}{n} + \chi \right) u_{,xx} + \frac{1}{n} w_{,xx} \right) \tag{5.17}$$

$$\ddot{u} + \frac{1}{n}\ddot{w} + \frac{g}{k}\dot{w} = c^2{}_w \left(\frac{1}{n} u_{,xx} + \frac{1}{n} w_{,xx} \right) \tag{5.18}$$

The above equations (5.16), (5.17) present the transfer of energy between solid and fluid phases, which result from the viscous forces of interaction between the solid and fluid phases. Biot showed that the energy dissipation per unit volume is :

$$E_d = 0.5 \frac{g\rho_f}{D_f} \left(\dot{w}\right)^2 . \tag{5.19}$$

5.2.2. Steady state response of the Biot column.

5.2.2.1. Analytical solution.

The Biot column (Fig. 5.9) is fixed and undrained at the bottom (x=L) but it is free to displace and drained at the top (x=0). It is subjected to normal, harmonic pressure at the top having the angular frequency ω.

Solutions of the steady state response of the Biot column are written in the form:

$$u(x,t) = U(x)e^{i\omega t} \tag{5.20}$$

$$w(x,t) = W(x)e^{i\omega t} \tag{5.21}$$

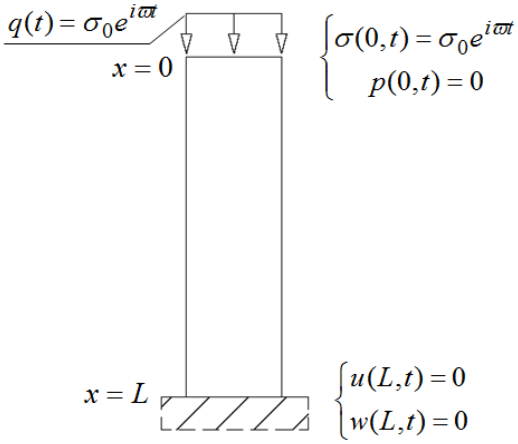

Fig. 5.9: Geometry and boundary conditions of the Biot column

where $i = \sqrt{-1}$ and *U(x)* and *W(x)* are

$$U(x) = Ae^{\lambda x} \tag{5.22}$$

$$W(x) = Be^{\lambda x}. \tag{5.23}$$

When substituting them into the equation of energy transfer (5.17) and (5.18) between solid and fluid we obtain (Bardet, 1995)

$$A\left(\psi^2\left(\chi + \frac{1}{n}\right) + \frac{1}{\beta}\right) + B\left(\frac{\psi^2}{n} + 1\right) = 0 \tag{5.24}$$

$$A\left(\frac{\psi^2}{n} + 1\right) + B\left(\frac{\psi^2}{n} + \frac{1}{n} - i\frac{g}{k\omega}\right) = 0 \tag{5.25}$$

where

$\psi = \frac{c_w \lambda}{\omega}$,

c_w – wave velocity in the fluid defined in section 5.2.1

λ – unknown, number characterizing the wave length corresponding to the frequency ω

A, B – unknowns.

If we want to have a nontrivial solution, the determinant of the above equations must be equal to zero, which gives the characteristic equation :

$$\frac{\chi}{n}\psi^4 + a\psi^2 + b = 0 \tag{5.26}$$

where

$$a = \left(\chi + \frac{1}{n}\right)\frac{1}{n} + \frac{1}{n\beta} - \frac{2}{n} - i\frac{g}{k\omega}\left(\frac{1}{n} + \chi\right) \tag{5.27a}$$

$$b = \frac{1}{n\beta} - 1 - i\frac{g}{k\omega}\frac{1}{\beta} \tag{5.27b}$$

The above characteristic equation always has four complex roots:

$$\psi_{1,3} = \pm\sqrt{\frac{-an-\sqrt{n^2a^2-4bn\chi}}{2\chi}} \tag{5.28a}$$

$$\psi_{2,4} = \pm\sqrt{\frac{-an+\sqrt{n^2a^2-4bn\chi}}{2\chi}} \tag{5.28b}$$

After calculating these roots, $U(x)$ and $W(x)$ can be found from:

$$U(x) = A_1e^{\lambda_1 x} + A_2e^{\lambda_2 x} + A_3e^{-\lambda_1 x} + A_4e^{-\lambda_2 x} \tag{5.29}$$

$$W(x) = K_1A_1e^{\lambda_1 x} + K_2A_2e^{\lambda_2 x} + K_1A_3e^{-\lambda_1 x} + K_2A_4e^{-\lambda_2 x} \tag{5.30}$$

where the complex constants are:

$$K_1 = -\frac{\psi_1^2(1+n\chi)+\frac{n}{\beta}}{\psi_1^2+n} \tag{5.31a}$$

$$K_2 = -\frac{\psi_2^2(1+n\chi)+\frac{n}{\beta}}{\psi_2^2+n} \tag{5.31b}$$

In order to calculate A_1, A_2, A_3 and A_4 it is necessary to analyze the boundary solutions for the aforementioned Biot column. As we can see in Fig. 5.9, the applied stress is harmonic with a frequency ω and amplitude σ_0. The D is given and defined in Appendix 1 by (Z1.10). The boundary conditions are :

$$\sigma'(0,t) = \sigma_0 e^{i\varpi t} \rightarrow u_{,x} = \frac{\sigma_0}{D}e^{i\varpi t}$$

$$p(0,t) = 0 \rightarrow w,_x = -\frac{\sigma_0}{D}$$

$$u(L,t) = 0 \rightarrow U(L) = 0$$

$$w(L,t) = 0 \rightarrow W(L) = 0 \tag{5.32}$$

When substituting the formulas of $U(x)$ and $W(x)$ we have :

$$A_1 e^{\lambda_1 L} + A_2 e^{\lambda_2 L} + A_3 e^{-\lambda_1 L} + A_4 e^{-\lambda_2 L} = 0$$

$$A_1 K_1 e^{\lambda_1 L} + A_2 K_2 e^{\lambda_2 L} + A_3 K_1 e^{-\lambda_1 L} + A_4 K_2 e^{-\lambda_2 L} = 0$$

$$A_1 \lambda_1 + A_2 \lambda_2 - A_3 \lambda_1 - A_4 \lambda_2 = \frac{\sigma_0}{D}$$

$$A_1 K_1 \lambda_1 + A_2 K_2 \lambda_2 + A_3 K_1 \lambda_1 + A_4 K_2 \lambda_2 = -\frac{\sigma_0}{D} \tag{5.33}$$

After solving this set of equations we obtain:

$$A_1 = \frac{L\sigma_0}{D} \frac{K_2 + 1}{(K_2 - K_1)\lambda_1 L} \frac{1}{1 + e^{2\lambda_1 L}}$$

$$A_2 = \frac{L\sigma_0}{D} \frac{K_1 + 1}{(K_1 - K_2)\lambda_2 L} \frac{1}{1 + e^{2\lambda_2 L}}$$

$$A_3 = -A_1 e^{2\lambda_1 L}$$

$$A_4 = -A_2 e^{2\lambda_2 L} \tag{5.34}$$

As a consequence the amplitude $U(x)$ of the solid phase displacement $u(x,t)$ is

$$U(x) = \frac{L\sigma_0}{D} \frac{1}{K_2 - K_1} \left(\frac{(K_2 + 1)\sinh[\lambda_1 (x - L)]}{\lambda_1 L \cosh[\lambda_1 L]} - \frac{(K_1 + 1)\sinh[\lambda_2 (x - L)]}{\lambda_2 L \cosh[\lambda_2 L]} \right) \tag{5.35}$$

and the amplitude $W(x)$ of the solid phase displacement $w(x,t)$ is

$$W(x) = \frac{L\sigma_0}{D} \frac{1}{K_2 - K_1} \left(\frac{K_1 (K_2 + 1)\sinh[\lambda_1 (x - L)]}{\lambda_1 L \cosh[\lambda_1 L]} - \frac{K_2 (K_1 + 1)\sinh[\lambda_2 (x - L)]}{\lambda_2 L \cosh[\lambda_2 L]} \right) \tag{5.36}$$

Knowing the expression for change in the fluid pressure and the meaning of relative displacement we can write :

$$\Delta p = \frac{D_f}{n}\left(\frac{\partial u}{\partial x} + \frac{\partial w}{\partial x}\right) \tag{5.37}$$

For harmonic solutions, the above becomes

$$\Delta p(x,t) = \frac{D_f}{n}\left(\frac{\partial U}{\partial x} + \frac{\partial W}{\partial x}\right) e^{i\omega t} = \Delta P(x) e^{i\omega t} \tag{5.38}$$

If we substitute into the above expression the formulas of $U(x)$ and $W(x)$, we obtain:

$$\Delta P(x) = \frac{\sigma_0}{n\chi} \frac{(K_1+1)(K_2+1)}{K_2 - K_1} \left(\frac{\cosh[\lambda_1 (x-L)]}{\cosh[\lambda_1 L]} - \frac{\cosh[\lambda_2 (x-L)]}{\cosh[\lambda_2 L]} \right). \tag{5.39}$$

5.2.2.2. Variations of parameters.

In order to make the calculations more clear, it is appropriate to introduce the dimensionless circular frequency Δ and dimensionless permeability K :

$$\Delta = \frac{\omega L}{c_0} \tag{5.40}$$

$$K = \frac{gL}{kc_0} \tag{5.41}$$

where

$$c_0 = c_w \sqrt{\beta\left(\chi + \frac{1}{n}\right)} \tag{5.42}$$

In terms of Δ and K eq.(5.26a), (5.26b) becomes

$$a = \left(\chi + \frac{1}{n}\right)\frac{1}{n} + \frac{1}{n\beta} - \frac{2}{n} - i\frac{K}{\Delta}\left(\frac{1}{n} + \chi\right) \tag{5.43a}$$

$$b = \frac{1}{n\beta} - 1 - i\frac{K}{\Delta}\frac{1}{\beta} \tag{5.42b}$$

As a consequence the analytical solutions for U, W and ΔP depend on five dimensionless parameters : n, β, c, Δ and K which depend on soil properties n, G_s, k and D , the water properties S and p, the geometry L, and the circular frequency ω.

5.2.2.3. Water properties.

As it was mentioned before we take into consideration only nearly saturated soils, which consist of the skeleton and the homogenous fluid made of water and dissolved gas. The bulk modulus of the fluid strongly depends on the degree of saturation *S*. It is equal to 2200MPa for *S*=100%, 100MPa for *S*=99.9%, 10MPa for *S*=99%, 2MPa for *S*=95% and 1MPa for *S*=90%.

5.2.2.4. Soil properties.

The ranges of variation of typical soil properties are quite wide. The approximate values for gravel are summarized below.

n = 0.12 – 0.46
G_s = 2.6 – 2.7
k = 10 – 10^{-1} cm/s
D = 200 MPa

The thesis does the calculations for the average coefficients. Knowing the extent of fluid bulk modulus D_f, we can summarize that the coefficient K ranges from 0.1 to about 50.

5.2.3. Examples of spectral response for gravel.

5.2.3.1. Amplification factor of solid displacement.

As it was mentioned before, the Biot column is analyzed, which might be considered as a layer of saturated soils that underlies the porous base of a structure or a piece of machinery. Its dynamic properties are characterized by the amplitude $U(x)$ of the solid phase.

$$U(x) = \frac{L\sigma_0}{D} G(\Delta, x) \tag{5.44}$$

An amplification factor $G(\Delta)$ can be easily obtained from eq.(5.35)

$$G(\Delta) = \frac{1}{K_2 - K_1}\left(\frac{(K_2+1)\sinh[\lambda_1(x-L)]}{\lambda_1 L \cosh[\lambda_1 L]} - \frac{(K_1+1)\sinh[\lambda_2(x-L)]}{\lambda_2 L \cosh[\lambda_2 L]} \right) \tag{5.45}$$

If we are interested in the amplitudes at the top of the column, we have to equate x to 0 and as a consequence we achieve the following graphs Fig. 5.10 and Fig. 5.11 showing the variety of the spectral response for different degrees of saturation and dimensionless permeability. The same

relations but in three dimensions are presented in Fig. 5.16 and Fig. 5.17. Irrespective of the soil parameters, the Biot column experiences a large dynamic amplification with very sharp peaks when $\Delta = \pi/2, 3\pi/2$ and $5\pi/2$. It can be deduced, that $\pi/2$ is a fundamental period of the column and for these frequencies the solid phase is in resonance. The peaks gradually decrease as the degree of saturation increases. What is more, for lower dimensionless permeability the peaks became less attenuated and their number increases for S=100%. Fig. 5.12 and Fig. 5.13 present a range of variety of the same factor but versus the depth of the column (x coordinate) for different frequencies and permeabilities. As it was expected, the amplitudes would decrease as we go deeper in the ground.

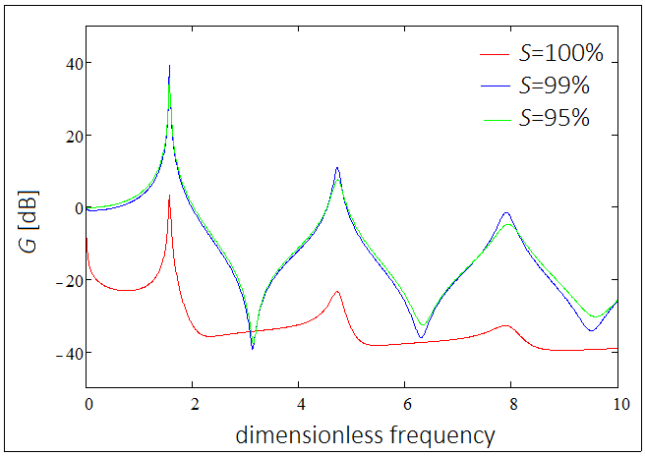

Fig. 5.10: Amplification factor $G(\Delta)$ versus Δ for conductivity coefficient K=50 and different degrees of saturation S

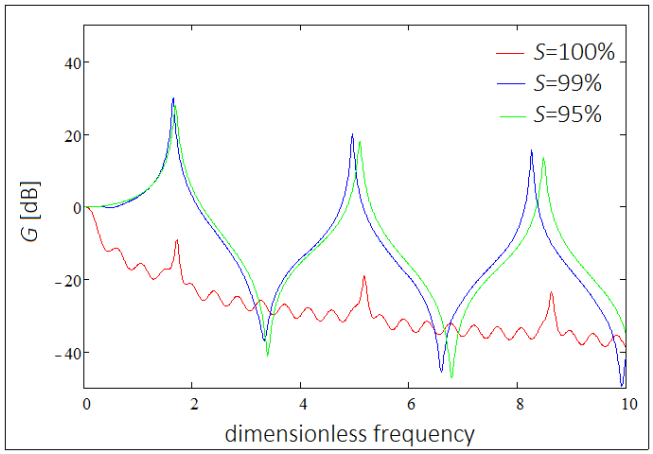

Fig. 5.11: Amplification factor $G(\Delta)$ versus Δ for conductivity coefficient K=1 and different degrees of saturation S

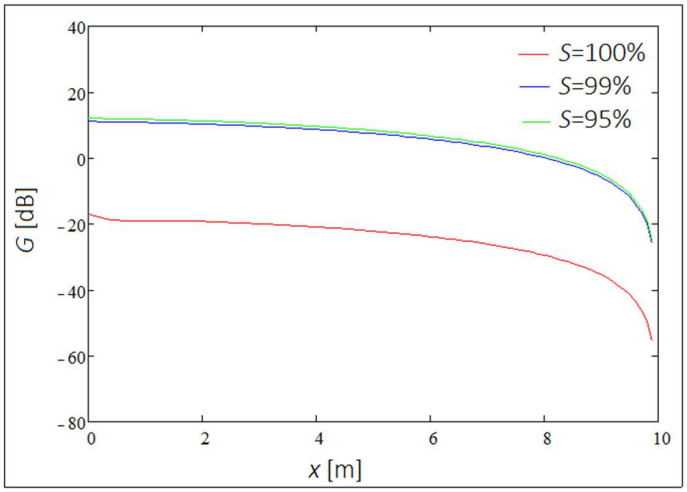

Fig. 5.12: Amplification factor $G(\Delta)$ versus depth x for conductivity coefficient K=50 and Δ =1.4 and different degrees of saturation S

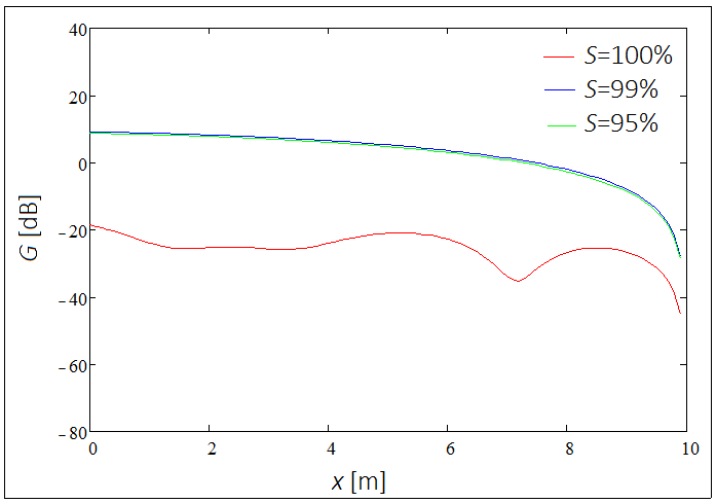

Fig. 5.13: Amplification factor $G(\Delta)$ versus depth x for conductivity coefficient K=1 and Δ =1.4 and different degrees of saturation S

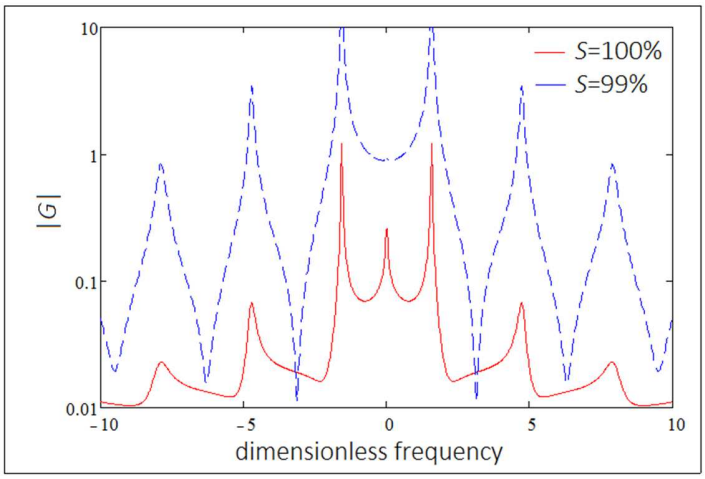

Fig. 5.14: Absolute value of amplification factor $G(\Delta)$ versus dimensionless frequency Δ for conductivity coefficient K=50 and x=0m, and different degrees of saturation S

Fig. 5.14 presents the absolute value of the $G(0)$ for K=1 and two different degrees of saturation. This graph has an important physical interpretation, for values $G(0) < 1$ the dynamic response becomes smaller than the static one ($\Delta = 0$ and $G(0) = 1$ for the static case). For $G(0) > 1$ there is always a dynamic amplification. The next Figure shows the same relation but for a different value of K.

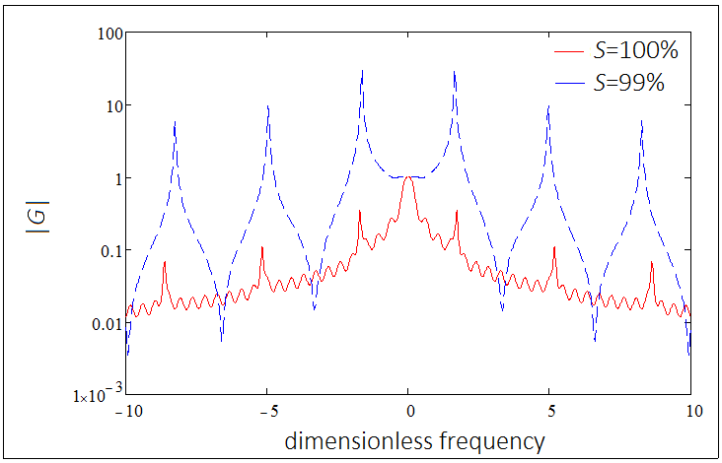

Fig. 5.15: Absolute value of amplification factor $G(\Delta)$ versus dimensionless frequency Δ for conductivity coefficient K=1 and x=0m, and different degrees of saturation S

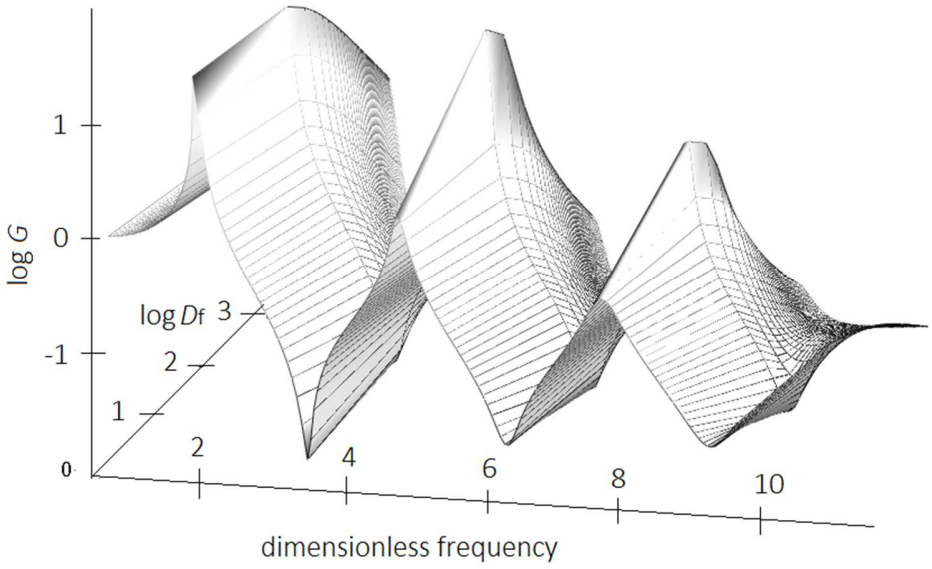

Fig. 5.16: Amplification factor $G(\Delta)$ versus dimensionless frequency Δ and $\log D_f$ for conductivity coefficient K=50 and x=0m

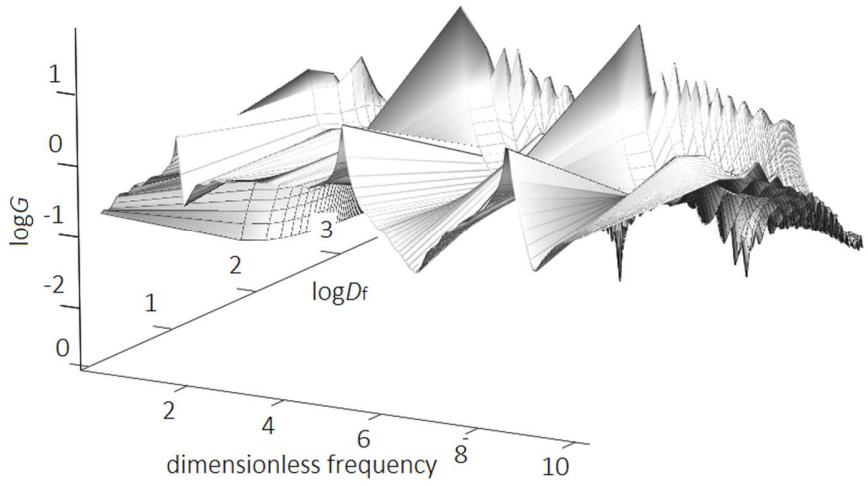

Fig. 5.17: Amplification factor $G(\Delta)$ versus dimensionless frequency Δ and $\log D_f$ for conductivity coefficient K=1 and x=0m

5.2.3.2. Velocity of compressional wave.

The velocity of the fast compressional wave is defined as :

$$c_1 = \frac{-c_w}{Im(\psi_1)} \tag{5.46}$$

where

$c_w = \sqrt{\frac{D_f}{\rho_f}}$ - wave velocity in the fluid

ψ_1 - defined in 5.2.2.1.

Fig. 5.18 and Fig. 5.19 show the velocity c_1 versus dimensionless frequency for different degrees of saturation S and K. In Fig. 5.18 the velocity strongly depends on the frequency of applied load. It means that for K=50 the soil is a dispersive media, while for K=1 and Δ>1 (Fig. 5.19) the soil is an elastic media, which on the contrary means that the applied load frequency does not affect the wave velocity.

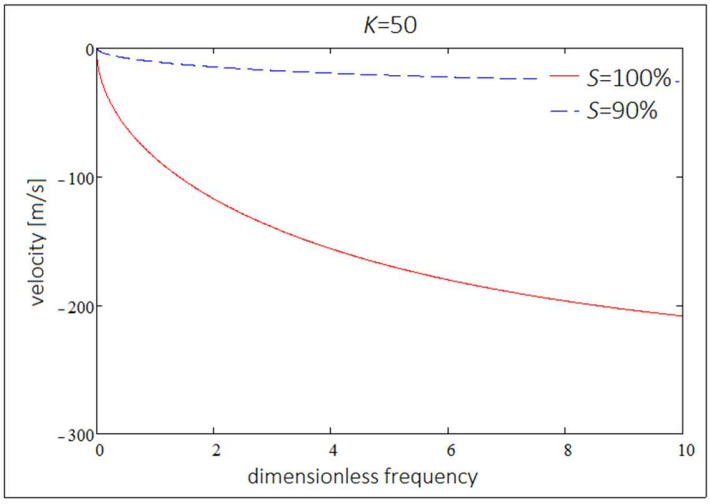

Fig. 5.18: Velocity c_1 versus dimensionless frequency Δ for two different degrees of saturation for *K*=50

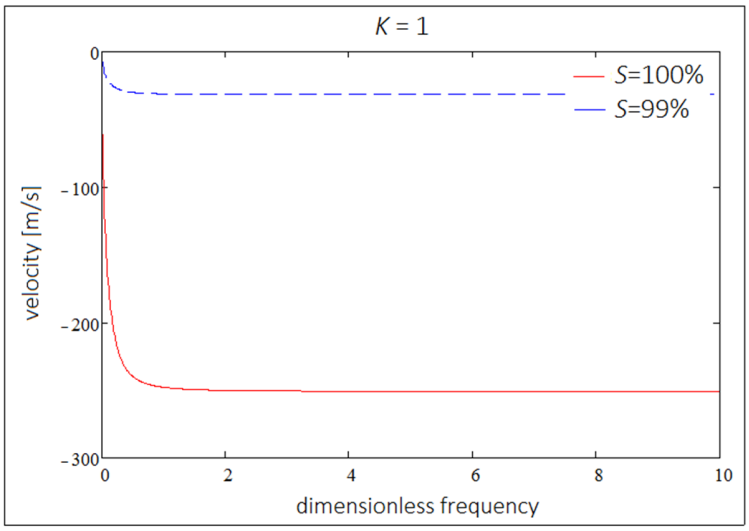

Fig. 5.19: Velocity c_1 versus dimensionless frequency Δ for two different degrees of saturation for K=1

5.2.3.3. Solid phase displacement.

As we can see in Fig. 5.20 (according to eq. (5.44) and (5.45)), the amplitude is the highest at the top of the Biot column, which is obvious, because that is the place where the extortion is applied. As it was mentioned before, $\Delta=\pi/2$ is the column's fundamental period and as the result the solid phase displacement violently increases around this value. The Biot column is clamped at the bottom, which explains the zero displacements for x=10m.

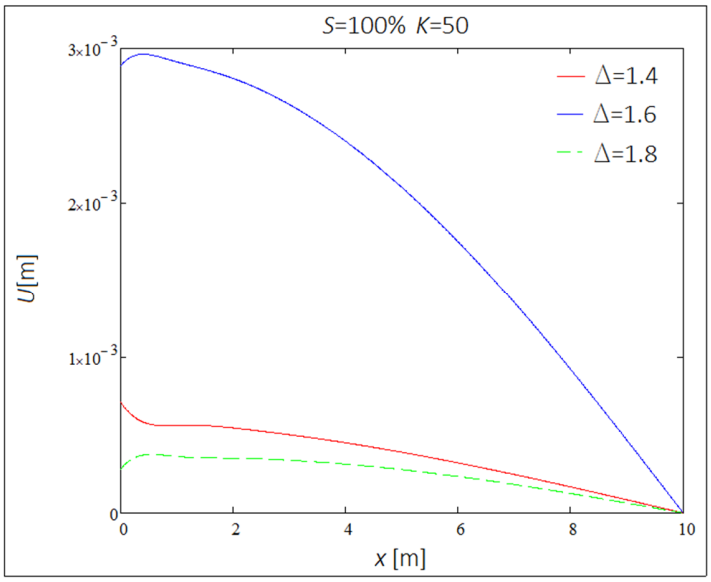

Fig. 5.20: Solid displacement versus *x* coordinate for three different extortions Δ for K=50

5.2.3.4. Relative displacement of the fluid.

At first it is appropriate to introduce an amplification factor for the relative displacement of the fluid. Similarly as for the solid phase, we can write

$$W(x) = \frac{L\sigma_0}{D} G_w(\Delta, x) \tag{5.47}$$

where

$$G_w(\Delta, x) = \frac{1}{K_2 - K_1}\left(\frac{K_1(K_2+1)\sinh[\lambda_1(x-L)]}{\lambda_1 L\cosh(\lambda_1 L)} - \frac{K_2(K_1+1)\sinh[\lambda_2(x-L)]}{\lambda_2 L\cosh(\lambda_{2L})}\right) \tag{5.48}$$

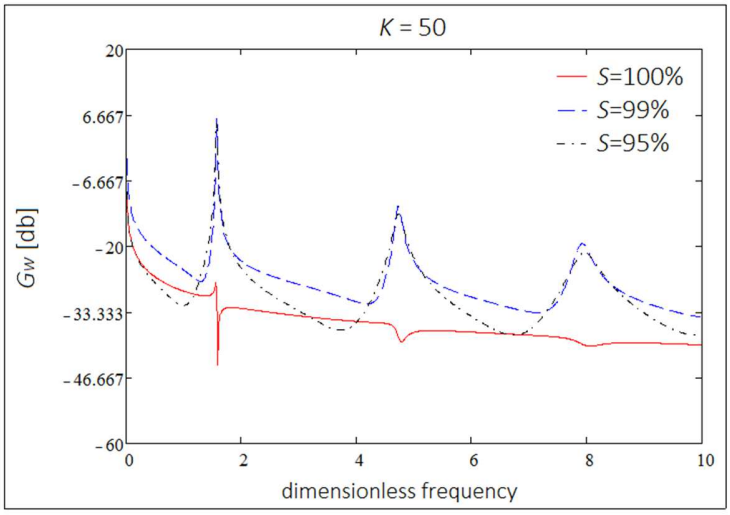

Fig. 5.21: Amplification factor $G_w(\Delta)$ versus Δ for conductivity coefficient K=50 and three different degrees of saturation S

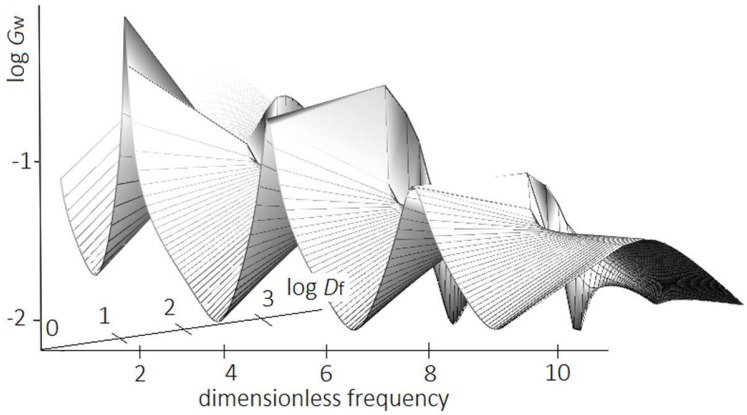

Fig. 5.22:Amplification factor $G_w(\Delta)$ versus Δ and log(D_f) for conductivity coefficient K=50

Fig. 5.23 shows the variation of an amplitude $W(x)$ versus Δ for various values of K and S. The relative displacement $W(x)$ is more chaotic then $U(x)$. There are local drops and pickups. For S=99% and less, $W(x)$ for the resonance frequency is about ten times bigger from other amplitudes. This occurrence does not happen for fully saturated soils contrary to solid displacement, where the differences of the displacements for the resonance frequencies and the remaining ones are substantial. For the static case (Δ =0) the relative displacement is the biggest, which means that fluid damping is considerable.

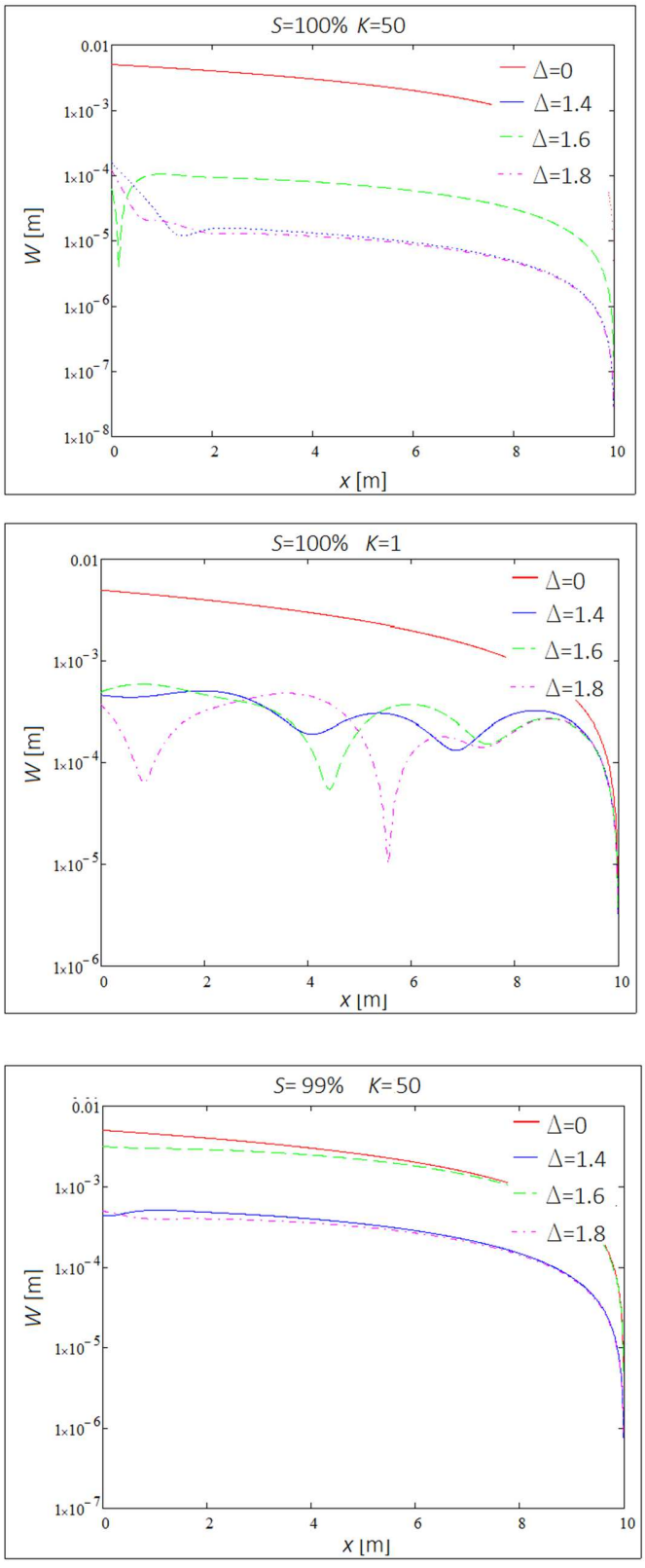

Fig. 5.23: Fluid relative displacement versus *x* coordinate for four different extortions Δ and for various *K* and *S*

5.2.3.5. Amplitude of the pore pressure.

We apply the same approach as previously. We can write :

$$\Delta P = \frac{\sigma_0}{n\chi} G_{\Delta P}(\Delta, x) \tag{5.49}$$

where

$$G_{\Delta P}(\Delta, x) = \frac{(K_1+1)(K_2+1)}{K_2-K_1}\left(\frac{\cosh[\lambda_1(x-1)]}{\cosh[\lambda_1 L]} - \frac{\cosh[\lambda_2(x-1)]}{\cosh[\lambda_2 L]}\right) \tag{5.50}$$

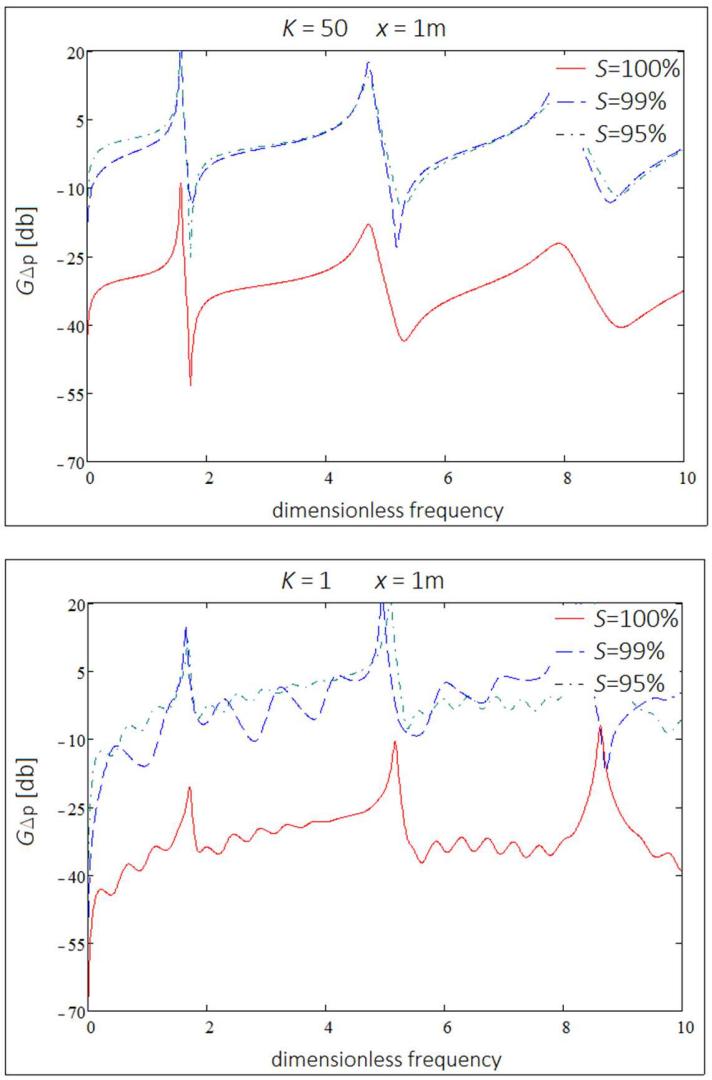

Fig. 5.24: Amplification factor $G_{\Delta p}(\Delta)$ versus Δ for two different conductivity coefficients and for x=1m for different degrees of saturation S

Fig. 5.24 presents an amplification factor $G_{\Delta p}$ versus dimensionless frequency. The above graph is for a depth x=1m, because for x=0m, as it is expected, the fluid pressure is equal to zero. Water can freely drain from the soil. It is noticeable that for high permeability, the amplification factor has lots of local drops and pickups. As shown in Fig. 5.25 the water pressure is quite turbulent for high permeability, while it increases evenly with depth for lower permeabilities.

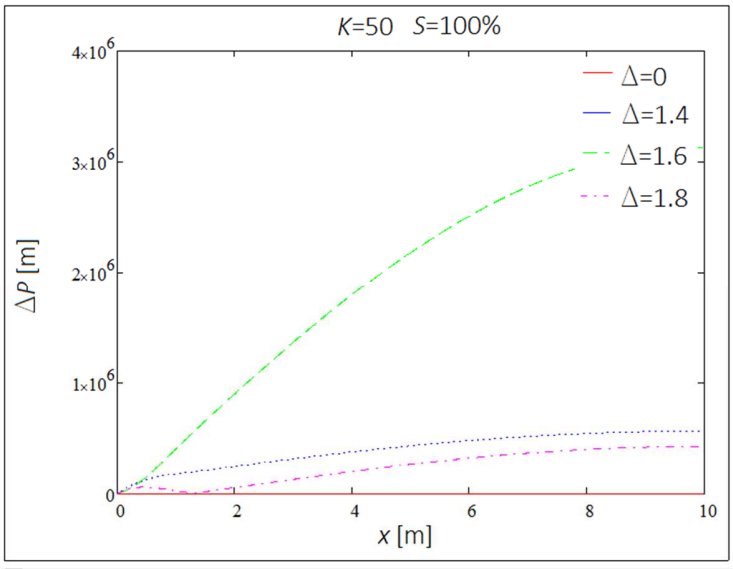

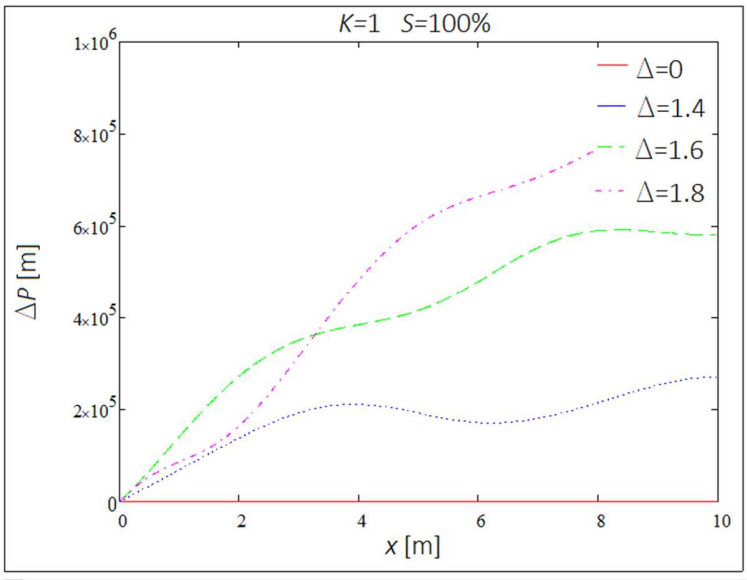

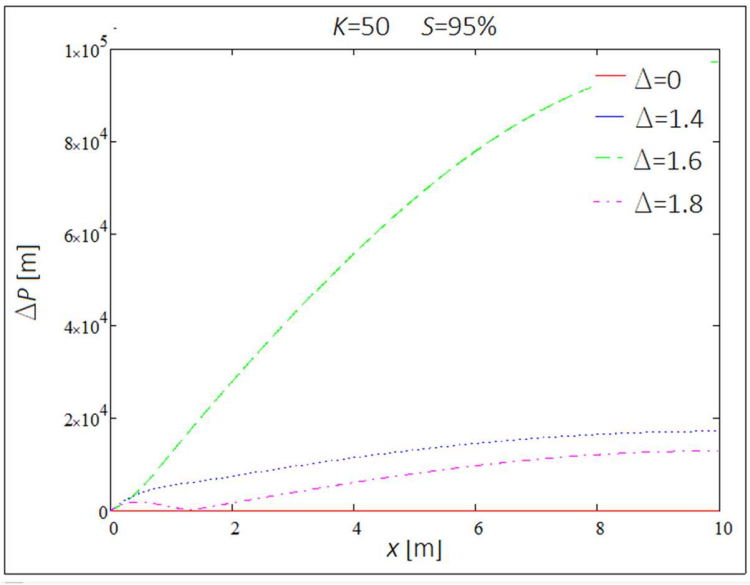

Fig. 5.25: Pore pressure amplitude versus *x* coordinate for four different extortions and various *K* and *S*

As we can see in Fig. 5.26, for fully saturated gravels at the fundamental frequency, the water pressure is much higher than in nearly saturated soils.

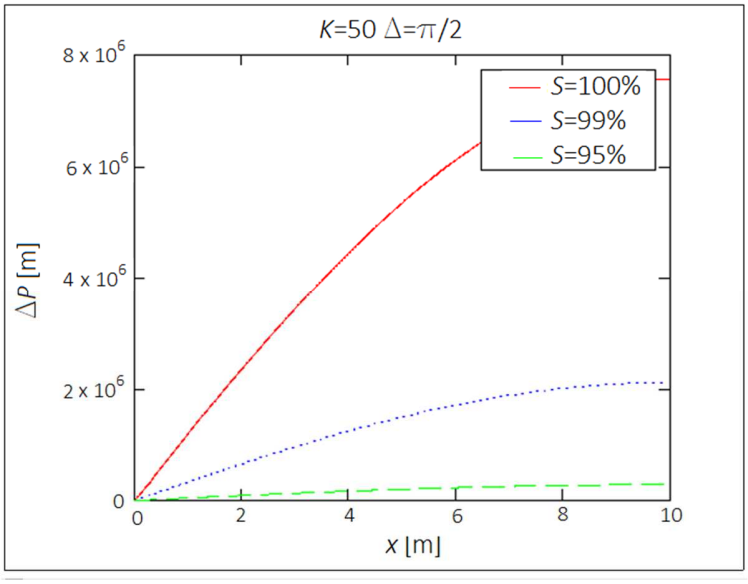

Fig. 5.26: Pore pressure amplitude versus *x* coordinate for *K*=1 and $\Delta=\pi/2$ and for various *S*

5.2.4. Conclusions.

The chapter included the analytical solution of the harmonic response of a column made of nearly and fully-saturated poroelastic materials using the Biot's theory. The study revealed the relative influence of the degree of saturation, permeability, and matrix rigidity on the fundamental period , the maximum amplitude and the dissipated energy. Parameters used in the article concern gravels. In the future work it is needed to find the solution for an undrained case, which is clay.

As it was proved in previous sections, the water diffusion plays an important role in the dynamic behavior of nearly and fully-saturated gravels, which vary from undamped ($|G|>1$) to overdamped ($|G|<<1$) depending on the degree of saturation.

6. Solution methods. Two dimensional problem of consolidation and dynamics.

6.1. Basic equations.

For the two dimensional problem the partly dynamic idealization ($\mathbf{u}^s$ –p formulation) is applied described in Section (5.1.2). Simplified set of equations (4.24), (4.27) and (4.33) eliminating the members of relative velocity $\mathbf{w}$ of pore water with respect to skeleton.

The following simplification in the equations used:

- omitted in equations (4.24) and (4.27) member $\dot{\mathbf{w}} + \mathbf{w}\nabla^{\mathrm{T}}\mathbf{w} = \mathbf{0}$, as small with respect to $\mathbf{u}^{\boldsymbol{s}} = \mathbf{u}$ – displacement of skeleton and with respect to p – pore water pressure.
- assumed the linear Darcy seepage law $\mathbf{kR} = \mathbf{w}$,
- omitted the water density changes in time, $\dot{\rho}^f = 0$,
- omitted the effects of temperature changes in time $\dot{s}_0 = \mathbf{0}$.

Equation (4.24) takes the form

$$\mathbf{L}^{\mathrm{T}}\boldsymbol{\sigma} - \rho\ddot{\mathbf{u}}^{\boldsymbol{s}} + \rho\mathbf{b} = 0 \qquad \text{n} \qquad (6.1)$$

where $\mathbf{L}$ is the differential operator defined in Appendix 1.

From the eq.(4.27) determine the force $\mathbf{R} = -\nabla p - \rho^f \ddot{\mathbf{u}}^s + \rho^f \mathbf{b} = 0$, hence Darcy seepage law can be written as $\mathbf{kR} = \mathbf{k}\left(-\nabla p - \rho^f \ddot{\mathbf{u}}^s + \rho^f \mathbf{b}\right) = \mathbf{w}$. Then, substituting to (4.33) received

$$\nabla^{\mathrm{T}}\mathbf{k}\left(-\nabla p - \rho^f \ddot{\mathbf{u}}^s + \rho^f \mathbf{b}\right) + \alpha \mathbf{m}\dot{\boldsymbol{\varepsilon}} + \frac{1}{Q}\dot{p} + \dot{s}_o = 0. \tag{6.2}$$

Equations (6.1) and (6.2) are dynamics consolidation equations which take into account the inertia forces $\rho\ddot{\mathbf{u}}^s$and $\rho^f \ddot{\mathbf{u}}^s$.

Omitting members of inertia forces we can obtained the two phase soil equations for static consolidation problem

$$\mathbf{L}^{\mathrm{T}}\boldsymbol{\sigma} + \rho\mathbf{b} = 0$$
$$\nabla^{\mathrm{T}}\mathbf{k}\left(-\nabla p + \rho^f \mathbf{b}\right) = 0. \tag{6.3}$$

Initial conditions

The initial conditions for the soil skeleton are: known the displacement at time t_o, $\mathbf{u}^s(t = t_o) = \mathbf{u}_o^s$ and known the velocity at time t_o, $\dot{\mathbf{u}}^s(t = t_o) = \dot{\mathbf{u}}_o^s$.

The initial condition for the pore water is - known the pore water pressure at time t_o, $p(t = t_o) = p_o$.

Boundary conditions

The boundary conditions for the soil skeleton are: known the displacement $\bar{\mathbf{u}}^s$ on the boundary Γ_u and known the normal stress $\mathbf{n}\boldsymbol{\sigma} = \bar{\mathbf{t}}$ on the boundary Γ_u^q, where $\Gamma = \Gamma_u \cup \Gamma_u^q$

The boundary conditions for the pore water are: known the pore water pressure $p = q$ on the boundary Γ_p and the water flow q^f through the boundary Γ_p^q, where $\Gamma = \Gamma_p \cup \Gamma_p^q$

Determined values of the boundary conditions:

- displacement of skeleton $\mathbf{u}^s = \bar{\mathbf{u}}^s$, on Γ_u, (6.4)
- normal stress $\mathbf{N}^T\boldsymbol{\sigma} = \bar{\mathbf{t}}$, on Γ_u^q, (6.5)
- pore water pressure $p = \bar{p}$, on Γ_p. (6.6)

where $\mathbf{N} = \begin{bmatrix} n_1 & 0 & 0 & n_2 & 0 & n_3 \\ 0 & n_2 & 0 & n_1 & n_3 & 0 \\ 0 & 0 & n_3 & 0 & n_2 & n_1 \end{bmatrix}$

- water flow condition

$$\frac{\rho^f}{\mu^w}\mathbf{k}\left(-\text{grad}p_f + \rho^f\mathbf{b} - \rho^f\ddot{\mathbf{u}}^s\right)^{\mathrm{T}}\mathbf{n} = q^w \text{ on } \Gamma_p^q \tag{6.7}$$

where q^w – known the external water flow normal to the boundary, $\mathbf{n} = \{n_1, n_2, n_3\}^{\mathrm{T}}$.

6.2. Weak formulation.

In case of the two-dimensional task, it is impossible to solve it analytically. The Finite Element Method is applied for the $\mathbf{u}^s$ –p formulation. In order to discretize the momentum equation (strong form) (6.1), (6.2), a weak form, often called a variational form or the principle of virtual work (or virtual power) will be developed. The weak form will be used to approximate the strong form by finite elements; solutions obtained by finite elements are approximate solutions to the strong form.

A weak form will now be developed for the momentum equation and the traction boundary conditions. For this purpose we define trial functions ($\mathbf{u}^s$, p^f) which satisfy any displacement boundary conditions and are smooth enough so that all derivatives in the momentum equation are well defined. The weight function ($\mathbf{w}$,p) are assumed to be smooth enough so that all of the following steps are well defined and to vanish on the prescribed displacement boundary. The weak form is obtained by taking the product of the momentum equation expressed in terms of the trial function with the test function. This gives

$$\int_\Omega \mathbf{w}^{\mathrm{T}}\left(\mathbf{L}^{\mathrm{T}}\boldsymbol{\sigma} - \rho\ddot{\mathbf{u}}^s + \rho\mathbf{b}\right)\mathrm{d}\Omega + \int_\Gamma \mathbf{w}^{\mathrm{T}}\left(\mathbf{N}^{\mathrm{T}}\boldsymbol{\sigma} - \bar{\mathbf{t}}\right)\mathrm{d}\Gamma_u = 0 \tag{6.8}$$

where for displacement of skeleton, trial function $\mathbf{u}^s$, once differentiable, adopted so as to satisfy the boundary conditions (6.4) and (6.5) on Γ_u, and weight function $\mathbf{w}$ satisfy vanish and prescribed condition on boundary

$\mathbf{w} = 0$ na Γ_u

$\bar{\mathbf{w}} = -\mathbf{w}$ na Γ_u^q. (6.9)

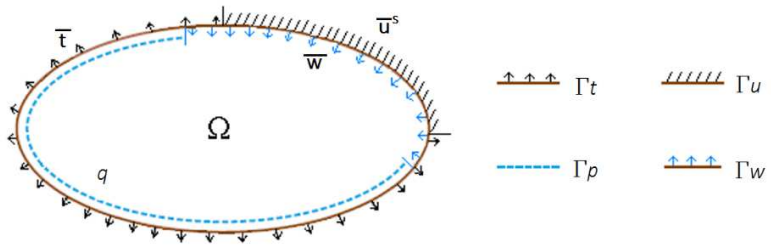

Fig. 6.1. Boundary conditions of two phase fully saturated soil model, more precisely discussed in Fig. 4.3.

Use of the Green theorem $\int_\Omega \varphi \frac{\partial \psi}{\partial x} \mathrm{d}\Omega = -\int_\Omega \frac{\partial \varphi}{\partial x} \psi \mathrm{d}\Omega + \int_\Gamma \varphi\psi \, n_x \mathrm{d}\Gamma$ with respect to the equation (6.43) one can receive

$$-\int_\Omega (\mathbf{Lw})^{\mathrm{T}} \boldsymbol{\sigma} \mathrm{d}\Omega + \int_\Gamma \mathbf{w}^{\mathrm{T}} \mathbf{N}^{\mathrm{T}} \boldsymbol{\sigma} \mathrm{d}\Gamma - \int_\Omega \mathbf{w}^{\mathrm{T}} \rho \ddot{\mathbf{u}}^s \mathrm{d}\Omega + \int_\Omega \mathbf{w}^{\mathrm{T}} \rho \mathbf{b} \mathrm{d}\Omega +$$

$$+ \int_{\Gamma_u^q} \bar{\mathbf{w}}^{\mathrm{T}} \left(\mathbf{N}^{\mathrm{T}} \boldsymbol{\sigma} - \bar{\mathbf{t}}\right) \mathrm{d}\Gamma = 0 \qquad (6.10)$$

and after taking into account eq.(6.9) finally obtained

$$\int_\Omega (\mathbf{Lw})^{\mathrm{T}} \boldsymbol{\sigma} \mathrm{d}\Omega = \int_\Omega \mathbf{w}^{\mathrm{T}} \rho \mathbf{b} \mathrm{d}\Omega - \int_\Omega \mathbf{w}^{\mathrm{T}} \rho \ddot{\mathbf{u}}^s \mathrm{d}\Omega + \int_{\Gamma_u^q} \bar{\mathbf{w}}^{\mathrm{T}} \bar{\mathbf{t}} \mathrm{d}\Gamma = 0. \qquad (6.11)$$

Now the weak formulation to mass balance equation for the soil-water mixture (6.2) is used and to boundary condition (6.7), obtained

$$\int_\Omega \mathbf{w}^{*\mathrm{T}} \left\{ \nabla^{\mathrm{T}} \left[\frac{\mathbf{k}}{\mu^w} \left(-\nabla p - \rho^f \ddot{\mathbf{u}}^s + \rho^f \mathbf{b} \right) \right] + \alpha \mathbf{m}^{\mathrm{T}} \mathbf{L} \dot{\mathbf{u}}^s + \left(\frac{\alpha - n}{K^s} + \frac{n}{K^w} \right) \frac{\partial p}{\partial t} \right\} \mathrm{d}\Omega +$$
$$+ \int_\Gamma \mathbf{w}^{*\mathrm{T}} \left[\frac{\mathbf{k}}{\mu^w} \left(-\nabla p - \rho^f \ddot{\mathbf{u}}^s + \rho^f \mathbf{b} \right)^{\mathrm{T}} \mathbf{n} - \frac{q^w}{\rho^f} \right] \mathrm{d}\Gamma = 0 \qquad (6.12)$$

where for pore pressure, trial function p, twice differentiable, adopted so as to satisfy the boundary condition (6.6) on Γ_p, and weight function $\mathbf{w}^*$ satisfy vanish and prescribed condition on boundary (6.13)

$$\mathbf{w}^* = 0 \qquad \text{na } \Gamma_p$$
$$\bar{\mathbf{w}}^* = -\mathbf{w}^* \qquad \text{na } \Gamma_p^q \qquad (6.13)$$

Use of the Green theorem to equation (6.12) finally obtained

$$\int_\Omega \left[-(\nabla \mathbf{w}^*)^{\mathrm{T}} \left(-\frac{\mathbf{k}}{\mu^w}\nabla p - \frac{\mathbf{k}}{\mu^w}\rho^f \ddot{\mathbf{u}}^s + \frac{\mathbf{k}}{\mu^w}\rho^f \mathbf{b}\right) + \mathbf{w}^{*\mathrm{T}}\alpha \mathbf{m}^{\mathrm{T}}\mathbf{L}\dot{\mathbf{u}}^s + \mathbf{w}^{*\mathrm{T}}\left(\frac{\alpha-n}{K^s}+\frac{n}{K^w}\right)\frac{\partial p}{\partial t}\right] \mathrm{d}\Omega +$$

$$+ \int_{\Gamma_{\mathrm{p}}^{\mathrm{q}}} \mathbf{w}^{*\mathrm{T}} \frac{q^w}{\rho^w} \mathrm{d}\Gamma = 0 \qquad (6.14)$$

6.3. Finite Element Method formulation.

6.3.1. FEM discretization.

FEM discretization was used, for the skeleton displacement the following approximation was introduced

$$\mathbf{u}^s = \mathbf{N}^u \mathbf{u} \qquad (6.15)$$

and for pore water pressure

$$p_f = \mathbf{N}^p \mathbf{p} \qquad (6.16)$$

Similarly, in place of the weight function **w** the shape function $\mathbf{N}^u$ used, and in place of weight function $\mathbf{w}^*$ the shape function $\mathbf{N}^p$ introduced.

Discretization of the linear momentum balance for the soil-water mixture

After implementation of the above approximation functions, the Equation (4.24) can be written:

$$\underbrace{\int_\Omega (\mathbf{N}^u)^T \mathbf{L}^T \boldsymbol{\sigma} d\Omega}_{\text{Green theorem}} - \int_\Omega (\mathbf{N}^u)^T \rho \mathbf{N}^u \ddot{\mathbf{u}} d\Omega + \int_\Omega (\mathbf{N}^u)^T \rho \mathbf{b} d\Omega = 0. \qquad (6.17)$$

After transformations we obtain

$$\int_\Omega (\mathbf{L}\mathbf{N}^u)^T \boldsymbol{\sigma} d\Omega + \underbrace{\left[\int_\Omega \rho (\mathbf{N}^u)^T \mathbf{N}^u d\Omega\right]}_{\mathbf{M}} \ddot{\mathbf{u}} = \underbrace{\int_\Omega \rho (\mathrm{N}^u)^T \mathbf{b} d\Omega + \int_{\Gamma_t} \rho (\mathrm{N}^u)^T \mathbf{t} d\Gamma_t}_{\mathbf{f}^{(1)}} \qquad (6.18)$$

When introducing the differential operator:

$$\mathbf{B} = \mathbf{L}\mathbf{N}^{u} \tag{6.19}$$

one can receive :

$$\mathbf{M}\ddot{\mathbf{u}} + \int_{\Omega} \mathbf{B}^{T}\, \boldsymbol{\sigma} d\Omega = \mathbf{f}^{(1)} \tag{6.20}$$

where

$\boldsymbol{\sigma}$ - total stress defined by eq.(4.7) or similarly:

$$\boldsymbol{\sigma}' = \boldsymbol{\sigma} + \alpha \mathbf{m}^{\boldsymbol{T}} p \tag{6.21}$$

when using it, one can obtain:

$$\mathbf{M}\ddot{\mathbf{u}} + \int_{\Omega} (\mathbf{B}^{T}\, \boldsymbol{\sigma}' - \mathbf{B}^{T} \alpha \mathbf{m}^{\mathrm{T}} \tilde{\mathbf{p}}) d\Omega = \mathbf{f}^{(1)} \tag{6.22}$$

$$\mathbf{M}\ddot{\mathbf{u}} + \int_{\Omega} \mathbf{B}^{T}\, \boldsymbol{\sigma}' d\Omega - \underbrace{\int_{\Omega} (\mathbf{B}^{T} \alpha \mathbf{m}^{\mathrm{T}} \mathbf{N}^{p}) d\Omega \mathbf{p}}_{\mathbf{Q}} = \mathbf{f}^{(1)} \tag{6.23}$$

In case of small strains $d\boldsymbol{\sigma}' = \mathbf{D}(\mathbf{B}d\mathbf{u} - d\boldsymbol{\varepsilon}^{\mathbf{0}})$ and neglecting all the thermal strains the above equation can be written in a form:

$$\mathbf{M}\ddot{\mathbf{u}} + \underbrace{[\int_{\Omega} \mathbf{B}^{T}\, \mathbf{D}\mathbf{B} d\Omega]}_{\mathbf{K}}\mathbf{u} - \mathbf{Q}\mathbf{p} = \mathbf{f}^{(1)} \tag{6.24}$$

Eventually :

$$\mathbf{M}\ddot{\mathbf{u}} + \mathbf{K}\mathbf{u} - \mathbf{Q}\mathbf{p} = \mathbf{f}^{(1)} \tag{6.25}$$

where:

$\mathbf{M} = \int_{\Omega} \rho (\mathbf{N}^{u})^{T}\, \mathbf{N}^{u} d\Omega$ – mass matrix,

$\mathbf{K} = \int_{\Omega} \mathbf{B}^{T}\, \mathbf{D}\mathbf{B} d\Omega$ – stiffness matrix,

$\mathbf{Q} = \int_{\Omega} (\mathbf{B}^{T} \alpha \mathbf{m}^{\mathrm{T}} \mathbf{N}^{p}) d\Omega$ – water coupling matrix

The mass matrix $\mathbf{M}$ and the stiffness matrix $\mathbf{K}$ are symmetrical because of chosen weight functions. Unfortunately the water coupling matrix $\mathbf{Q}$ proved to be asymmetrical.

Discretization of the linear momentum balance for the water including mass balance for the mixture

Equation (6.2) if neglecting the $\rho^f \ddot{\mathbf{u}}^s$ term and the term representing the temperature changes $\dot{s}_o$, as being negligible for the thesis' purpose, and implementing the differential operator (6.19):

$$\nabla^{\mathrm{T}}\mathbf{k}\left(-\nabla p + \rho^f \mathbf{b}\right) + \alpha \mathbf{m}^{\boldsymbol{T}}\dot{\mathbf{u}} + \frac{1}{Q}\dot{p} = 0. \tag{6.26}$$

Similarly, after introduction into eq.(6.26) the shape functions (6.16) in place of weight functions and integration over the Ω area, received

$$\int_\Omega (\mathbf{N}^p)^{\mathrm{T}} \nabla^{\mathrm{T}}\mathbf{k}\left(-\nabla p + \rho_f \mathbf{b}\right) d\Omega + \int_\Omega (\mathbf{N}^p)^{\mathrm{T}} \alpha \mathbf{m}^{\mathrm{T}}\mathbf{L}\dot{\mathbf{u}} d\Omega + \int_\Omega (\mathbf{N}^p)^{\mathrm{T}} \frac{\dot{p}}{Q} d\Omega = 0 \tag{6.27}$$

After further transformations :

$$\overbrace{\left[\int_\Omega (\nabla \mathbf{N}^p)^{\mathrm{T}}\, \mathbf{k} (\nabla \mathbf{N}^p) d\Omega\right]}^{\mathbf{H}} \mathbf{p} + \overbrace{\left[\int_\Omega (\mathbf{N}^p)^{\mathrm{T}}\, \alpha \mathbf{m}^{\mathrm{T}} \mathbf{L} \mathbf{N}^u d\Omega\right]}^{\mathbf{Q}^{\mathbf{T}}} \dot{\mathbf{u}} +$$

$$+ \underbrace{\left[\int_\Omega (\mathbf{N}^p)^{\mathrm{T}} \frac{1}{Q} \mathbf{N}^p d\Omega\right]}_{\mathbf{S}} \dot{\mathbf{p}} = \mathbf{f}^{(2)} \tag{6.28}$$

where

$$\mathbf{f}^{(2)} = \int_\Omega (\mathbf{N}^p)^{\mathrm{T}} \nabla^{\mathrm{T}} (k \rho_f \mathbf{b}) d\Omega + \int_{\Gamma_w} (\mathbf{N}^p)^{\mathrm{T}} \mathbf{q} d\Gamma_w . \tag{6.29}$$

Finally:

$$\mathbf{Q}^T \dot{\mathbf{u}} + \mathbf{H}\mathbf{p} + \mathbf{S}\dot{\mathbf{p}} = \mathbf{f}^{(2)} \tag{6.30}$$

where:

$\mathbf{H} = \int_\Omega (\nabla \mathbf{N}^p)^{\mathrm{T}}\, \mathbf{k} (\nabla \mathbf{N}^p) d\Omega$ – water permeability matrix;

$\mathbf{S} = \int_\Omega (\mathbf{N}^p)^{\mathrm{T}} \frac{1}{Q} \mathbf{N}^p d\Omega$ – compressibility matrix

Again all of the matrices are symmetrical except $\mathbf{Q}^T$.

6.3.2. FEM set of equations.

6.3.2.1. Partly dynamic formulation.

Full set of Finite Element Method equations, called Partly Dynamic Formulation (or **u**-*p* formulation), regarding the aforementioned matrices is as follows:

$$\begin{bmatrix} \mathbf{M} & \mathbf{0} \\ \mathbf{0} & \mathbf{0} \end{bmatrix} \begin{bmatrix} \ddot{\mathbf{u}} \\ \ddot{\mathbf{p}} \end{bmatrix} + \begin{bmatrix} \mathbf{0} & \mathbf{0} \\ \mathbf{Q}^T & \mathbf{S} \end{bmatrix} \begin{bmatrix} \dot{\mathbf{u}} \\ \dot{\mathbf{p}} \end{bmatrix} + \begin{bmatrix} \mathbf{K} & -\mathbf{Q} \\ \mathbf{0} & \mathbf{H} \end{bmatrix} \begin{bmatrix} \mathbf{u} \\ \mathbf{p} \end{bmatrix} = \begin{bmatrix} \mathbf{f}^{(1)} \\ \mathbf{f}^{(2)} \end{bmatrix} \tag{6.31}$$

The unknowns are:

- pore water pressure **p** and rate of change of the pore water pressure $\dot{\mathbf{p}}$
- soil skeleton displacements **u,** velocities $\dot{\mathbf{u}}$ and accelerations $\ddot{\mathbf{u}}$

Most of the literature, for example (Zienkiewicz & Shiomi, 1984) and (Smith & Griffiths, 2006), omit the water compressibility matrix **S** as being irrelevant, see eq.(6.32).

$$\begin{bmatrix} \mathbf{M} & \mathbf{0} \\ \mathbf{0} & \mathbf{0} \end{bmatrix} \begin{bmatrix} \ddot{\mathbf{u}} \\ \ddot{\mathbf{p}} \end{bmatrix} + \begin{bmatrix} \mathbf{0} & \mathbf{0} \\ \mathbf{Q}^T & \mathbf{0} \end{bmatrix} \begin{bmatrix} \dot{\mathbf{u}} \\ \dot{\mathbf{p}} \end{bmatrix} + \begin{bmatrix} \mathbf{K} & -\mathbf{Q} \\ \mathbf{0} & \mathbf{H} \end{bmatrix} \begin{bmatrix} \mathbf{u} \\ \mathbf{p} \end{bmatrix} = \begin{bmatrix} \mathbf{f}^{(1)} \\ \mathbf{f}^{(2)} \end{bmatrix} \tag{6.32}$$

This thesis examines the influence of this matrix on the displacements and pore water pressure. The matrix is responsible for storage increase. It describes the energy storage and it is associated with water compressibility.

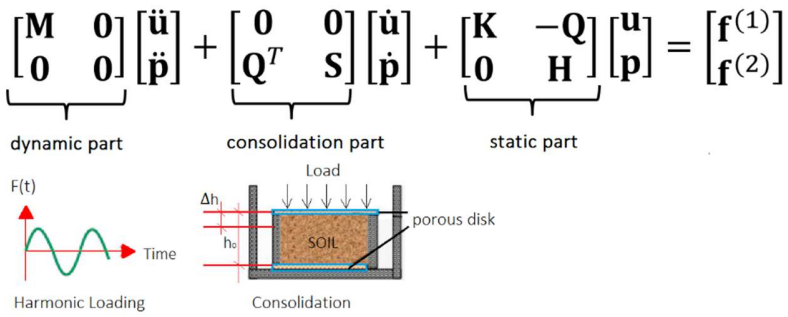

Fig. 6.2: Components of the FEM set of equations if harmonic loading is applied

6.3.2.2. Partly dynamic formulation without consolidation.

Consolidation is a process by which soil decreases in volume (Fig. 6.2). According to Karl von Terzaghi consolidation is any process which involves a decrease in water content of saturated

soil without replacement of water by air. In general it is the process in which reduction in volume takes place by expulsion of water under long term static loads. When this occurs in soil that is saturated with water, water will be squeezed out of the soil. If we analyze the fast short-term period, the consolidation part from eq.(6.31) can be omitted.

In case of harmonic loading we can predict the solution of the FEM set of equation in the following form

$$\begin{bmatrix}\mathbf{u}(t)\\ \mathbf{p}(t)\end{bmatrix} = \begin{bmatrix}\mathbf{U}\\ \mathbf{P}\end{bmatrix} e^{i\omega t}, \begin{bmatrix}\dot{\mathbf{u}}(t)\\ \dot{\mathbf{p}}(t)\end{bmatrix} = i\omega \begin{bmatrix}\mathbf{U}\\ \mathbf{P}\end{bmatrix} e^{i\omega t}, \begin{bmatrix}\ddot{\mathbf{u}}(t)\\ \ddot{\mathbf{p}}(t)\end{bmatrix} = -\omega^2 \begin{bmatrix}\mathbf{U}\\ \mathbf{P}\end{bmatrix} e^{i\omega t}, \begin{bmatrix}\mathbf{f}^{(1)}(t)\\ \mathbf{f}^{(2)}(t)\end{bmatrix} = \begin{bmatrix}\mathbf{F}^{(1)}\\ \mathbf{F}^{(2)}\end{bmatrix} e^{i\omega t}. \quad (6.33)$$

Equation (6.31) omitting the consolidation term can be expressed:

$$\begin{bmatrix}\mathbf{M} & \mathbf{0}\\ \mathbf{0} & \mathbf{0}\end{bmatrix}\begin{bmatrix}\ddot{\mathbf{u}}\\ \ddot{\mathbf{p}}\end{bmatrix} + \begin{bmatrix}\mathbf{K} & -\mathbf{Q}\\ \mathbf{0} & \mathbf{H}\end{bmatrix}\begin{bmatrix}\mathbf{u}\\ \mathbf{p}\end{bmatrix} = \begin{bmatrix}\mathbf{f}^{(1)}\\ \mathbf{f}^{(2)}\end{bmatrix} \quad (6.34)$$

and after introducing the relations (6.33):

$$\left\{-\omega^2 \begin{bmatrix}\mathbf{M} & \mathbf{0}\\ \mathbf{0} & \mathbf{0}\end{bmatrix} + \begin{bmatrix}\mathbf{K} & -\mathbf{Q}\\ \mathbf{0} & \mathbf{H}\end{bmatrix}\right\}\begin{bmatrix}\mathbf{U}\\ \mathbf{P}\end{bmatrix} = \begin{bmatrix}\mathbf{F}^{(1)}\\ \mathbf{F}^{(2)}\end{bmatrix} \quad (6.35)$$

The above approach allows for the omission of integration over time domain. The results obtained are for a specific frequency only.

6.3.2.3. Partly dynamic formulation – omitting the change of water pressure with time.

It was mentioned in the previous section, that the water compressibility matrix **S** is sometimes omitted (Zienkiewicz & Shiomi, 1984). This approach excludes the change of water pressure with time, in other words, the significant part of storage increase terms are excluded from the equations. It is then possible to eliminate the pore water pressure *p* as follows:

From the second eq.(6.31) we obtain:

$$\mathbf{Q}^{\mathrm{T}}\dot{\mathbf{u}} + \mathbf{H}\mathbf{p} = \mathbf{f}^{(2)}$$

$$\mathbf{p} = \mathbf{H}^{-1}(\mathbf{f}^{(2)} - \mathbf{Q}^{\mathrm{T}}\dot{\mathbf{u}}) \quad (6.36)$$

Afterwards we put this formula into the first eq.(6.31):

$$\mathbf{M}\ddot{\mathbf{u}} + \mathbf{K}\mathbf{u} - (-\mathbf{Q}\mathbf{H}^{-1}\mathbf{Q}^{\mathrm{T}}\dot{\mathbf{u}}) - \mathbf{Q}\mathbf{H}^{-1}\mathbf{f}^{(2)} = \mathbf{f}^{(1)} \quad (6.37)$$

or $$\mathbf{M\ddot{u} + QH^{-1}Q^{T}\dot{u} + Ku = f^{(1)} + QH^{-1}f^{(2)}} \quad (6.38)$$

The above formula is relatively easy, symmetric and valid for both linear and nonlinear cases. What is most important is that it outlines a very relevant fluid parameter, which is damping. Unfortunately this approach is problematic. The inverse of the **H** matrix or the solution of the equation $\mathbf{H^{-1}f^{(2)}}$ needs to be calculated.

Regarding the harmonic loading, the eq.(6.38) can be written in this form:

$$\{-\omega^2\mathbf{M} + i\omega\mathbf{QH^{-1}Q^{T}} + \mathbf{K}\}\mathbf{u} = \mathbf{F^{(1)}} + \mathbf{QH^{-1}F^{(2)}}\ . \quad (6.39)$$

6.3.2.4. Set of equations for the consolidation model.

If dynamic loading is slow enough, it can be assumed that quasi static formulation (the consolidation model in other words) is sufficient. Unfortunately the boundary is not very clear and its range is planned to be estimated in a future study.

The Finite Element Method set of equations for the consolidation model (all inertia forces are omitted) are as follows:

$$\begin{bmatrix} \mathbf{0} & \mathbf{0} \\ \mathbf{Q}^{T} & \mathbf{S} \end{bmatrix}\begin{bmatrix} \dot{\mathbf{u}} \\ \dot{\mathbf{p}} \end{bmatrix} + \begin{bmatrix} \mathbf{K} & -\mathbf{Q} \\ \mathbf{0} & \mathbf{H} \end{bmatrix}\begin{bmatrix} \mathbf{u} \\ \mathbf{p} \end{bmatrix} = \begin{bmatrix} \mathbf{f}^{(1)} \\ \mathbf{f}^{(2)} \end{bmatrix} \quad (6.40)$$

In Section 6.3.3 the comparison of some of the above formulations can be found in numerical examples. In Appendix 1 all the matrices introduced above are presented in a more detailed way for an eight-node Serendipity quadrilateral finite element in a plane strain condition.

6.3.3. Examples for individual formulations.

6.3.3.1. Introduction.

The example presented in this section is a limited region of the plane strain elastic model as shown in Fig. 6.4. The eight node Serendipity finite element is introduced for the skeleton, which is a higher order element with only exterior nodes. For the pore water pressure the four node Lagrangian finite element is used (Fig. 6.4).

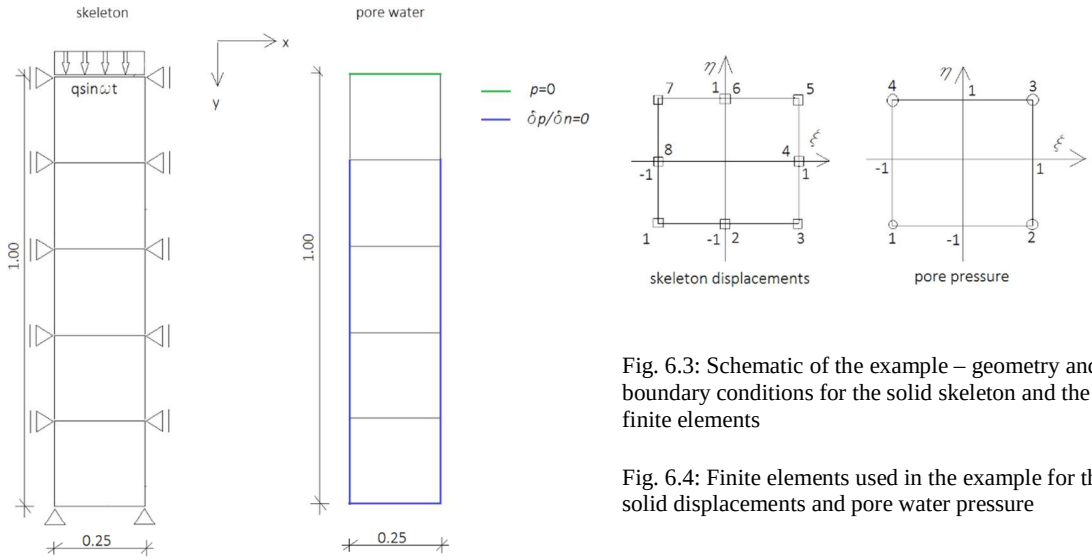

Fig. 6.3: Schematic of the example – geometry and boundary conditions for the solid skeleton and the fluid; finite elements

Fig. 6.4: Finite elements used in the example for the solid displacements and pore water pressure

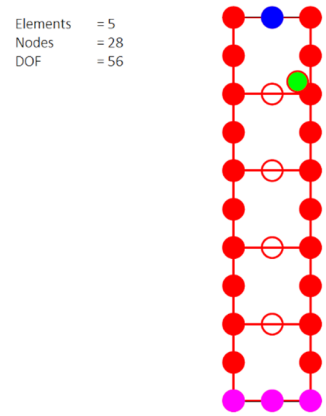

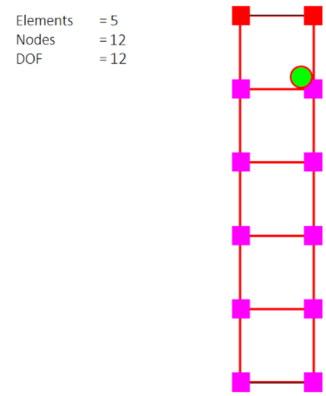

- pore pressure equal to zero
- normal derivative equal to zero

Fig. 6.5 presents the discretized region for the skeleton consisting of 28 nodes. Each of the nodes can move in both horizontal and vertical direction, which implies 56 degrees of freedom if boundary conditions are disregarded. Fig. 6.6 on the contrary shows the discretization for the pore water pressure. This time the four node finite element is introduced. Each of the node has only one degree of freedom (which is pressure), which implies 12x1=12 degrees of freedom if not considering the boundary conditions.

Fig. 6.5: The region after discretization (skeleton) consisting of 5 elements, having 28 nodes and 56 degrees of freedom

Fig. 6.6: The region after discretization (fluid in the pores) consisting of 5 elements, having 13 nodes and 12 degrees of freedom

Generally the results in the following sections are presented for two types of soil – clay and sand, which parameters' are shown in Table 6.1. The harmonic loading with various frequencies ω is applied at the top with an amplitude of q=100kN.

	SOIL TYPE 1 -**CLAY**	SOIL TYPE 2 -**SAND**
I_L / I_D	0,2	0,5
Modulus of Elasticity E [MPa]	25	80
Poisson Ratio ν	0,37	0,25
porosity *n*	0,35	0,35
permeability coefficient k [m/s]	10^(-10)	10^(-4)
Biot constant *Q* [GPa]	6,2	6,7
density ρ [kg/m^3]	2000	2000

Table 6.1 Soil parameters used in the computational examples.

In order to make it more clear and precise, all the formulations from Section 6.3.2 are named:

$$\begin{bmatrix} \mathbf{0} & \mathbf{0} \\ \mathbf{Q}^{\mathrm{T}} & \mathbf{S} \end{bmatrix} \begin{bmatrix} \dot{\mathbf{u}} \\ \dot{\mathbf{p}} \end{bmatrix} + \begin{bmatrix} \mathbf{K} & -\mathbf{Q} \\ \mathbf{0} & \mathbf{H} \end{bmatrix} \begin{bmatrix} \mathbf{u} \\ \mathbf{p} \end{bmatrix} = \begin{bmatrix} \mathbf{f}^{(1)} \\ \mathbf{f}^{(2)} \end{bmatrix} \qquad \text{Model 1 (Equation 6.40)}$$

$$\begin{bmatrix} \mathbf{M} & \mathbf{0} \\ \mathbf{0} & \mathbf{0} \end{bmatrix} \begin{bmatrix} \ddot{\mathbf{u}} \\ \ddot{\mathbf{p}} \end{bmatrix} + \begin{bmatrix} \mathbf{K} & -\mathbf{Q} \\ \mathbf{0} & \mathbf{H} \end{bmatrix} \begin{bmatrix} \mathbf{u} \\ \mathbf{p} \end{bmatrix} = \begin{bmatrix} \mathbf{f}^{(1)} \\ \mathbf{f}^{(2)} \end{bmatrix} \qquad \text{Model 2 (Equation 6.34)}$$

$$\begin{bmatrix} \mathbf{M} & \mathbf{0} \\ \mathbf{0} & \mathbf{0} \end{bmatrix} \begin{bmatrix} \ddot{\mathbf{u}} \\ \ddot{\mathbf{p}} \end{bmatrix} + \begin{bmatrix} \mathbf{0} & \mathbf{0} \\ \mathbf{Q}^{T} & \mathbf{S} \end{bmatrix} \begin{bmatrix} \dot{\mathbf{u}} \\ \dot{\mathbf{p}} \end{bmatrix} + \begin{bmatrix} \mathbf{K} & -\mathbf{Q} \\ \mathbf{0} & \mathbf{H} \end{bmatrix} \begin{bmatrix} \mathbf{u} \\ \mathbf{p} \end{bmatrix} = \begin{bmatrix} \mathbf{f}^{(1)} \\ \mathbf{f}^{(2)} \end{bmatrix} \qquad \text{Model 3 (Equation 6.31)}$$

$$\begin{bmatrix} \mathbf{M} & \mathbf{0} \\ \mathbf{0} & \mathbf{0} \end{bmatrix} \begin{bmatrix} \ddot{\mathbf{u}} \\ \ddot{\mathbf{p}} \end{bmatrix} + \begin{bmatrix} \mathbf{0} & \mathbf{0} \\ \mathbf{Q}^{T} & \mathbf{0} \end{bmatrix} \begin{bmatrix} \dot{\mathbf{u}} \\ \dot{\mathbf{p}} \end{bmatrix} + \begin{bmatrix} \mathbf{K} & -\mathbf{Q} \\ \mathbf{0} & \mathbf{H} \end{bmatrix} \begin{bmatrix} \mathbf{u} \\ \mathbf{p} \end{bmatrix} = \begin{bmatrix} \mathbf{f}^{(1)} \\ \mathbf{f}^{(2)} \end{bmatrix} \qquad \text{Model 4 (Equation 6.32)}$$

6.3.3.2. Comparison of partly dynamic idealization including and omitting the change of water pressure with time.

Hereunder, the results of the Model 3 and Model 4 - equations (6.31) and (6.32) are presented and compared. Model 4, which omits the change of water pressure with time, is the simplified version of Model 3, which is equivalent to eliminating the compressibility matrix **S** from eq.(6.30). Direct numerical integration of the equations over time is introduced, which means, that integration step-by-step is performing, where the word "direct" means that there is no transformation of the equation of motion. The HHT-α method, proposed by Hilbert, Hughes and Taylor in 1977, is used with the α parameter equal to zero (Lacoma & Romero, 2007).

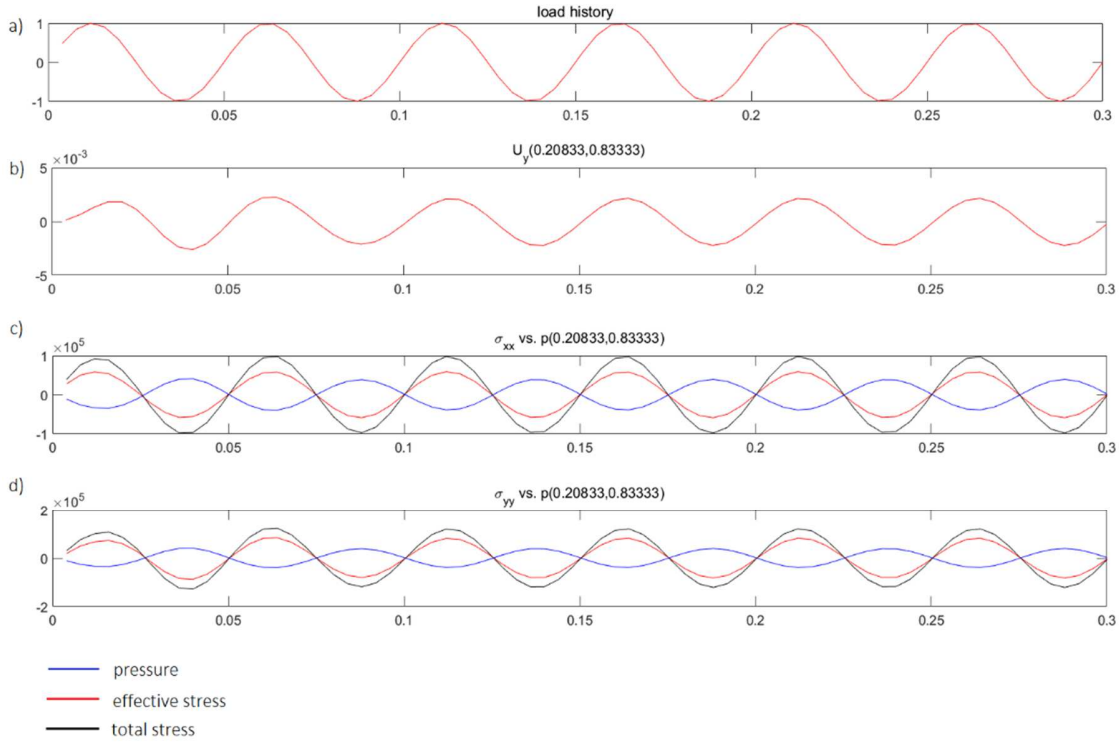

Fig. 6.7: The results for soil Type 1, including compressibility matrix **S** for the excitation frequency equal to 20Hz a) load multiplier b) displacement u_y [m] c) effective stress σ'_{xx} vs. pressure p and total stress [Pa] d) effective stress σ'_{yy} vs. pressure p and total stress [Pa]

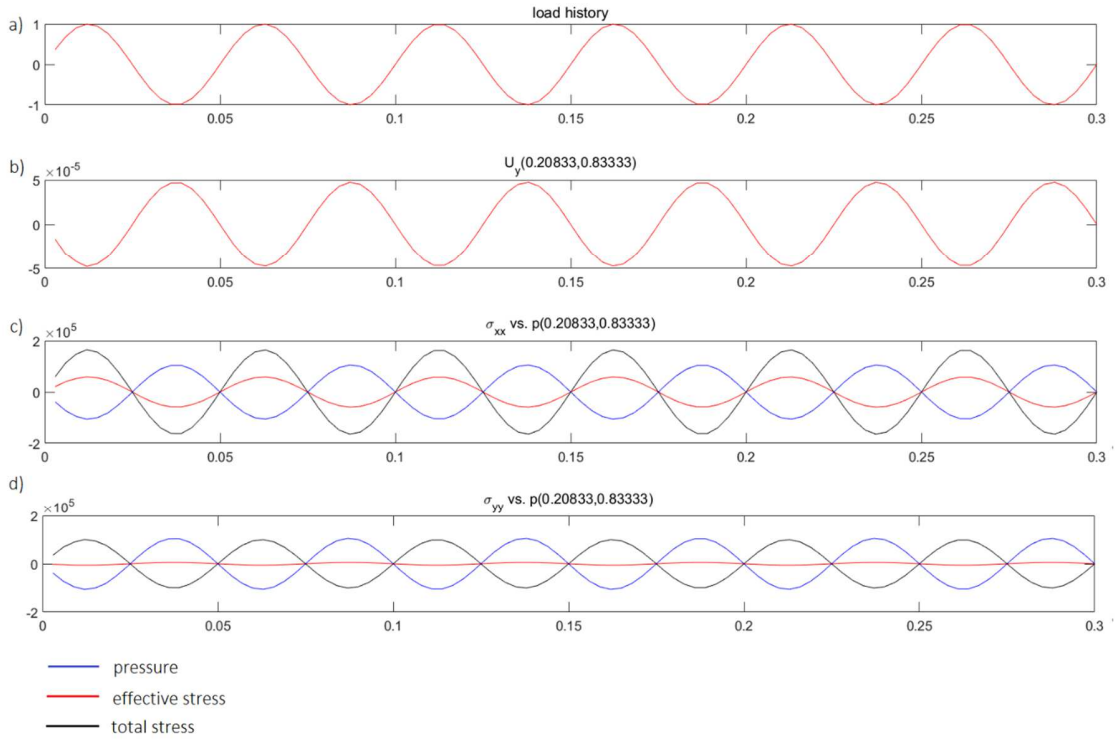

Fig. 6.8: The results for soil Type 1, omitting compressibility matrix **S** for the excitation frequency equal to 20Hz a) load multiplier b) displacement u_y [m] c) effective stress σ'_{xx} vs. pressure p and total stress [Pa] d) effective stress σ'_{yy} vs. pressure p and total stress [Pa]

The calculations are done for soil Type 1 and soil Type 2 from Table 6.1. At first, the study concentrates on soil Type 1 (clay). The excitation has two exemplary frequencies – 20Hz and 40Hz. The graphs below (from Fig. 6.7 to Fig. 6.13) present the nature of loading applied at the top of the area, the displacements, effective stresses, pressure and finally total stresses for the exemplary point shown in green in Fig. 6.5 and Fig. 6.6., where time is on x- axis.

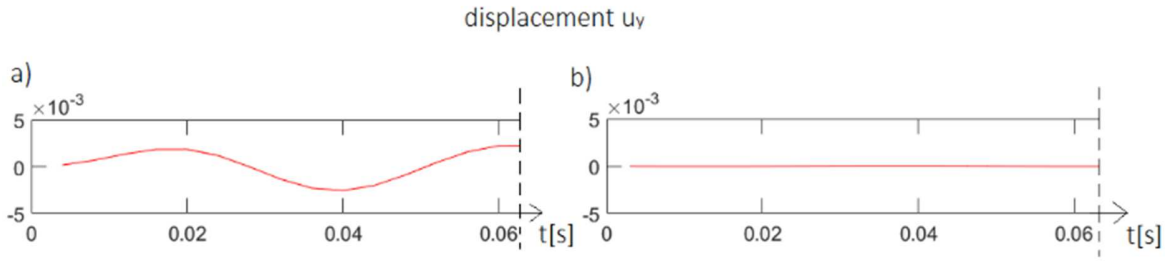

Fig. 6.9: The comparison of displacements u_y [m] for soil Type 1 for excitation frequency equal to 20Hz a) including compressibility matrix **S** b) omitting compressibility matrix **S**

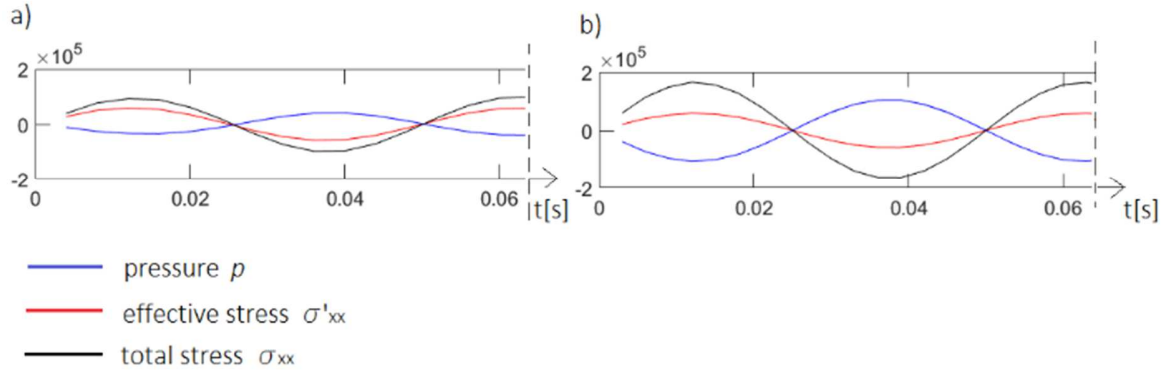

Fig. 6.10: The comparison of effective stress σ'_{xx} vs. pressure p and total stress [Pa] for soil Type 1 for excitation frequency equal to 20Hz a) including compressibility matrix **S** b) omitting compressibility matrix **S**

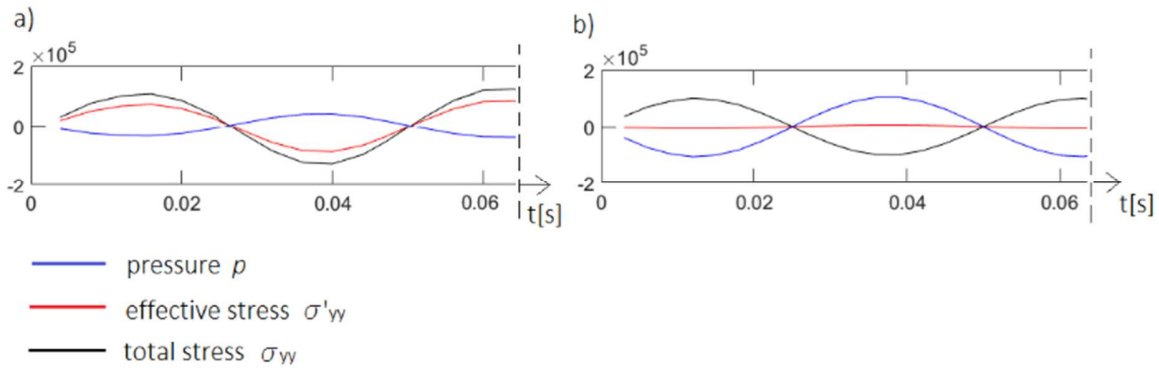

Fig. 6.11: The comparison of effective stress σ_{yy} vs. pressure *p* and total stress [Pa] for soil Type 1 for excitation frequency equal to 20Hz a) including compressibility matrix **S** b) omitting compressibility matrix **S**

As we can see in Fig. 6.9 the compressibility matrix, which involves the change of water pressure with time, has a huge impact on the displacements. If we include it in our equations, the settlements are much higher (over ten times). However, for the pore water pressure, the values are smaller, whereas the effective stress in the skeleton is higher. For the Model 4 on the contrary, the vertical effective stress σ'_{yy} (for the analyzed short time interval) is close to zero, see Fig. 6.11b and Fig. 6.16b. The total applied at the top stress is carried by pore water.

All of the aforementioned tendencies can be observed for higher frequencies, but the proportional relationship between the effective stress and the pressure in Fig. 6.15 and Fig. 6.16 is even higher.

What is also worth mentioning here is, if we omit the change of water pressure with time, values of the horizontal total stress σ_{xx} are higher for both lower (Fig. 6.10) and higher frequencies (Fig. 6.15).

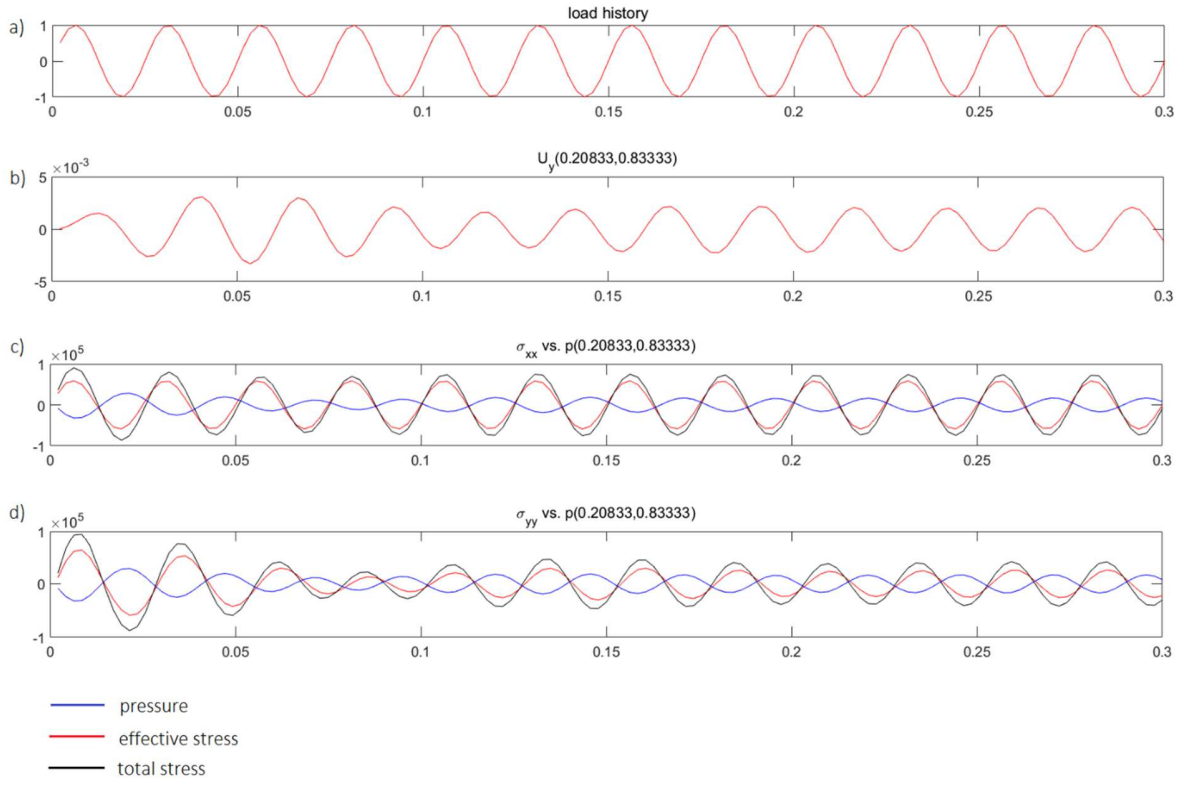

Fig. 6.12: The results for soil Type 1, including compressibility matrix **S** for the excitation frequency equal to 40Hz a) load multiplier b) displacement u_y [m] c) effective stress σ'_{xx} vs. pressure p and total stress σ_{xx} [Pa] d) effective stress σ_{yy} vs. pressure p and total stress [Pa]

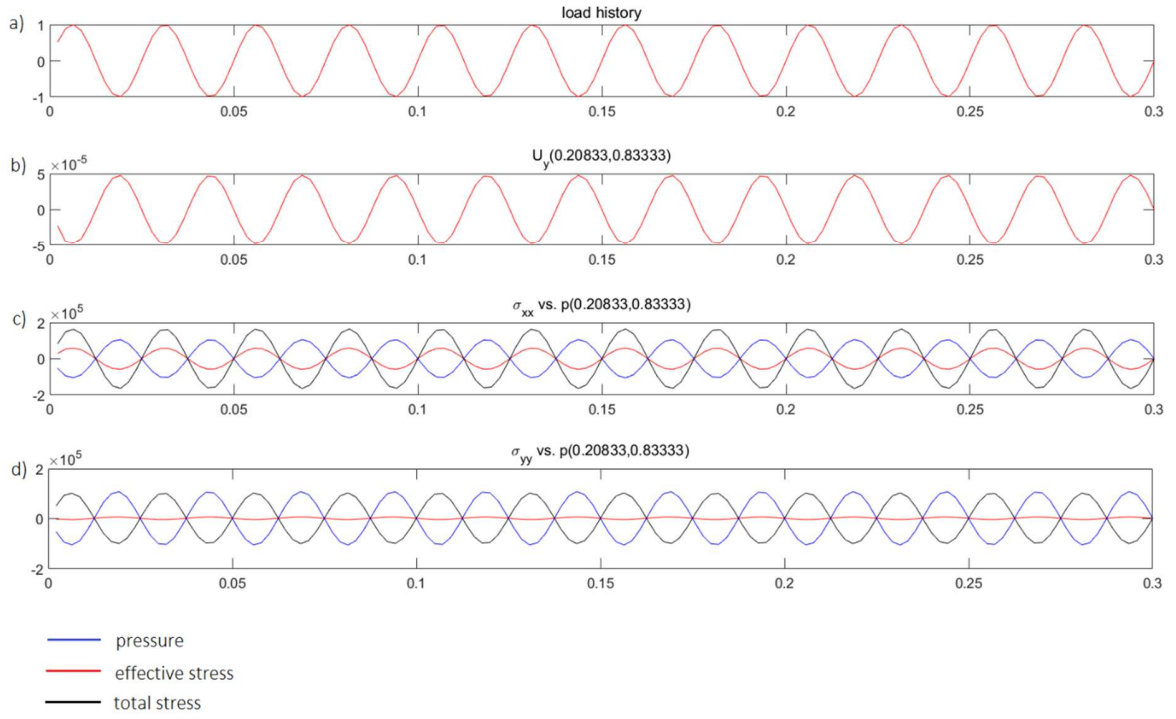

Fig. 6.13: The results for soil Type 1, omitting compressibility matrix **S** for the excitation frequency equal to 40Hz a) load multiplier b) displacement u_y [m] c) effective stress σ_{xx} vs. pressure p and total stress [Pa] d) effective stress σ_{yy} vs. pressure p and total stress [Pa]

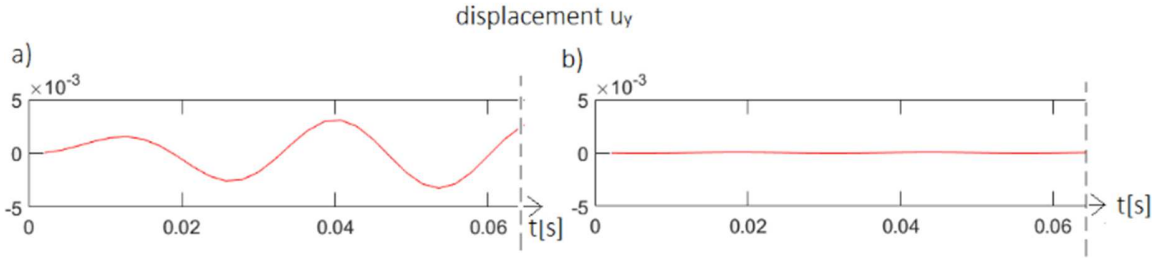

Fig. 6.14: The comparison of displacements u_y [m] for soil Type 1 for excitation frequency equal to 40Hz a) including compressibility matrix **S** b) omitting compressibility matrix **S**

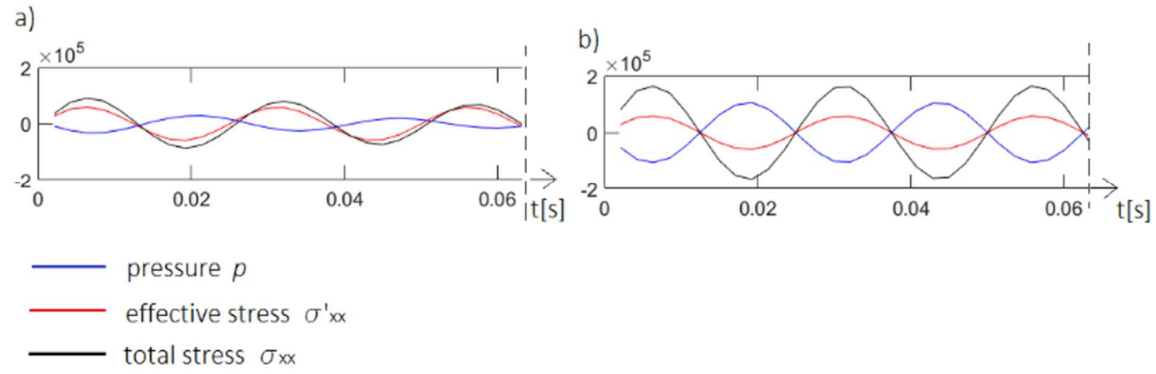

Fig. 6.15: The comparison of effective stress σ'_{xx} vs. pressure p and total stress [Pa] for soil Type 1 for excitation frequency equal to 40Hz a) including compressibility matrix **S** b) omitting compressibility matrix **S**

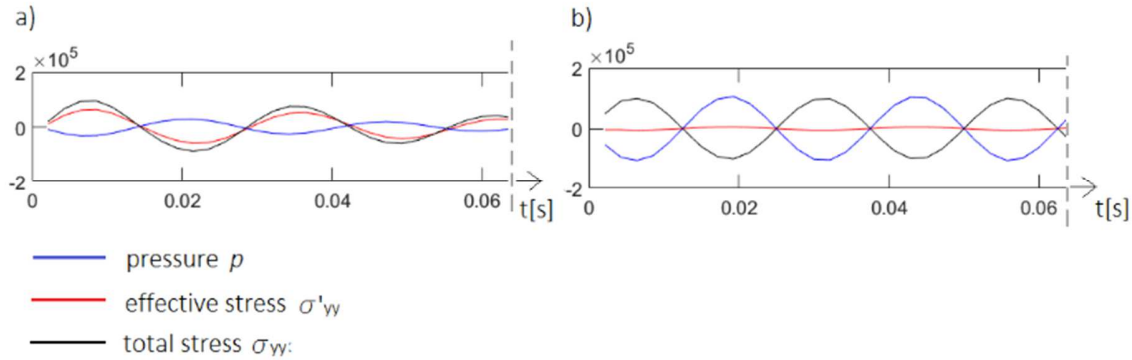

Fig. 6.16: The comparison of effective stress σ'_{yy} vs. pressure p and total stress [Pa] for soil Type 1 for excitation frequency equal to 40Hz a) including compressibility matrix **S** b) omitting compressibility matrix **S**

The same calculations were done for soil Type 2 (medium sand). The outcomes are presented in Fig. 6.17 through Fig. 6.23. There are two relevant differences between the results for two types of analyzed soils. Firstly, the pressure for the Model 3 in Fig. 6.21a) and Fig. 6.26a) is almost equal to zero for soil Type 2 if compared relatively with the vertical effective stress. Secondly, this time not only pore water, but also the skeleton takes part in carrying the applied loading for Model 4. The vertical effective stress σ'_{yy} in Fig. 6.21b) and Fig. 6.26b) is definitely different from zero.

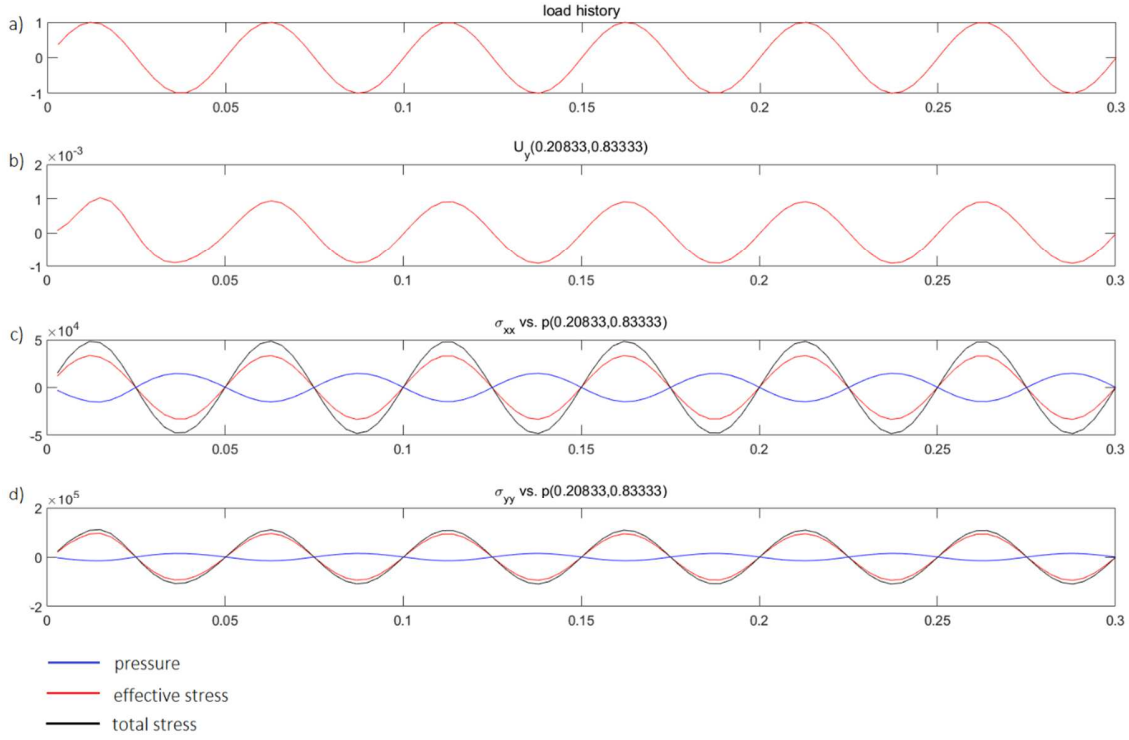

Fig. 6.17: The results for soil Type 2, including compressibility matrix **S** for the excitation frequency equal to 20Hz a) load multiplier b) displacement u_y [m] c) effective stress σ_{xx} vs. pressure p and total stress [Pa] d) effective stress σ_{yy} vs. pressure p and total stress [Pa]

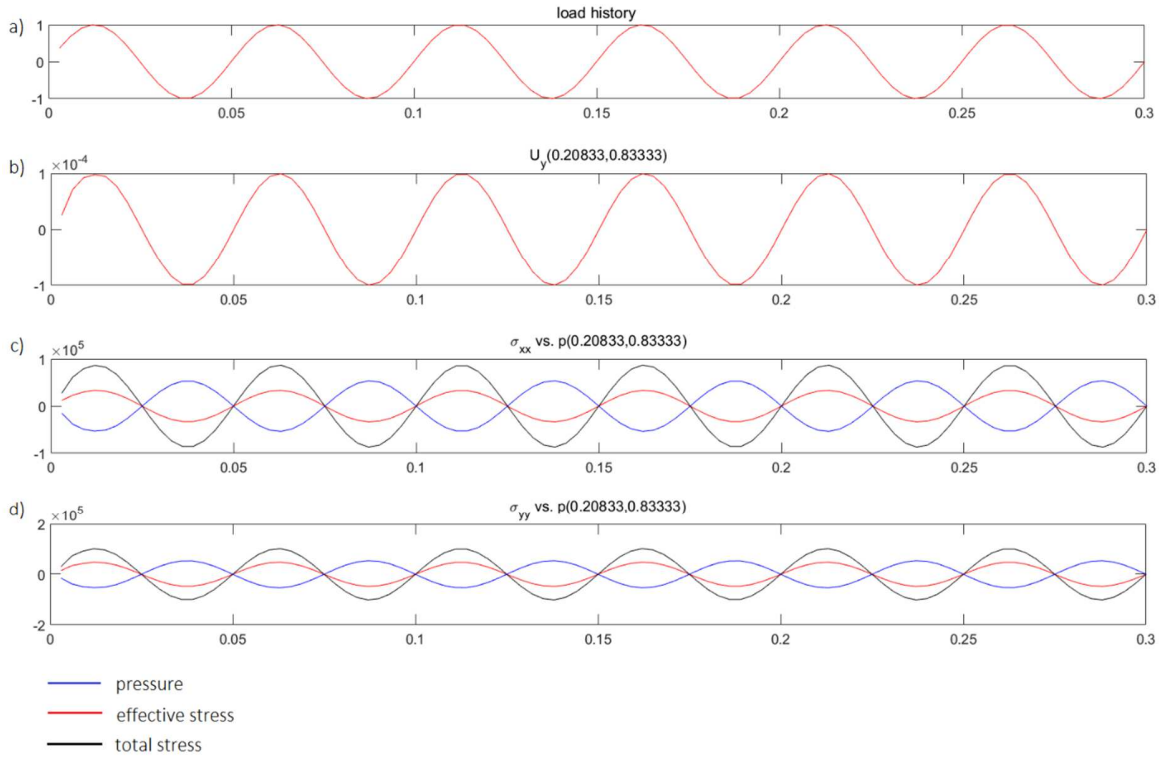

Fig. 6.18: The results for soil Type 2, omitting compressibility matrix **S** for the excitation frequency equal to 20Hz a) load multiplier b) displacement u_y [m] c) effective stress σ_{xx} vs. pressure p and total stress [Pa] d) effective stress σ_{yy} vs. pressure p and total stress [Pa]

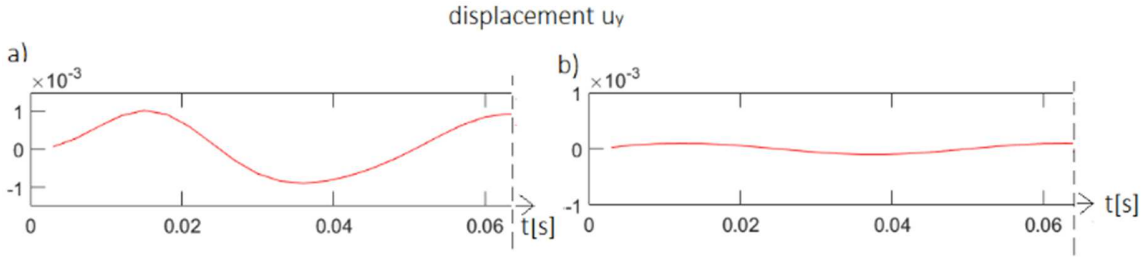

Fig. 6.19: The comparison of displacements u_y [m] for soil Type 2 for excitation frequency equal to 20Hz a) including compressibility matrix **S** b) omitting compressibility matrix **S**

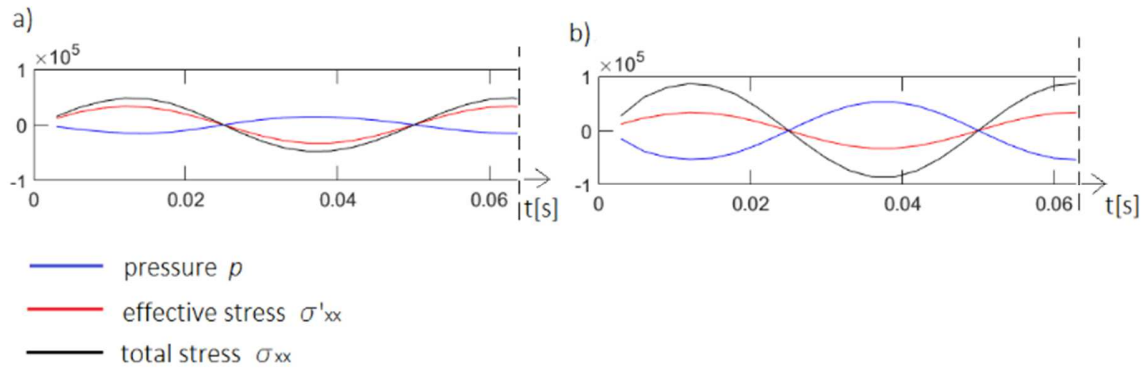

Fig. 6.20: The comparison of effective stress σ'_{xx} vs. pressure p and total stress [Pa] for soil Type 2 for excitation frequency equal to 20Hz a) including compressibility matrix **S** b) disregarding compressibility matrix **S**

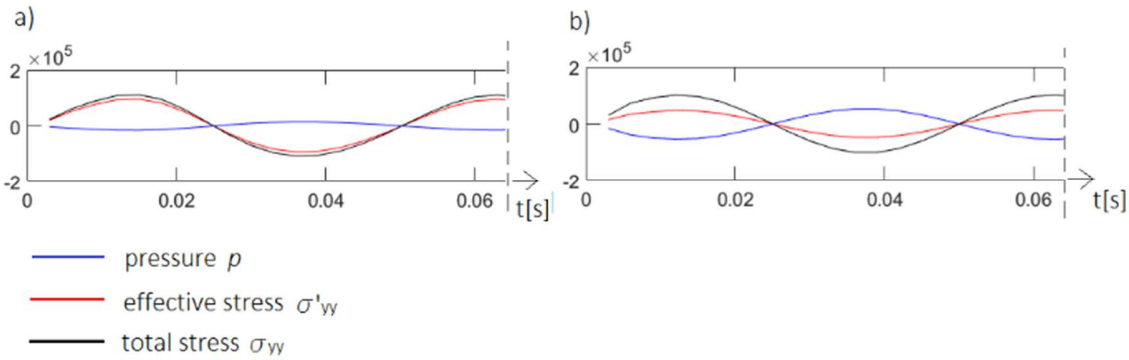

Fig. 6.21: The comparison of effective stress σ'_{yy} vs. pressure p and total stress [Pa] for soil Type 2 for excitation frequency equal to 20Hz a) omitting compressibility matrix **S** b) disregarding compressibility matrix **S**

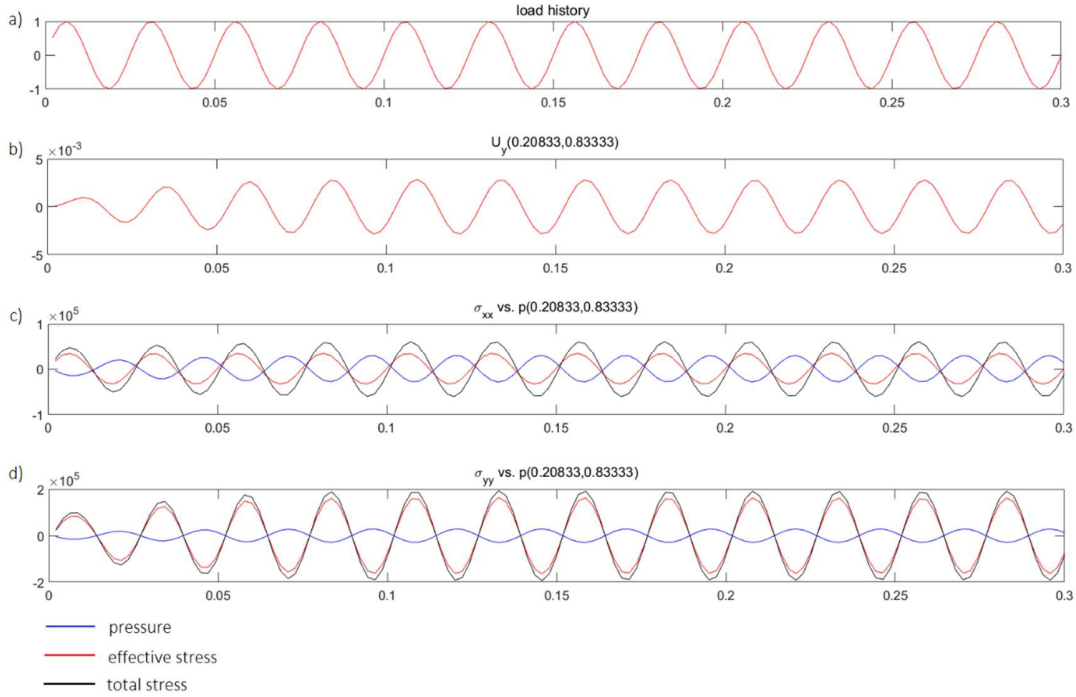

Fig. 6.22: The results for soil Type 2, including compressibility matrix **S** for the excitation frequency equal to 40Hz a) load multiplier b) displacement u_y [m] c) effective stress σ_{xx} vs. pressure p and total stress [Pa] d) effective stress σ_{yy} vs. pressure p and total stress [Pa]

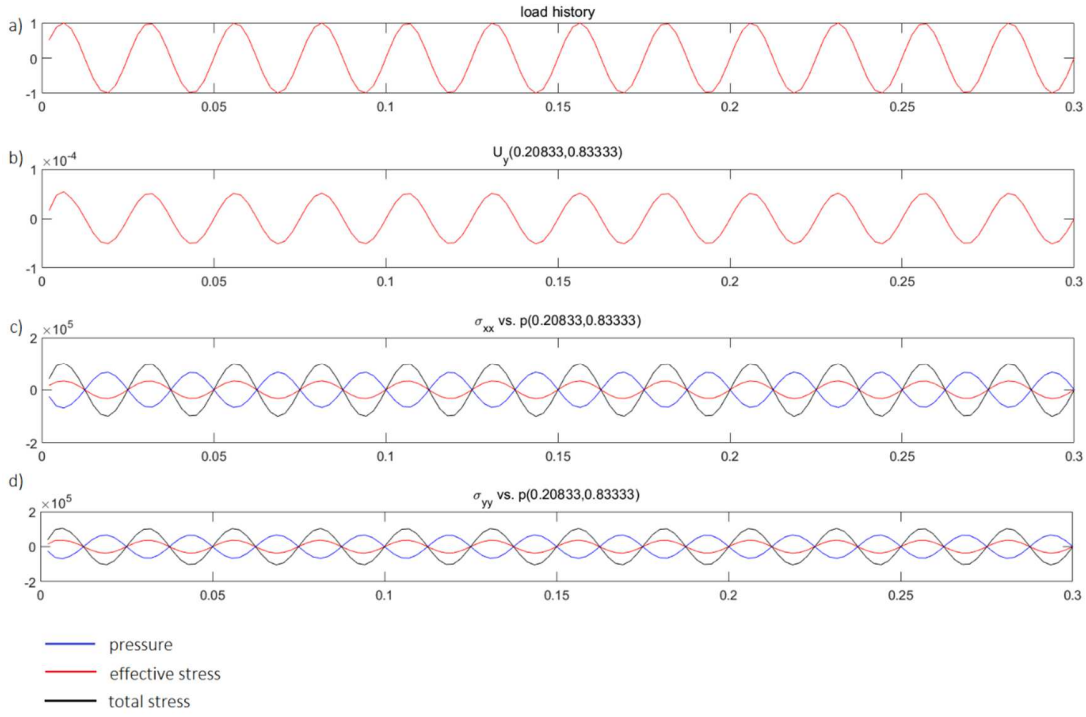

Fig. 6.23: The results for soil Type 2, omitting compressibility matrix **S** for the excitation frequency equal to 40Hz a) load multiplier b) displacement u_y [m] c) effective stress σ_{xx} vs. pressure p and total stress [Pa] d) effective stress σ_{yy} vs. pressure p and total stress [Pa]

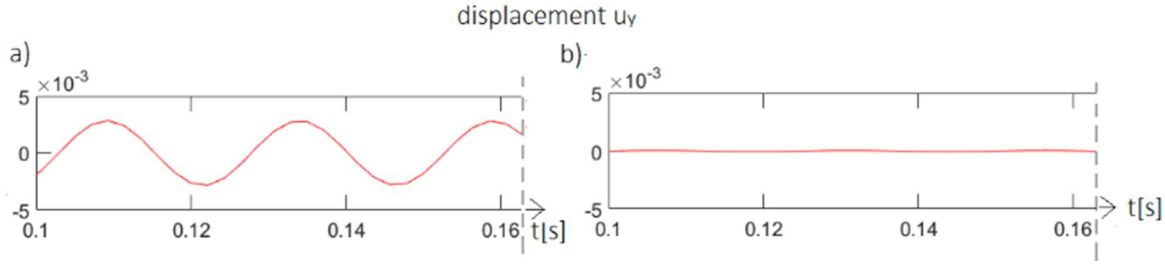

Fig. 6.24: The comparison of displacements u_y [m] for soil Type 2 for excitation frequency equal to 40Hz a) including compressibility matrix **S** b) omitting compressibility matrix **S**

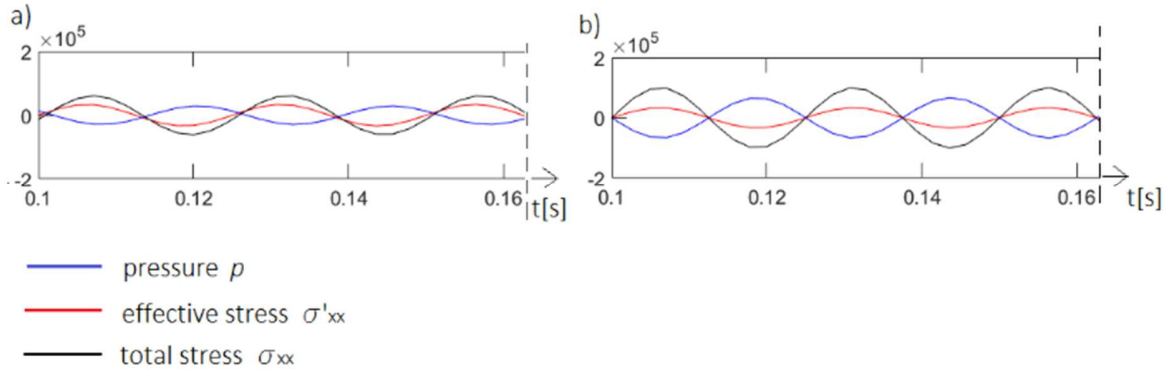

Fig. 6.25: The comparison of effective stress σ'_{xx} vs. pressure p and total stress [Pa] for soil Type 2 for excitation frequency equal to 40Hz a) including compressibility matrix **S** b) omitting compressibility matrix **S**

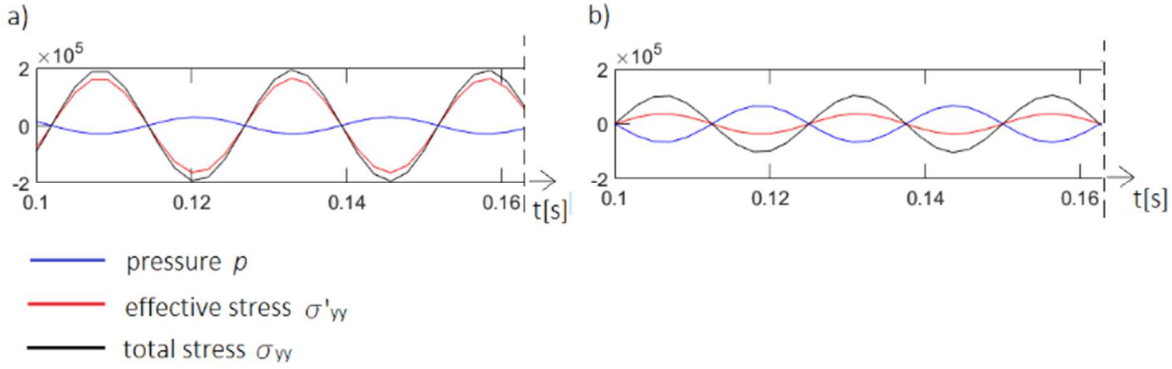

Fig. 6.26: The comparison of effective stress σ'_{yy} vs. pressure p and total stress [Pa] for soil Type 2 for excitation frequency equal to 40Hz a) including compressibility matrix **S** b) disregarding compressibility matrix **S**

6.3.3.3. Comparison of partly dynamic formulation with and without consolidation part.

The Equation including the consolidation part (Model 3 – eq.(6.31)) and the one omitting it (Model 2 – eq.(6.34)) are hereunder discussed and compared. Additionally Model 4, which assumes the water being stiff and uncompressible, is also compared in the figures, but only for the Soil Type 2 (medium sand). Regarding Soil Type 1 (clay), the comparison can be done analogously when analyzing the figures in Section 6.3.3.2. Only a short-term period is analyzed. The purpose of this section is to estimate if the consolidation part does have any impact on the results even if a long-term period is not considered.

The results from Model 2 are the individual values (the displacement or the total stresses in both directions) for the specified value of the frequency. In accordance with the set of equations (6.34), as there is no loading applied to the pore water, the fluid pressure is equal to zero. The figures below (Fig. 6.27 through Fig. 6.29) show the comparison of the values which resulted from Model 2 and the extreme values which resulted from Model 3 and 4 for the medium sand (soil Type 2 from Table 6.1).

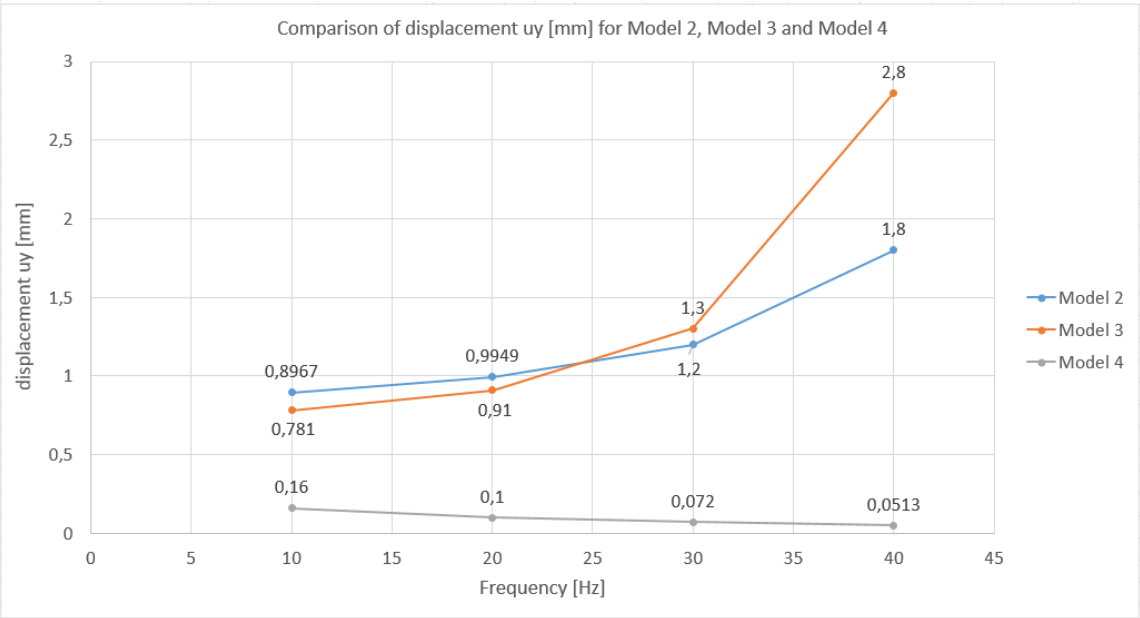

Fig. 6.27: The comparison of Soil Type 2 displacements for the sample point for four arbitrarily chosen frequencies - 10,20,30 and 40Hz, for three analyzed models.

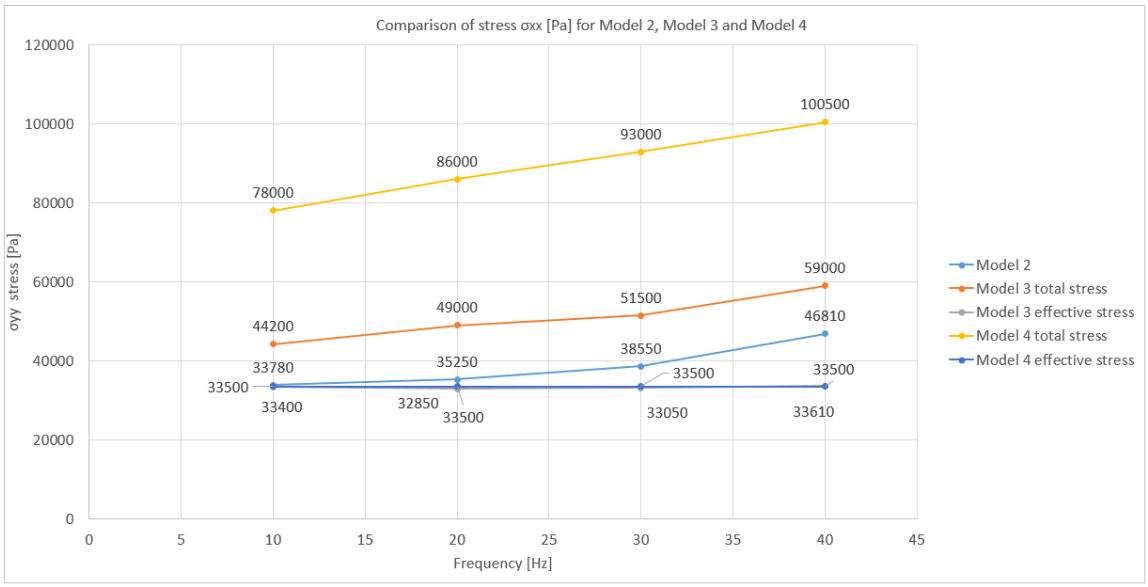

Fig. 6.28: The comparison of Soil Type 2 stresses in the horizontal direction for the sample point for four arbitrarily chosen frequencies -10,20,30 and 40Hz, for three analyzed models.

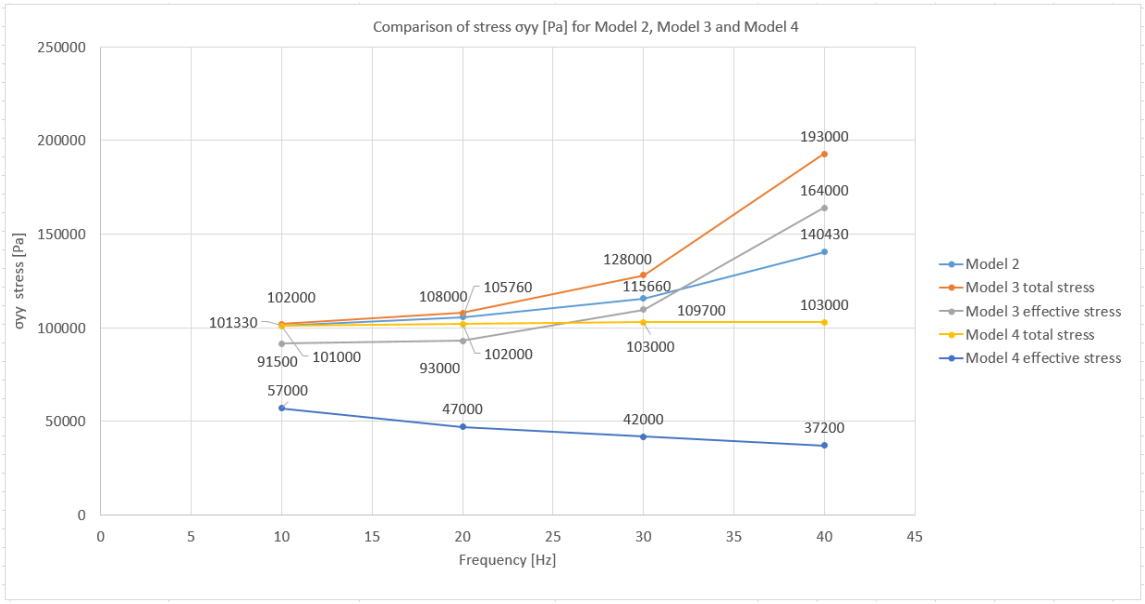

Fig. 6.29: The comparison of Soil Type 2 stresses in the vertical direction for the sample point for four arbitrarily chosen frequencies -10,20,30 and 40Hz, for three analyzed models.

In Fig. 6.27 the displacements of the point shown in green in Fig. 6.5 are compared for four arbitrarily chosen frequencies. The results from Model 2 are shown in blue, the results from Model 3 are shown in orange, and results from Model 4 are shown in grey . As we can see Model 3 is the most vulnerable to frequency increase. The values of the displacement for this model grow faster

with the frequency. Model 4 on the contrary, which reflects the uncompressible skeleton, is almost frequency independent and the displacements are not only much smaller but also do not react dynamically. The confirmation of this conclusion is in Fig. 6.29 which shows the stresses in the vertical axis (the external load direction). It can be seen that the effective stress for Model 4 is much smaller, if compared with other models, and almost does not change with the growing frequency. The total stress is also almost frequency independent.

Fig. 6.28 presents the comparison of the stresses in the horizontal direction σ_{xx} (perpendicular to the external harmonic loading). For Model 3 and 4 not only the total stress, but also the effective stress is presented. As it was mentioned before, for Model 2, there is only one type of stress shown in blue in the figure. Since the applied loading is in the opposite (*y*) direction, the effective stresses σ'_{xx} hardly change with the increasing frequency. Only the water pressure reacts, which has its reflection in the form of the growing total stresses σ_{xx} for both Model 3 and 4. This phenomenon does not occur in the vertical *y* direction (Fig. 6.29), where both total σ_{yy} and effective stress σ'_{yy} increase with the growing frequency except for the frequency-independent Model 4.

To sum up it can be observed that there are noticeable differences in displacements and stresses between the models. The differences between Model 2 and 3 can also be seen for Soil Type 1 (clay) in Fig. 6.30, Fig. 6.31 and Fig. 6.32. One should be aware that the single phase model (Model 2) implies an apparent difference in the results.

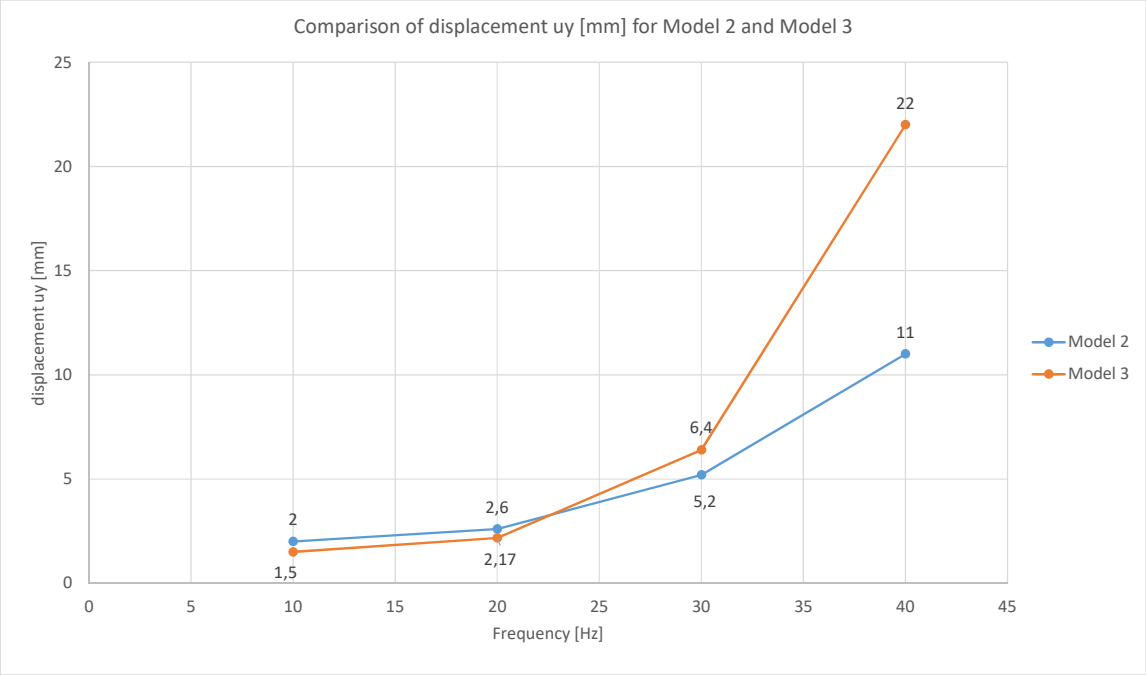

Fig. 6.30: The comparison of Soil Type 1 displacements for the sample point for four arbitrarily chosen frequencies - 10,20,30 and 40Hz, for two analyzed models.

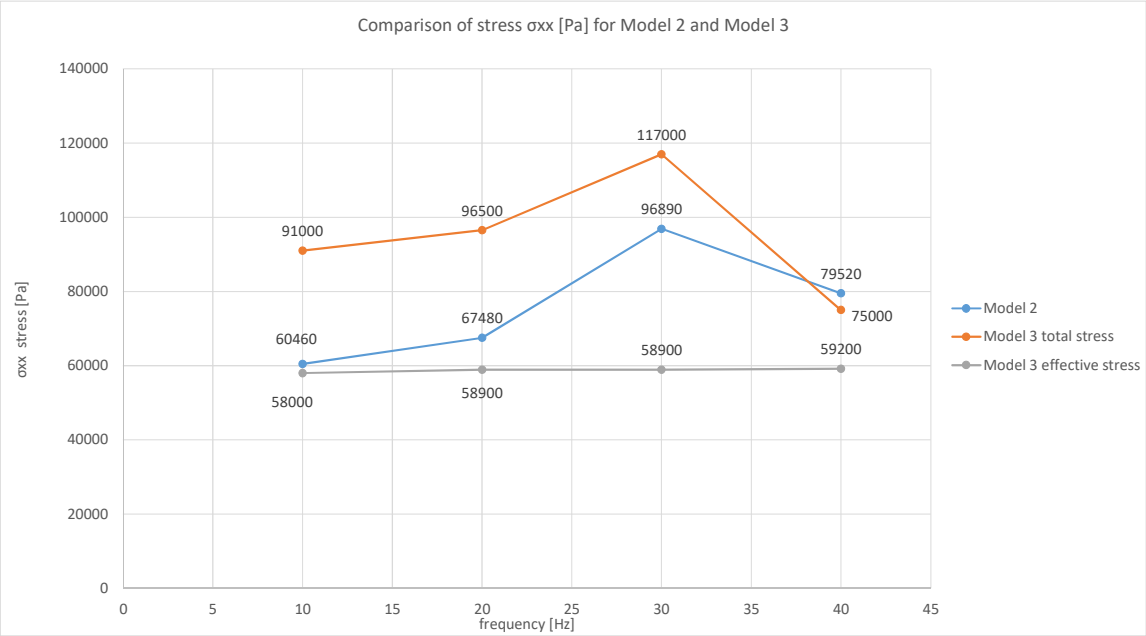

Fig. 6.31: The comparison of Soil Type 1 stresses in the vertical direction for the sample point for four arbitrarily chosen frequencies -10,20,30 and 40Hz, for two analyzed models.

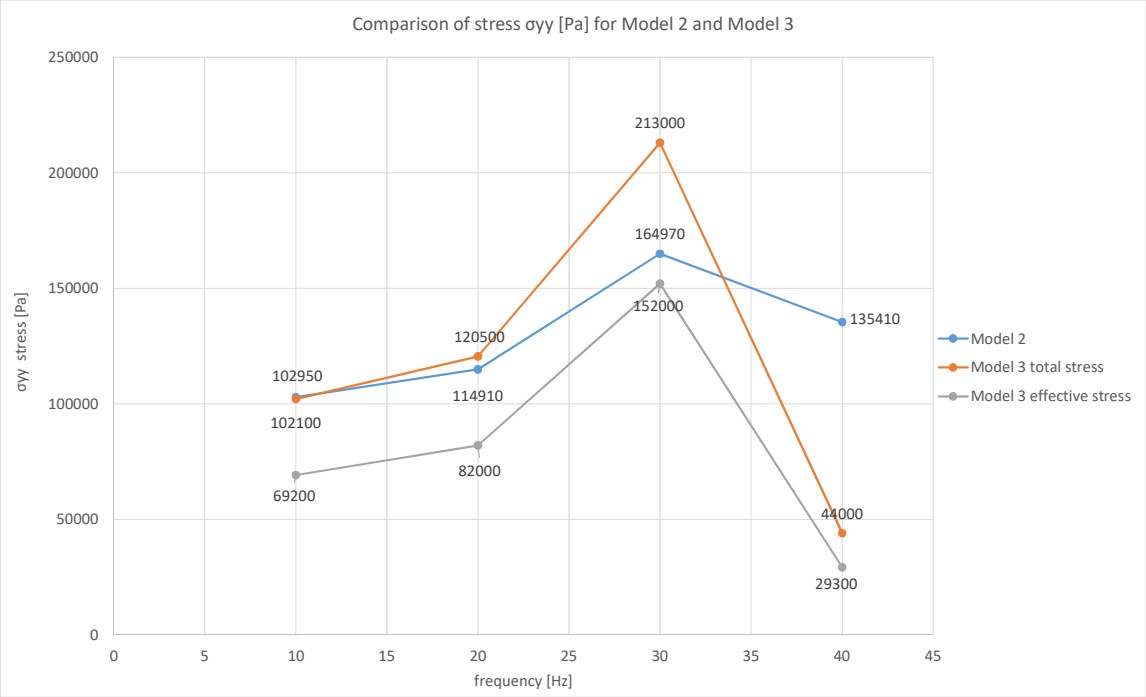

Fig. 6.32: The comparison of Soil Type 1 stresses in the vertical direction for the sample point for four arbitrarily chosen frequencies -10,20,30 and 40Hz, for two analyzed models.

7. Conclusions and future development plans.

7.1. Conclusions.

The analysis portion of the thesis is divided into two parts. The first part of the thesis (Chapter 5) concerns the one dimensional problem, whereas the second part (Chapter 6) refers to the two dimensional problem, for two-phase media under harmonic loading. The objectives for each part are defined in Section 1.2.

The first objective (A.1) for the one dimensional problem was to define the three possible formulations for two phase media - fully dynamic, partly dynamic, and quasi-static. After deriving the equations, the author moved forward to the second objective (A.2) for one dimensional problem, which was the comparison of the abovementioned models. The discrepancies between the different models vary depending on the excitation frequency and soil parameters. The dissertation proposed the limits of validity for each model in Section 5.1.4. The last (third) objective for the one dimensional problem (A.3) was to examine the influence of the physical parameters and degree of

saturation on the fundamental period, the maximum amplitude and dissipated energy. The evident dependence of these parameters can be seen on all desired results.

Regarding the two dimensional problem, firstly, the possible simplifications were introduced and implemented into the Finite Element Method , than presented in Section 6.3.3.1. This was a prelude to the second objective of the thesis (B.3), which was the comparison of the u-p model including (Model 3) and omitting the change of water pressure with time (Model 4). It was observed that the compressibility matrix does have a significant influence on the results, especially on the displacements, which are over ten times higher if incorporating the compressibility of the fluid. It can be deduced that Model 4 is not appropriate for the short-term period dynamic analysis. The last but not least (B.3) objective was to highlight the divergences of the very common single phase model (Model 2) with the two phase model including the compressibility term (Model 3). The strong influence of the frequency was noticed in the results. The higher the frequencies, the bigger differences between the models can be observed. Additionally in Section 6.3.3.3 the comparison of Model 4 with already discussed Model 2 and 3, for Soil Type 2, (sand) was done. It revealed that Model 4 is almost frequency independent and should be avoided in dynamic analysis.

To sum up, the main goal of the thesis was to show the influence of inertia forces on the amplitude of soil displacement, velocity, and acceleration when exposed to harmonic loading. An inertia force in soil for the two-phase media model, is the product of mass (skeleton or water) and acceleration (skeleton or water respectively). Consequently, the magnitude of inertia forces is affected by mass or acceleration change.

For the one dimensional case the comparison of the FD model, where all the inertia forces are included, with a simplified model was presented. This is the PD model, where water inertia forces are excluded from the equations. Additionally, the above results were compared with the consolidation model. The results presented proved the increasing divergence between the models with the increasing frequency of extortion.

For the two dimensional case, the influence of the inertia forces was also investigated. Similarly, the results proved the significant impact of the inertia forces. The comparison revealed significant differences in skeleton acceleration and pore water pressure results with the constant skeleton mass. A detailed analysis for the two dimensional case can be found in Chapter 6.

7.2. Future research plans.

The thesis concentrated on linear elastic material. Hooke's Law for the effective stress is defined by eq.(4.21). This approach is reasonable if we encounter small strains when designing turbine, pump or ventilator foundations. Unfortunately, it will not be adequate when analyzing, for example, the process of pile driving or impact loading, where the strain is relatively high. Then it is necessary to apply the nonlinear stress-strain relations, which is obviously a topic of research for the future.

In the thesis, the one and two dimensional problems were analyzed using adequately analytical solutions for the former and finite element method implementation for the latter. Firstly, a future study will widen the problem to three dimensions. Moreover, the nonlinear stress-strain relationships will be introduced.

In the study only short-term intervals were analyzed. This is the reason why the consolidation process itself was not deeply considered. It needs much more time for the water to be squeezed out of the soil. For clay soil this activity can take up to a few years. The purpose of a future study will be a profound investigation of the consolidation process. The soil settlements will be compared using two models. The first model will be a pure long-term consolidation, whereas the second model will additionally consider the harmonic loading at the first stage of the process. The initial dynamic loading can possibly shorten the consolidation mechanism and therefore it may have a significant impact on the construction industry.

APPENDIX 1

Finite Element Method Matrices for the Plane Strain Condition.

The finite elements used for the soil skeleton and the pore water pressure in the thesis are presented in Fig. 6.4.

Soil skeleton displacements in both the horizontal (*x*) direction and vertical (*y*) direction are as follows:

$$u_x(\xi,\eta) = N_1^u \bar{u}_{x1} + N_2^u \bar{u}_{x2} + N_3^u \bar{u}_{x3} + N_4^u \bar{u}_{x4} +$$

$$+N_5^u \bar{u}_{x5} + N_6^u \bar{u}_{x6} + N_7^u \bar{u}_{x7} + N_8^u \bar{u}_{x8} \quad \text{(Z1.1a)}$$

$$u_y(\xi,\eta) = N_1^u \bar{u}_{y1} + N_2^u \bar{u}_{y2} + N_3^u \bar{u}_{y3} + N_4^u \bar{u}_{y4} +$$

$$+N_5^u \bar{u}_{y5} + N_6^u \bar{u}_{y6} + N_7^u \bar{u}_{y7} + N_8^u \bar{u}_{y8} \quad \text{(Z1.2a)}$$

where the shape functions :

$$N_1^u = \frac{1}{4}(1-\xi)(1-\eta)(-\xi-\eta-1) \quad \text{(Z1.3a)}$$

$$N_2^u = \frac{1}{2}(1-\xi^2)(1-\eta) \quad \text{(Z1.3b)}$$

$$N_3^u = \frac{1}{4}(1+\xi)(1-\eta)(\xi-\eta-1) \quad \text{(Z1.3c)}$$

$$N_4^u = \frac{1}{2}(1+\xi)(1-\eta^2) \quad \text{(Z1.3d)}$$

$$N_5^u = \frac{1}{4}(1+\xi)(1+\eta)(\xi+\eta-1) \quad \text{(Z1.3e)}$$

$$N_6^u = \frac{1}{2}(1-\xi^2)(1+\eta) \quad \text{(Z1.3f)}$$

$$N_7^u = \frac{1}{4}(1-\xi)(1+\eta)(-\xi+\eta-1) \quad \text{(Z1.3g)}$$

$$N_8^u = \frac{1}{2}(1-\xi)(1-\eta^2) \quad \text{(Z1.3h)}$$

Pore water pressure is defined as:

$$p(\xi,\eta) = N_1^p \bar{p}_1 + N_2^p \bar{p}_2 + N_3^p \bar{p}_3 + N_4^p \bar{p}_4 \quad \text{(Z1.4)}$$

where :

$$N_1^p = \frac{1}{4}(1-\xi)(1-\eta) \quad \text{(Z1.5a)}$$

$$N_2^p = \frac{1}{4}(1+\xi)(1-\eta) \quad \text{(Z1.5b)}$$

$$N_3^p = \frac{1}{4}(1+\xi)(1+\eta) \quad \text{(Z1.5c)}$$

$$N_4^p = \frac{1}{4}(1-\xi)(1+\eta) \quad \text{(Z1.5d)}$$

In the equations of strong and weak formulation (eq.(6.1), (6.18) and (6.28)) the differential operator, **L,** is used which has the following form for x_1, x_2, x_3 coordinate system:

$$\mathbf{L} = \begin{bmatrix} \frac{\partial}{\partial x_1} & 0 & 0 \\ 0 & \frac{\partial}{\partial x_2} & 0 \\ 0 & 0 & \frac{\partial}{\partial x_3} \\ \frac{\partial}{\partial x_2} & \frac{\partial}{\partial x_1} & 0 \\ 0 & \frac{\partial}{\partial x_3} & \frac{\partial}{\partial x_2} \\ \frac{\partial}{\partial x_3} & 0 & \frac{\partial}{\partial x_1} \end{bmatrix} \quad \text{for 3D tasks}$$

$$\mathbf{L} = \begin{bmatrix} \frac{\partial}{\partial x_1} & 0 \\ 0 & \frac{\partial}{\partial x_2} \\ \frac{\partial}{\partial x_2} & \frac{\partial}{\partial x_1} \end{bmatrix} \quad \text{for 2D tasks}$$

SHAPE FUNCTION MATRIX

The shape functions in matrix notation are as written below. This notation is necessary to derive all the finite element matrices.

$$\mathbf{N}^u = \begin{bmatrix} N_1^u & 0 & N_2^u & 0 & N_3^u & 0 & N_4^u & 0 & N_5^u & 0 & N_6^u & 0 & N_7^u & 0 & N_8^u & 0 \\ 0 & N_1^u & 0 & N_2^u & 0 & N_3^u & 0 & N_4^u & 0 & N_5^u & 0 & N_6^u & 0 & N_7^u & 0 & N_8^u \end{bmatrix} \quad \text{(Z1.6)}$$

$$\mathbf{N}^p = [N_1^p \quad N_2^p \quad N_3^p \quad N_4^p] \quad \text{(Z1.7)}$$

ELEMENT STIFFNESS MATRIX

The stiffness matrix for the plane strain condition is defined as:

$$\mathbf{K} = \int_\Omega \mathbf{B}^\mathrm{T}\mathbf{D}\mathbf{B}d\Omega \quad \text{(Z1.8)}$$

Where **B** and **D** represent the strain-displacement and stress-strain matrices respectively:

$$\mathbf{B} = \nabla \mathbf{N}^u \tag{Z1.9}$$

where $\nabla = \begin{bmatrix} \frac{\partial}{\partial \xi} & 0 \\ 0 & \frac{\partial}{\partial \eta} \\ \frac{\partial}{\partial \eta} & \frac{\partial}{\partial \xi} \end{bmatrix}$, $\mathbf{D} = \frac{E(1-\nu)}{(1+\nu)(1-2\nu)} \begin{bmatrix} 1 & \frac{\nu}{1-\nu} & 0 \\ \frac{\nu}{1-\nu} & 1 & 0 \\ 0 & 0 & \frac{1-2\nu}{2(1-\nu)} \end{bmatrix}$ (Z1.10)

ELEMENT MASS MATRIX

$$\mathbf{M} = \int_\Omega (\mathbf{N}^u)^{\mathrm{T}} \rho \mathbf{N}^u d\Omega \tag{Z1.11}$$

The ρ is the mass of the element per unit volume and again $\mathbf{N}^u$ holds the shape functions. In further calculations, in order to make the notation clearer, the shape functions regarding the skeleton displacements are written without *u* index. After multiplication we obtain the following matrix ready to be integrated:

$\mathbf{M} =$

$$\int_\Omega \begin{bmatrix}
N_1^2 & 0 & N_1N_2 & 0 & N_1N_3 & 0 & N_1N_4 & 0 & N_1N_4 & 0 & N_1N_4 & 0 & N_1N_4 & 0 & N_1N_4 & 0 \\
0 & N_1^2 & 0 & N_1N_2 & 0 & N_1N_3 & 0 & N_1N_4 & 0 & N_1N_4 & 0 & N_1N_4 & 0 & N_1N_4 & 0 & N_1N_4 \\
N_1N_2 & 0 & N_2^2 & 0 & N_2N_3 & 0 & N_2N_4 & 0 & N_2N_5 & 0 & N_2N_6 & 0 & N_2N_7 & 0 & N_2N_8 & 0 \\
0 & N_1N_2 & 0 & N_2^2 & 0 & N_2N_3 & 0 & N_2N_4 & 0 & N_2N_5 & 0 & N_2N_6 & 0 & N_2N_7 & 0 & N_2N_8 \\
N_1N_3 & 0 & N_2N_3 & 0 & N_3^2 & 0 & N_3N_4 & 0 & N_3N_5 & 0 & N_3N_6 & 0 & N_3N_7 & 0 & N_3N_8 & 0 \\
0 & N_1N_3 & 0 & N_2N_3 & 0 & N_3^2 & 0 & N_3N_4 & 0 & N_3N_5 & 0 & N_3N_6 & 0 & N_3N_7 & 0 & N_3N_8 \\
N_1N_4 & 0 & N_2N_4 & 0 & N_3N_4 & 0 & N_4^2 & 0 & N_5N_4 & 0 & N_6N_4 & 0 & N_7N_4 & 0 & N_8N_4 & 0 \\
0 & N_1N_4 & 0 & N_2N_4 & 0 & N_3N_4 & 0 & N_4^2 & 0 & N_5N_4 & 0 & N_6N_4 & 0 & N_7N_4 & 0 & N_8N_4 \\
N_1N_5 & 0 & N_2N_5 & 0 & N_3N_5 & 0 & N_4N_5 & 0 & N_5^2 & 0 & N_6N_5 & 0 & N_7N_5 & 0 & N_8N_5 & 0 \\
0 & N_1N_5 & 0 & N_2N_5 & 0 & N_3N_5 & 0 & N_4N_5 & 0 & N_5^2 & 0 & N_6N_5 & 0 & N_7N_5 & 0 & N_8N_5 \\
N_1N_6 & 0 & N_2N_6 & 0 & N_3N_6 & 0 & N_4N_6 & 0 & N_5N_6 & 0 & N_6^2 & 0 & N_7N_6 & 0 & N_8N_6 & 0 \\
0 & N_1N_6 & 0 & N_2N_6 & 0 & N_3N_6 & 0 & N_4N_6 & 0 & N_5N_6 & 0 & N_6^2 & 0 & N_7N_6 & 0 & N_8N_6 \\
N_1N_7 & 0 & N_2N_7 & 0 & N_3N_7 & 0 & N_4N_7 & 0 & N_5N_7 & 0 & N_6N_7 & 0 & N_7^2 & 0 & N_8N_7 & 0 \\
0 & N_1N_7 & 0 & N_2N_7 & 0 & N_3N_7 & 0 & N_4N_7 & 0 & N_5N_7 & 0 & N_6N_7 & 0 & N_7^2 & 0 & N_8N_7 \\
N_1N_8 & 0 & N_2N_8 & 0 & N_3N_8 & 0 & N_4N_8 & 0 & N_5N_8 & 0 & N_6N_8 & 0 & N_7N_8 & 0 & N_8^2 & 0 \\
0 & N_1N_8 & 0 & N_2N_8 & 0 & N_3N_8 & 0 & N_4N_8 & 0 & N_5N_8 & 0 & N_6N_8 & 0 & N_7N_8 & 0 & N_8^2
\end{bmatrix} \rho \, d\Omega$$

(Z1.12)

ELEMENT WATER COUPLING MATRIX

$$\mathbf{Q} = \int_\Omega \mathbf{B}^{\mathrm{T}} \alpha \mathbf{m}^{\mathbf{T}} (\mathbf{N}^p)^{\mathrm{T}} d\Omega \tag{Z1.13}$$

where : $\mathbf{m} = [1 \quad 1 \quad 0]$.

After multiplication we obtain the following matrix [16x3]:

$$\mathbf{Q} = \int_{\Omega} \begin{bmatrix} \frac{\partial N_1}{\partial \xi} N_1^p & \frac{\partial N_1}{\partial \xi} N_2^p & \frac{\partial N_1}{\partial \xi} N_3^p & \frac{\partial N_1}{\partial \xi} N_4^p \\ \frac{\partial N_1}{\partial \eta} N_1^p & \frac{\partial N_1}{\partial \eta} N_2^p & \frac{\partial N_1}{\partial \eta} N_3^p & \frac{\partial N_1}{\partial \eta} N_4^p \\ \frac{\partial N_2}{\partial \xi} N_1^p & \frac{\partial N_2}{\partial \xi} N_2^p & \frac{\partial N_2}{\partial \xi} N_3^p & \frac{\partial N_2}{\partial \xi} N_4^p \\ \frac{\partial N_2}{\partial \eta} N_1^p & \frac{\partial N_2}{\partial \eta} N_2^p & \frac{\partial N_2}{\partial \eta} N_3^p & \frac{\partial N_2}{\partial \eta} N_4^p \\ \frac{\partial N_3}{\partial \xi} N_1^p & \frac{\partial N_3}{\partial \xi} N_2^p & \frac{\partial N_3}{\partial \xi} N_3^p & \frac{\partial N_3}{\partial \xi} N_4^p \\ \frac{\partial N_3}{\partial \eta} N_1^p & \frac{\partial N_3}{\partial \eta} N_2^p & \frac{\partial N_3}{\partial \eta} N_3^p & \frac{\partial N_3}{\partial \eta} N_4^p \\ \frac{\partial N_4}{\partial \xi} N_1^p & \frac{\partial N_4}{\partial \xi} N_2^p & \frac{\partial N_4}{\partial \xi} N_3^p & \frac{\partial N_4}{\partial \xi} N_4^p \\ \frac{\partial N_4}{\partial \eta} N_1^p & \frac{\partial N_4}{\partial \eta} N_2^p & \frac{\partial N_4}{\partial \eta} N_3^p & \frac{\partial N_4}{\partial \eta} N_4^p \\ \frac{\partial N_5}{\partial \xi} N_1^p & \frac{\partial N_5}{\partial \xi} N_2^p & \frac{\partial N_5}{\partial \xi} N_3^p & \frac{\partial N_5}{\partial \xi} N_4^p \\ \frac{\partial N_5}{\partial \eta} N_1^p & \frac{\partial N_5}{\partial \eta} N_2^p & \frac{\partial N_5}{\partial \eta} N_3^p & \frac{\partial N_5}{\partial \eta} N_5^p \\ \frac{\partial N_5}{\partial \xi} N_1^p & \frac{\partial N_5}{\partial \xi} N_2^p & \frac{\partial N_5}{\partial \xi} N_3^p & \frac{\partial N_5}{\partial \xi} N_4^p \\ \frac{\partial N_5}{\partial \eta} N_1^p & \frac{\partial N_5}{\partial \eta} N_2^p & \frac{\partial N_5}{\partial \eta} N_3^p & \frac{\partial N_5}{\partial \eta} N_4^p \\ \frac{\partial N_6}{\partial \xi} N_1^p & \frac{\partial N_6}{\partial \xi} N_2^p & \frac{\partial N_6}{\partial \xi} N_3^p & \frac{\partial N_6}{\partial \xi} N_4^p \\ \frac{\partial N_6}{\partial \eta} N_1^p & \frac{\partial N_6}{\partial \eta} N_2^p & \frac{\partial N_6}{\partial \eta} N_3^p & \frac{\partial N_6}{\partial \eta} N_4^p \\ \frac{\partial N_8}{\partial \xi} N_1^p & \frac{\partial N_8}{\partial \xi} N_2^p & \frac{\partial N_8}{\partial \xi} N_3^p & \frac{\partial N_8}{\partial \xi} N_4^p \\ \frac{\partial N_8}{\partial \eta} N_1^p & \frac{\partial N_8}{\partial \eta} N_2^p & \frac{\partial N_8}{\partial \eta} N_3^p & \frac{\partial N_8}{\partial \eta} N_4^p \end{bmatrix} d\Omega \qquad \text{(Z1.14)}$$

The **Q** matrix, in contrast to other matrices, is asymmetrical.

ELEMENT COMPRESSIBILITY MATRIX

As it was stated in Section 6.3.1 the matrix is as follows:

$$\mathbf{S} = \int_{\Omega} (\mathbf{N}^{\boldsymbol{p}})^{\mathrm{T}} \frac{1}{Q} \mathbf{N}^{\boldsymbol{p}} d\Omega \qquad \text{(Z1.15)}$$

After multiplication we obtain::

$$\mathbf{S} = \frac{1}{Q} \int_{\Omega} \begin{bmatrix} N_{1p}N_{1p} & N_{1p}N_{2p} & N_{1p}N_{3p} & N_{1p}N_{4p} \\ N_{2p}N_{1p} & N_{2p}N_{2p} & N_{2p}N_{3p} & N_{2p}N_{4p} \\ N_{3p}N_{1p} & N_{3p}N_{2p} & N_{3p}N_{3p} & N_{3p}N_{3p} \\ N_{4p}N_{1p} & N_{4p}N_{2p} & N_{4p}N_{3p} & N_{4p}N_{4p} \end{bmatrix} \mathrm{d}\Omega \qquad \text{(Z1.16)}$$

where the inverse Biot constant $\frac{1}{Q}$ according to (4.31), if we assume that $\alpha = 1$, is defined as:

$$\frac{1}{Q} = \frac{n}{K^f} + \frac{1-n}{K^s} \tag{Z1.17}$$

K^s- bulk modulus of skeleton phase in soil

K^f - – bulk modulus of fluid phase in soil.

ELEMENT PERMEABILITY MATRIX

$$\mathbf{H} = \int_{\Omega} (\nabla \mathbf{N}^{\boldsymbol{p}})^{\mathrm{T}} \mathbf{k} \mathbf{N}^{p} d\Omega \tag{Z1.18}$$

where

$\mathbf{k} = \begin{bmatrix} k_\xi & 0 \\ 0 & k_\eta \end{bmatrix}$ - water permeability coefficients for each direction

$$\nabla \mathbf{N}^{p} = \begin{bmatrix} \frac{\partial N_1^p}{\partial \xi} & \frac{\partial N_2^p}{\partial \xi} & \frac{\partial N_3^p}{\partial \xi} & \frac{\partial N_4^p}{\partial \xi} \\ \frac{\partial N_1^p}{\partial \eta} & \frac{\partial N_2^p}{\partial \eta} & \frac{\partial N_3^p}{\partial \eta} & \frac{\partial N_4^p}{\partial \eta} \end{bmatrix}. \tag{Z1.19}$$

After detailed writing we finally obtain the following matrix [4x4]:

$$\mathbf{H} = \begin{bmatrix} k_\xi \frac{\partial N_1^p}{\partial \xi}\frac{\partial N_1^p}{\partial \xi} + k_\eta \frac{\partial N_1^p}{\partial \eta}\frac{\partial N_1^p}{\partial \eta} & \cdots & k_\xi \frac{\partial N_1^p}{\partial \xi}\frac{\partial N_4^p}{\partial \xi} + k_\eta \frac{\partial N_1^p}{\partial \eta}\frac{\partial N_4^p}{\partial \eta} \\ \vdots & \ddots & \vdots \\ k_\xi \frac{\partial N_4^p}{\partial \xi}\frac{\partial N_1^p}{\partial \xi} + k_\eta \frac{\partial N_4^p}{\partial \eta}\frac{\partial N_1^p}{\partial \eta} & \cdots & k_\xi \frac{\partial N_4^p}{\partial \xi}\frac{\partial N_4^p}{\partial \xi} + k_\eta \frac{\partial N_4^p}{\partial \eta}\frac{\partial N_4^p}{\partial \eta} \end{bmatrix} \tag{Z1.20}$$

Bibliography

Bardet, J. P., 1995. The Damping of Saturated Poroelastic Soils during Steady-State Vibrations. *Applied Mathematics and Computation 67,* pp. 3-31.

Berryman, J. G., 1980. Confirmation of Biot' s theory. *Appl.Phys.Lett.,37*, pp. 382-384.

Biot, M. A., 1940. Consolidation Settlement Under a Rectangular Load Distribution. *Journal of Applied Physics*, 7 December, pp. 426-430.

Biot, M. A., 1940. General Theory of Three-Dimensional Consolidation. *Journal of Applied Physics, vol.12, No.2,* February, pp. 155-164.

Biot, M. A., 1941. General Theory of Three-Dimensional Consolidation. *Journal of Applied Physics, Vol.12, No. 2,* February, pp. 155-164.

Biot, M. A., 1955. Theory of Elasticity and Consolidation for a Porous Anisotropic Solid. *Journal of Applied Physics, vol. 26*, pp. 182-185.

Biot, M. A., 1955. Theoryof Elasticity and Consolidation for a Porous Anisotropic Solid. *Journal of Applied Physics, Vol. 26, No. 2,* February, pp. 182-185.

Biot, M. A., 1956. General Solutions of the Equations of Elasticity and Consoliadation for a Porous Material. *Journal of Applied Mechanics,* March, pp. 91-96.

Biot, M. A., 1956. Theory of propagation of elastic waves in a fluid-saturated porous soild. I. Low-Frequency Range. *The Journal of the Acoustical Society of America, vol.28, No.2*, March, pp. 168-178.

Biot, M. A., 1956. Theory of propagation of elastic waves in a fluid-saturated porous solid. II. Higher Frequency Range. *The Journal of the Acoustical Society of America, Vol.28, No. 2*, March, pp. 179-191.

Biot, M. A., 1962. Mechanics of Deformation and Acoustic Propagation in Porous Media. *Journal of Applied Physics*, pp. 1482-1498.

Biot, M. A. & Clingan, F. M., 1941. Consolidation Settlement of Soil with an Impervious Top Surface. *Journal of Applied Physics, vol 12*, July, pp. 578-581.

Biot, M. A. & Willis, D. G., 1957. The Elastic Coefficients of the Theory of Consolidation. *Journal of Applied Mechanics*, December, pp. 594--601.

Bishop, A. W., 1959. The principle of effective stress. *Teknisk Ukeblad*, pp. 859-863.

Boer, R., 1996. Highlights in the historical development of the porous media theory - toward the consistent macroscopic theory. *Applied Mechanics Reviews*, October, pp. 201-262.

Boer, R., 1999. Theory of Porous Media — Past and Present. *ZAMM Journal of applied mathematics and mechanics*, 4 February, pp. 441-466.

Bourbie, T., Coussy, O. & Zinszner, B., 1987. *Bourbie, T., Coussy, O., Zinszner, B., 1987, Acoustics of Porous Media.* s.l.:Gulf, Houston.

Brutsaert, W., 1964. The propagation of elastic waves in unconsolidated unsaturated granular mediums. *Journal of Geophysical Research 69 (2)*, pp. 243-257.

Carcione, J. M., 1998. Viscoelastic effective rheologies for modeling wave propagation in porous media. *Geophysical Prospecting*, pp. 249-270.

Cauchy, A. L., 1828. Sur l'equilibre et le mouvement d'un systeme de points materiels sollicites par des forces d'atraction ou de repulsion mutuelle. *Exercises de mathematiques 3*, pp. 188-212.

Cauchy, A. L., 1828. Sur les equations qui experiment les conditions d'equilibre, ou les lois du mouvement interieur d'un corps solide, elastique, ou non elastique. *Exercises de mathematiques 3*, pp. 160-187.

Coussy, O., 2004. *Poromechanics.* s.l.:John Wiley & Sons .

Coussy, O., 2004. *Poromechasnsics.* France: John Wiley & Sons Ltd.

de Boer, R., Schiffman, R. & Gibson, R. E., 1996. The orogins of the theory of consolidation : the Terzaghi-Fillungert dispute. *Geotechnique*, 46, pp. 175-186.

Desai, C. S., 2000. *Mechanics of Materials and Interfaces.* s.l.:CRC Press.

Desai, C. S. & Galagoda, H. M., 1989. Earthquake Analysis with generalized plasticity models for saturated soils. *International Journal of Earthquake Engineering and Structural Dynamics*, pp. 903-919.

Desai, C. S. & Zaman, M., 2014. *Advanced Geotechnical Engineering. Soil-Structure Interaction Using Computer and Material Models.*. s.l.:CRC Press, Taylor & Francis Group.

Detournay, E. & Cheng, A. H., 1993. Fundamentals of Poroelasticity. *Comprehensive Rock Engineering: Principles, Practice and Projects, Vol. II*, pp. 113-171.

Euler, L., 1736. *Mechanica sive motus scientia analytice.* s.l.:Acad. Sci..

Fick, A., 1855. Ueber Diffusion. *Ann. der Physik u. Chemie*, pp. 59-86.

Fillunger, P., 1913. Der Aufrieb in Talsperren. *Osterr. Wochenschr.f. offentl. Baudienst 19*, pp. 532-556.

Fillunger, P., 1936. Erdbaumechanik. *Selbstverlag des Verfassers, Vienna*.

Fredlund, D. G. & Morgenstern, N. R., 1977. Stress State Variables for Unsaturated Soils. *Journal of the Geotechnical Engineering Division*, May, pp. 447-466.

Fredlund, D. G., Morgenstern, N. R. & Widger, R. A., 1978. Shear strength of unsaturated soils. *Can. Geotech. J.*, pp. 313-321.

Fredlund, D. G. & Rahardjo, H., 1993. *Soil Mechanics for Unsaturated Soils.* United States of America: John Wiley & Sons.

Fredlung, D. G. & Morgenstern, N. R., 1976. Constitutive relations for volume change in unsaturated soils. *Canadian Geotechnical Journal*, pp. 261-276.

Frenkel, J., 1944. On the theory of seismic and seismoelectric phenomena in moist soil. *Journal of Physics III (4)*, pp. 230-241.

Fung, Y. C., 1965. *Foundations of solid mechanics.* New Jersey: Prentice Hall.

Gassmann, F., 1951. Über die elastizität poröser medien. *Viertel. Naturforsch. Ges.*, pp. 1-23.

Kosiński, W., 1986. *Field Singularities and Wave Analysis in Continuum Mechanics.* Warszawa: PWN - Polish Scientific Publishers.

Kubik, J., Cieszko, M. & Kaczmarek, M., 2000. *Podstawy dynamiki nasyconych ośrodków porowatych.* Warszawa: Biblioteka Mechaniki Stosowanej.

Lacoma, L. M. & Romero, I., 2007. Error Estimation for HHT method in non-linear soild mechanics. *Computer and Structures*, pp. 158-169.

Lewis, R. W. & Schrefler, B. A., 1998. *The Finite Element Method in the Static and Dynamic Deformationand Consolidation of Porous Media.* s.l.:John Wiley & Sons.

Loret, B. & Khalili, N., 2000. A three-phase model for unsaturated soils. *Internationa Journal for Numerical and Analytical Methods in geomechanics*, pp. 893-927.

Miura, K., Yoshida, N. & Kim, Y.-S., 2001. Frequency Dependent Property of Waves in Saturated Soil. *Soil and Foundations*, April, pp. 1-19.

Morland, L. W., 1972. A simple constitutive theory for a fluid-saturated porous solid. *J. Geoph. Res. 77*, pp. 890-900.

Morland, L. W., 1972. A Simple Constitutive Theory for a Fluid-Saturated Porous Solid. *Journal of Geophysical Research, Vol. 77*, January, pp. 590-600.

Murray, E. J. & Sivakumar, V., 2010. *Unsaturated Soils. A fundamental Interpretation of Soil Behaviour.*. s.l.:John Wiley & Sons.

Navier, C. L., 1827. *Mémoire sur les lois de l'équilibre et du mouvement des corps solides élastiques.* Paris, Mémoires de l'Académie Royal des Sciences 7, 375-393.

Nelson, J. T., 1988. *Acoustic emission in a fluid saturated heterogeneous porous layer with application to hydraulic fracture.* s.l.:Ph.D. thesis, Lawrence Berkeley Laboratory, Univ. of California.

Rice, J. R. & Cleary, M. P., 1976. Some basic stress diffusion solutions for fluid-saturated elastic porous media with compressible constituents. *Reviews of Geophysics and Space Physics (14)*, May, p. 227–241.

Santamarina , J. C., Klein, K. A. & Fam, M. A., 2001. *Soils and Waves.* s.l.:John Wiley & Sons Ltd..

Santamarina, J. C., Klein, K. A. & Fam, M. A., 2001. *Soils and Waves.* Chichester: John Wiley & Sons, LTD.

Shao , C., 1997. *Implementation of DSC Model for Nonlinear and Dynamic Analysis of Soil-Structure Interaction.* s.l.:s.n.

Smith, I. M. & Griffiths, D. V., 2006. *Programming the Finite Element Method.* 4th edition ed. s.l.:John Wiley & Sons.

Szefer, G., 1980. *Nonlinear problems of consolidation Theory*. Warszawa, PWN.

Terzaghi, K., 1924. *Die Theorie der hydrodynamischen Spannungserscheinungen und ihr erdbautechnisches Anwendungsgebiet.* Delft, Proceedings of the international congress for applied mechanics.

Terzaghi, K., 1936. *The shearing resitance of saturated soils and the Angle between the Planes of Shear.* Cambridge, s.n., pp. 54-56.

Terzaghi, K., 1943. *Theoretical Soil Mechanics.* New York: John Wiley and Sons.

Terzaghi, K., 1960. *From Theory to Practice in Soil Mechanics. Selections from the writings of Karl Terzaghi.*. s.l.:John Wiley & Sons.

Verruijt, A., 2010. *An Introduction to Soil Dynamics.* s.l.:Springer.

von Terzaghi, K., 1925. Principles of soil mechanics. *Engin. News-Record 95*, pp. 742-746, 796-800, 832-936, 974-978, 912-915, 1026-1029, 1060-1068.

von Terzaghi, K., 1933. Auftrieb und Kapillardruck an betonierten Talsperren. *Wasserwirtsch 26*, pp. 397-399.

Voyiadjis, G. Z. & Song, C. R., 2006. *The Coupled Theory of Mixtures in Geomechanics with Applications.* s.l.:Springer Berlin Heidelberg.

Wang, H. F., 2000. *Theory of Linear Poroelasticity with Applications to Geomechanics and Hydrogeology.* s.l.:Princeton University Press.

Wathugala, W. & Desai, C. S., 1990. *Nonlinear and Dynamic Analysis of Porous Media and Applications. Report on National Science Foundation.*, Washington,DC: s.n.

Woltman, R., 1794. *Beytr age zur Hydraulischen Architectur.* Gottingen: Dritter Band. Johann C. Dietrich.

Wrana, B., 2016. *Soil Dynamics. Computational Models.*. Kraków: s.n.

Wrana, B. & Pietrzak, N., 2013. INFLUENCE OF INERTIA FORCES ON SOIL SETTLEMENT UNDER HARMONIC LOADING. *Studia Geotechnica et Mechanica*, March, pp. 245-256.

Wrana, B. & Pietrzak, N., 2013. Soil Settlement of Two Phase Media under Harmonic Loading. *Czasopismo Techniczne PK*.

Wrana, B. & Pietrzak, N., 2015. *Deformation Analysis of the Kościuszko Mound in Cracow*. Gdańsk, 21st International Conference on Computer Methods in Mechanics.

Yoshida, N., Kobayashi, S., Suetomi, I. & Miura, K., 2002. Equivalent Linear Method considering frequency dependent characteristics of stiffness and damping. *Soil Dynamics and Earthquake Engineering*, April, pp. 205-222.

Zienkiewicz, O. C., 1982. Basic Formulation of Static and Dynamic Behaviour of Soil and Other Porous Media. *Applied Mathematics and Mechanics*, August.

Zienkiewicz, O. C. et al., 1990. Static and dynamic behaviour of soils: a rational approach to quantitive solutions.I.Fully saturated problems. *Proc R Soc Lond*, pp. 285-309.

Zienkiewicz, O. C., Chang, C. T. & Bettes, P., 1980. Drained, undrained, consolidating and dynamic behaviour assumptions in soils. *Geotechnique 30*, pp. 385-395.

Zienkiewicz, O. C. & Shiomi, T., 1984. Dynamic behaviour of saturated porous media; The generalized Biot formulation and its numerical solution. *International Journal for Numerical and Analytical Methods in Geomechanics, vol. 8*, pp. 71-96.

STRESZCZENIE

1. Wprowadzenie, motywacja oraz cele pracy naukowej

Wprowadzenie oraz motywacja

W pracy doktorskiej podejmowane jest zagadnienie dynamiki gruntów jako ośrodka dwufazowego z zastosowaniem teorii mieszaniny. Rozważa się zachowanie gruntu przy obciążeniach szybko zmiennych w czasie uwzględniając zmianę prędkości oraz zmianę przyspieszenia. Obciążenie tego typu, to obciążenie dynamiczne, w którym uwzględniana jest siła tłumienia oraz siła bezwładności składników mieszaniny.

W zależności od stopnia dokładności rozróżnia się trzy rodzaje modeli gruntu z uwagi na liczbę faz w analizie dynamicznej. Modelem obecnie najdokładniejszym jest model trójfazowy gruntu składający się ze szkieletu i płynu z gazem w porach gruntu. Uwzględnia on ich wzajemne relacje i wciąż jest rozwijany i stanowi pole badawcze w wielu ośrodkach naukowych. Model ten prowadzi do złożonego układu równań ruchu co wymaga sprzętu obliczeniowego o dużej mocy. W modelu jednofazowym występuje jeden materiał gruntu, jako mieszanina o określonych parametrach fizycznych i mechanicznych w każdym punkcie ośrodka. Model ten stosowany jest głównie do analizy rozchodzenia się fal sejsmicznych i parasejsmicznych w gruncie z założeniem liniowo-sprężystego prawa fizycznego. Model dwufazowy stosowany jest głównie w przypadku gruntu w pełni nasyconego wodą, np. w analizie zapór wodnych, skarp lub zboczy oraz w przypadku gruntu suchego. W zagadnieniach propagacji fal od źródła drgań do punktu odbioru drgań, jakim jest budynek, najczęściej stosowany jest model jednofazowy. Jeśli wymagana jest analiza drgań gruntu wokół obiektu budowlanego, to odpowiedni jest model dwufazowy. Model trójfazowy często stosowany jest w analizie zjawisk zachodzących lokalnie.

Praca naukowa zawiera analizę numeryczną odpowiedzi gruntu na obciążania harmoniczne (cykliczne). W pracy rozważany jest problem wpływu poszczególnych składników obowiązujących równań (w tym sił bezwładności szkieletu i wody w porach), przy założeniu gruntu w pełni nasyconego wodą, jako ośrodka dwufazowego. Uwzględniany jest wpływ deformacji szkieletu gruntowego na zmianę ciśnienia wody w porach. Problem tego rodzaju jest określany, jako „coupled problem”, gdzie woda w porach powoduje odkształcanie szkieletu gruntu. W równaniu ruchu uwzględnia się założenie laminarnego (zgodnie z prawem Darcy) przepływu wody. Ponadto, w równaniu ruchu zakłada się, że: przemieszczenie, prędkość i przyspieszenie cząstki wody są różne od przemieszczenie, prędkość i przyspieszenie szkieletu. Rozważania prowadzone są w zakresie teorii dynamicznej konsolidacji Biota przy uwzględnieniu wpływu sił bezwładności. Analizowany jest przypadek jednowymiarowy (rozwiązany analitycznie) oraz przypadek dwuwymiarowy (w ujęciu MES).

Cele pracy naukowej

W pacy doktorskiej rozważane jest zagadnienie wpływu definicji poszczególnych faz modelu dwufazowego gruntu, fazy szkieletu, jego bezwładności oraz fazy płynnej, wody, jej bezwładności i tłumienia drgań. Praca doktorska dotyczy zagadnienia modelowania gruntu w zakresie obciążeń dynamicznych. Rozważane są następujące sformułowania:

A) dla problemu jednowymiarowego:

1. Wpływ przyjętego modelu gruntu w sformułowaniu przemieszczeniowym: a) modelu dwufazowego dokładnego (*fully dynamic FD*) uwzględniającego przemieszczenia szkieletu, wody i ciśnienie wody w porach; b) modelu dwufazowego u-p (*partly dynamic PD*) przemieszczenia szkieletu i ciśnienia wody w porach, oraz c) modelu (*quasi-static QS*), stosowanego w zagadnieniach konsolidacji gruntu, bez udziału bezwładności szkieletu.
2. Przedstawienie różnic wyników trzech powyższych modeli oraz określenie dopuszczalnych zakresów zastosowań każdego a nich.
3. Analiza wpływu stopnia saturacji, parametrów fizycznych i częstotliwości wymuszenia na współczynnik amplifikacji drgań.

B) dla problemu dwuwymiarowego:

1. Określenie udziału szkieletu i ciśnienia wody w porach w modelu u-p, oraz analiza stosowanych obecnie uproszczeń tego modelu polegającego na pominięcie zmiany ciśnienia w czasie na tle powszechnie stosowanego modelu jednofazowego.
2. Przedstawienie różnic wyników obliczeń komputerowych (przemieszczeń, prędkości i przyspieszeń), przy zastosowaniu własnego autorskiego programu komputerowego, różnic pomiędzy modelem u-p z uwzględnieniem i bez uwzględnienia ciśnienia w czasie.
3. Zaprezentowanie różnic w przemieszczeniach, prędkościach i przyspieszeniach pomiędzy modelem dwufazowym z powszechnie stosowanym modelem jednofazowym.

W pracy ograniczono się do analizy gruntu w zakresie małych odkształceń. Założenie to stosowane jest w zagadnieniach inżynierskich, np. w dynamice gruntów pod fundamentami maszyn. Przedstawione są wyniki osiadania, ciśnienia, naprężenia gruntu na przykładzie zadania płaskiego stanu odkształcenia.

Jak wspomniano wcześniej faza szkieletu i wody jest ze sobą powiązana. Równania ruchu w pełni nasyconego ośrodka gruntowego to układ trzech równań spełniających trzy zasady:

- Zasada pędu mieszaniny szkieletu i wody
- Zasada pędu cieczy

- Zasada zachowania masy przepływu

W tych równaniach uwzględnia się: ρ_f - gęstość cieczy (wody); $\rho = n\rho_f + (1-n)$; ρ - gęstość całkowita; ρ_s - gęstość szkieletu ; **b** – wektor sił masowych (w ogólności grawitacja); *n* – porowatość; **w** – wektor średniej prędkości przepływu wody (Darcy'ego); K_f – moduł odkształcenia objętościowego cieczy w porach; **L** - macierz operatorów różniczkowania; **R** wektor wiskotycznej siły oporu przepływu zgodnie z równaniem **k R** = **w**. Macierz współczynników wodoprzepuszczalności **k** określona jest w jednostkach [długość]^3 [czas]/[masa].

Niewiadomymi dla powyższego układu równań są:

- przemieszczenia szkieletu $\mathbf{u}^s$,
- przemieszczenia wody $\mathbf{u}^f$
- ciśnienie wody w porach *p*.

2. Zakres pracy

Rozdział 1 obejmuje wprowadzenie, motywację oraz cele pracy naukowej.

Rozdział 2 pracy zawiera krótki opis historii rozwoju ośrodka porowatego. Wspomina najbardziej wpływowych naukowców oraz przedstawia zarys trzech epok w tej dziedzinie.

Rozdział 3 przedstawia szczegóły propagacji sprężystych fal w półprzestrzeni ośrodka gruntowego będącego pod wpływem obciążeń dynamicznych. Rozważany jest ośrodek jednofazowy (szkielet), dwufazowy (szkielet i woda) oraz trójfazowy (szkielet, woda i powietrze). Rozdział główną uwagę poświęca równaniom fal dylatacyjnych oraz poprzecznych.

Rozdział 4 jest wstępem do części obliczeniowej pracy doktorskiej. Przedstawia szczegółowy opis obowiązujących równań, które są bazą dla dalszej analizy. W ich skład wchodzą równania konstytutywne, równowagi, przedstawione są również na potrzeby pracy warunki początkowe oraz brzegowe.

Rozdział 5 wyjaśnia różnice między trzema możliwymi sformułowaniami dla przypadku jednowymiarowego. Oprócz różnic teoretycznych, przedstawione są różnice w wynikach na podstawie przykładu obliczeniowego rozwiązanego analitycznie. Rozbieżności te są szczegółowo przeanalizowane i zestawione ze sobą. Dla każdego modelu określone są dopuszczalne zakresy poprawności rozwiązań. W ostatni podrozdziale Rozdziału 5 analizowane są wartości współczynnika amplifikacji dla różnych rodzajów gruntu, częstotliwości wymuszenia oraz stopni saturacji.

Rozdział 6 razem z Załącznikiem 1 przedstawia równania w przypadku dwuwymiarowego płaskiego stanu odkształcenia. Podobnie jak dla przypadku jednowymiarowego wyprowadzone są

różne modele (uproszczenia), które następnie są ze sobą zestawione i porównane. Obliczenia prowadzone są w ramach aproksymacji metody elementów skończonych. Załącznik 1 prezentuje macierze MES dla ośmiowęzłowego elementu skończonego dla szkieletu oraz czterowęzłowego elementu skończonego dla ciśnienia.

Rozdział 7 zawiera podsumowanie całości pracy oraz przedstawiono dalsze kierunki rozwoju naukowego.

3. Wnioski z pracy

Obliczenia prezentowane w pracy doktorskiej podzielono na dwie części. Pierwsza (Rozdział 5) dotyczy przypadku jednowymiarowego, a druga (Rozdział 6) dotyczy przypadku dwuwymiarowego. Obie części dotyczą opisu zachowania się ośrodka dwufazowego pod działaniem obciążenia harmonicznego.

A) W ramach analizy zadania jednowymiarowego wyniki pracy doktorskiej obejmują:

- W ramach celu A.1 przedstawiono analizę i dyskusję wpływu poszczególnych składników równania dynamiki gruntu jako ośrodka dwufazowego.
- W ramach celu A.2 dla przypadku jednowymiarowego przedstawiono wyniki rozwiązań analitycznych porównania wyprowadzonych modeli. Rozbieżności w wynikach dla poszczególnych sformułowań różnią się w zależności od częstotliwości wymuszenia oraz parametrów fizycznych gruntów. W pracy zaproponowano zakresy praktycznych zastosowań poszczególnych modeli w podrozdziale 5.1.4.
- W ramach celu A.3 przedstawiono wyniki wpływu parametrów fizycznych oraz stopnia saturacji na podstawowy okres drgań układu, ekstremalną amplitudę drgań oraz współczynnik amplifikacji drgań. Wpływ każdego z czynników został zaprezentowany na zamieszczonych w pracy wykresach.

B) W ramach analizy zadania dwuwymiarowego w sformułowaniu MES wyniki pracy doktorskiego obejmują:

- W ramach celu B.1 przedstawiono analizę i dyskusję wpływu poszczególnych składników równania dynamiki gruntu w ramach pełnego modelu u-p, następnie modelu u-p z pominięciem zmiany ciśnienia w czasie oraz powszechnie stosowanego modelu jednofazowego. Każdy z tych modeli zapisano w postaci układu równań MES i zestawiono w podrozdziale 6.3.3.1.
- W ramach celu B.2 przedstawiono wyniki obliczeń komputerowych tzw. zadania „kolumny Biota" w którym wykazano znaczące różnice pomiędzy pełnym modelem u-p (Model 3) a modelem często stosowanym w praktycznych obliczeniach, w którym pomija się zmianę ciśnienia w czasie (Model 4). Udowodniono, że macierz ściśliwości w równaniu MES ma znaczący wpływ na wyniki, w szczególności na przemieszczenia, które są około 10 razy większe w przypadku jej uwzględnienia. Na

podstawie zamieszczonych wyników można wywnioskować, iż Model 4 nie jest odpowiednim modelem dla krótkiego w czasie zjawiska obciążenia dynamicznego.

- W ramach celu B.3 przedstawiono wyniki obliczeń dla „kolumny Biota", które wskazują na znaczące różnice w wynikach między modelem dwufazowym uwzględniającym zmianę ciśnienia wody w porach w czasie (Model 3) a powszechnie stosowanym modelem jednofazowym (Model 2). Występuje duża rozbieżność wyników między tymi modelami z uwagi na częstotliwość wymuszenia harmonicznego. Im wyższa częstotliwość wymuszenia, tym większe różnice w wynikach. Dodatkowo w podrozdziale 6.3.3.3 dokonano porównania Modelu 4 oraz dotychczas omówionych Modeli 2 i 3, dla gruntu typu 2 (piasek średni). Zamieszone wyniki wskazują , iż Model 4 jest praktycznie niezależny od częstotliwości wymuszenia, a więc powinien być unikany przy analizie dynamicznej.

Podsumowując, głównym celem pracy doktorskiej było wykazanie wpływu sił bezwładności na wielkości amplitud przemieszczenia (osiadania) gruntu oraz prędkości i przyspieszenia przy obciążeniu dynamicznym typu harmonicznego. Siła bezwładności występująca w gruncie w ramach modelu dwufazowego, to iloczyn masy szkieletu gruntu i wody w porach z przyspieszeniem szkieletu i wody. Zatem na wielkość sił bezwładności ma wpływ zmiana masy i zmiana przyspieszenia.

W zagadnieniu jednowymiarowym porównano wyniki obliczeń modelu PD, w którym występują siły bezwładności szkieletu i wody z modelem uproszczonym bez siły bezwładności wody. Wyniki obu modeli przedstawiono na tle modelu opisującego zjawisko konsolidacji gruntu. Przedstawione wyniki wykazują znaczące rozbieżności wraz ze wzrostem częstotliwości wymuszenia dynamicznego

W przypadku dwuwymiarowego podobnie jako w przypadku jednowymiarowego wyniki obliczeń wskazują na znaczące różnice wpływu definicji sił bezwładności. Porównanie wpływu tych sił przedstawiono przez pokazanie znaczących różnic w wielkościach przyspieszenia szkieletu i ciśnienia wody w porach przy założeniu niezmiennej masy szkieletu gruntu. Szczegółową analizę zamieszczono w Rozdziale 6.